

# CHARACTERIZATION AND DEVELOPMENT OF OCCIDIOFUNGIN

A Dissertation

by

AKSHAYA RAVICHANDRAN

Submitted to the Office of Graduate and Professional Studies of  
Texas A&M University  
in partial fulfillment of the requirements for the degree of

DOCTOR OF PHILOSOPHY

Chair of Committee,	James L. Smith
Committee Members,	Matthew Sachs
	Joseph Sorg
	Ravikumar Majeti
Head of Department,	Thomas McKnight

December 2016

Major Subject: Microbiology

Copyright 2016 Akshaya Ravichandran

## ABSTRACT

Fungal infections caused by opportunistic pathogens tend to be particularly severe and systemic in the case of immunocompromised patients. The current treatment options fall under classes such as azoles, polyenes, echinocandins and nucleoside analogs, to which resistance has been widely reported. Occidiofungin is a novel non-ribosomal peptide with a base mass of 1,200 Da that has sub-micromolar activity against a wide spectrum of fungi. Occidiofungin does not have a similar mechanism of action as the other classes of antifungals. Preliminary toxicological analyses suggested that occidiofungin was well tolerated in mice at high doses. This dissertation is aimed at characterizing the structural, functional and pharmacological aspects of occidiofungin. We describe the structural and functional characteristics of occidiofungin without the xylose group. Loss of the xylose group affected the secretion of occidiofungin by the bacterium but did not affect activity of the purified compound. We analyze a variant that is produced when a free standing thioesterase in the biosynthetic pathway is mutated. We observed that a distinct diastereomer of occidiofungin cyclized by the mutated thioesterase contributed to the activity of occidiofungin. Microscopy assays indicated that the wild type compound rapidly triggered apoptosis. Time course analysis showed immediate concentration of occidiofungin at the bud tips of *S. cerevisiae*; after an hour of exposure it distributed throughout the parent cells. In *S. pombe*, localization was seen at the poles and division septum. *In vivo* and *in vitro* affinity purification assays indicated binding of occidiofungin to actin. Pharmacokinetic evaluation of occidiofungin

indicated that highest peak plasma concentration could be achieved in a murine model via the intravenous route. Lipoformulation of occidiofungin led to a marked increase in the peak plasma concentration. Histopathology performed on mice that were exposed to long duration treatment indicated that changes in all organ tissues were within normal limits. Efficacy of occidiofungin in reducing the fungal load in a murine model of systemic candidiasis could not be demonstrated due to the possibility of high levels of binding of occidiofungin to serum proteins. Future studies will be aimed at the chemical modification of occidiofungin to reduce the binding of serum proteins.

## **DEDICATION**

To my parents for their endless patience and unconditional support throughout the course of my graduate studies.

## ACKNOWLEDGEMENTS

I would like to thank my committee chair, Dr. James Smith, for being instrumental in shaping my academic career. I wish to express my gratitude to him for being a patient mentor and an invaluable source of support in the last six years. I also wish to thank my committee members, Dr. Sachs, Dr. Sorg and Dr. Majeti, for their guidance and support throughout the course of this research. I would like to thank Dr. Dangott for his advice and for helping me understand mass spectrometry. I would also like to thank Dr. Andreas Holzenburg and Dr. Stanislav Vitha for helping me understand microscopy and providing their expertise with troubleshooting my experiments. I wish to thank the graduate student advisor, Dr. Arne Lekven and our Graduate Program Coordinator, Jennifer Bradford for their assistance.

I would like to express sincere thanks to Jerome Escano for all the help, advice, support and, especially, the cheerful company during all these years. I also wish to thank Michael Francis for the insightful discussions, scientific and otherwise. Thanks also go to my labmates, Adam Foxfire, Steven LaiHing, Mengxin Geng and Dr. Shaorong Chen for making my time at Texas A&M University a wonderful experience. I also want to extend my gratitude to the Cancer Prevention Research Institute of Texas for providing the funding for the studies presented herein.

Finally, thanks to my mother and father for their encouragement and love.

## TABLE OF CONTENTS

	Page
ABSTRACT .....	ii
DEDICATION .....	iv
ACKNOWLEDGEMENTS .....	v
TABLE OF CONTENTS .....	vi
LIST OF FIGURES.....	x
LIST OF TABLES .....	xiii
1. INTRODUCTION.....	1
1.1 Overview .....	1
1.2 Classes of antifungals.....	2
1.2.1 Polyenes.....	2
1.2.2 Azoles.....	4
1.2.3 Echinocandins .....	6
1.2.4 Allylamines .....	8
1.2.5 Nucleoside analog .....	9
1.3 Novel antifungals that target unique cellular components .....	9
1.4 NRPS antifungal agents .....	11
1.5 Occidiofungin.....	13
1.5.1 Mechanism of action and toxicity profile of occidiofungin .....	14
1.6 Conclusion.....	16
2. THE OCFC GENE ENCODES A XYLOSYLTRANSFERASE FOR THE ANTIFUNGAL OCCIDIOFUNGIN PRODUCTION BY <i>BURKHOLDERIA</i> <i>CONTAMINANS</i> MS14.....	19
2.1 Overview .....	19
2.2 Introduction .....	20
2.3 Materials and methods .....	21
2.3.1 Bacterial strains, plasmids and media .....	21
2.3.2 Mutagenesis of the <i>ocfC</i> gene .....	22
2.3.3 Reversion of the <i>ocfC</i> mutant into its wild genotype .....	24
2.3.4 In vitro susceptibility testing .....	25
2.3.5 NMR spectroscopy .....	25
2.4 Results .....	26

2.4.1	Sequence analysis of the <i>ocfC</i> gene .....	26
2.4.2	Site-directed mutagenesis of the <i>ocfC</i> gene .....	27
2.4.3	Effect of mutation in <i>ocfC</i> on antifungal activity.....	27
2.4.4	Effects of the <i>ocfC</i> mutation on production and antifungal activity of occidiofungin.....	29
2.5	Discussion .....	30
2.5.1	The <i>ocfC</i> gene encodes a member of the GT25 family of glycosyltransferases.....	30
2.5.2	The <i>ocfC</i> gene is important for the production of occidiofungin.....	31
2.6	Conclusion.....	33
3.	THE PRESENCE OF TWO CYCLASE THIOESTERASES EXPANDS THE CONFORMATIONAL FREEDOM OF THE CYCLIC PEPTIDE OCCIDIOFUNGIN	42
3.1	Overview .....	42
3.2	Introduction .....	43
3.3	Materials and methods .....	46
3.3.1	Materials .....	46
3.3.2	Site directed mutagenesis .....	46
3.3.3	NMR spectroscopy .....	47
3.3.4	Mass spectrometry.....	48
3.4	Results .....	49
3.4.1	Proportion of occidiofungin variants in the sample .....	49
3.4.2	Comparison of wild-type and <i>ocfN</i> mutant NMR spectra .....	51
3.4.3	Model for the coordinated function of two cyclase thioesterases .....	53
3.4.4	Comparison of the bioactivity of the wild-type and <i>ocfN</i> mutant product .....	54
3.5	Discussion .....	55
3.6	Conclusion.....	58
4.	THE ANTIFUNGAL OCCIDIOFUNGIN TRIGGERS AN APOPTOTIC MECHANISM OF CELL DEATH IN YEAST.....	70
4.1	Overview .....	70
4.2	Introduction .....	71
4.3	Materials and methods .....	74
4.3.1	Antifungal preparation .....	74
4.3.2	Strains, media, and plasmids .....	75
4.3.3	In vitro susceptibility testing .....	75
4.3.4	Monitoring cell-cycle progression.....	77
4.3.5	Protein extracts and Western blot analysis.....	78
4.3.6	Electron microscopy.....	79
4.3.7	Fluorescent microscopy.....	80
4.4	Results .....	82
4.4.1	Membrane and cell wall stability .....	82

4.4.2 Morphological changes following subinhibitory dosing of occidiofungin .....	84
4.4.3 Cell death experiments .....	85
4.5 Discussion .....	89
4.6 Conclusion.....	92
5. IDENTIFICATION OF THE CELLULAR TARGET FOR THE NOVEL ANTIFUNGAL OCCIDIOFUNGIN .....	109
5.1 Overview .....	109
5.2 Background .....	110
5.3 Materials and methods .....	110
5.3.1 Spectrum of activity of occidiofungin.....	110
5.3.2 Derivatization of occidiofungin.....	111
5.3.3 Confirmation of activity of alkyne-OF.....	112
5.3.4 Affinity purification of proteins with alkyne-OF .....	112
5.3.5 Localization of alkyne-OF over a time course of exposure .....	113
5.3.6 Estimation of endocytosis following occidiofungin treatment.....	114
5.3.7 Affinity purification of actin .....	115
5.3.8 Actin polymerization and depolymerization assays.....	116
5.3.9 Microscopic analysis of actin treated with occidiofungin.....	116
5.4 Results and discussion.....	117
5.5 Conclusion.....	122
6. PHARMACOLOGICAL DEVELOPMENT OF OCCIDIOFUNGIN: LIPOFORMULATION, TOXICOLOGICAL ANALYSIS AND EFFICACY STUDIES .....	139
6.1 Overview .....	139
6.2 Introduction .....	140
6.3 Materials and methods .....	142
6.3.1 In vitro quantification of occidiofungin in plasma.....	142
6.3.2 In vivo analysis of occidiofungin in a murine model.....	145
6.3.3 Estimation of the activity of occidiofungin in the presence of serum.....	147
6.4 Results .....	148
6.4.1 Estimation of peak plasma concentration of non-liposomal occidiofungin by different routes of administration .....	148
6.4.2 Determination of peak plasma concentration following liposomal occidiofungin administration.....	149
6.4.3 Comparison of pharmacodynamics between free and liposomal occidiofungin.....	150
6.4.4 Toxicology and histopathology analysis .....	150
6.4.5 Efficacy analysis of liposomal occidiofungin .....	151
6.4.6 Activity of occidiofungin in the presence of serum .....	151
6.5 Discussion .....	152



6.6 Conclusion.....	155
7. CONCLUSION.....	166
REFERENCES.....	169

## LIST OF FIGURES

	Page
Figure 1.1: Structures of clinically used antifungal classes .....	17
Figure 1.2: Antifungals in clinical development .....	18
Figure 2.1: Plates of bioassays for antifungal activities of <i>Burkholderia contaminans</i> strains (A: The wild type strain MS14; B: MS14KC1, <i>ocfC::nptII</i> ; C: MS14KC1-R, a revertant of the <i>ocfC</i> mutant; and D: MS14MT18, <i>ocfE::Tn5</i> ) against indicator fungus <i>Geotrichum candidum</i> .....	37
Figure 2.2: Absence of Xylose in the <i>ocfC</i> mutant product.....	38
Figure 2.3: TOCSY fingerprint region (NH correlations).....	39
Figure 2.4: Overlaid RP-HPLC chromatogram.....	40
Figure 2.5: Product analysis of the <i>ocfC</i> mutant revertant MS14 KC1-R.....	41
Figure 3.1: Covalent structure of occidiofungin .....	61
Figure 3.2: RP-HPLC Chromatograms .....	62
Figure 3.3: TOCSY (left panel) and HSQC (right panel) spectra of BHY4 in the wild-type sample.....	63
Figure 3.4: ESI mass spectrometry.. ..	64
Figure 3.5: TOCSY fingerprint region (NH correlations).....	64
Figure 3.6: One-dimensional NMR temperature titration curves for occidiofungin derived from <i>ocfN</i> mutant MS14GG88 and wild-type strain MS14. ....	65
Figure 3.7: Time-kill experiments performed against <i>Candida glabrata</i> ATCC66032...66	66
Figure 3.8: Schematic of occidiofungin ring closure .....	67
Figure 3.9: Comparison of the bioactivity from the wild-type and <i>ocfN</i> mutant occidiofungin fractions .....	68
Figure 3.10: Potato dextrose agar plates were inoculated with each of the strains and incubated for 3 days at 28°C.....	69
Figure 4.1: RP-HPLC chromatogram of 50 µg of purified occidiofungin.....	95

Figure 4.2: Western blot detection of MAPK activation .....	96
Figure 4.3: Western blot detection of MAPK activation in <i>Candida glabrata</i> .....	97
Figure 4.4: Scanning electron microscopy (SEM) images of <i>Candida albicans</i> .....	98
Figure 4.5: TEM Micrographs. ....	99
Figure 4.6: Cell wall mannoprotein distribution in <i>Candida glabrata</i> treated with occidiofungin remains unchanged. ....	100
Figure 4.7: Chitin staining in <i>Candida glabrata</i> .....	101
Figure 4.8: FUN-1 Assay. ....	102
Figure 4.9: Fluorescent Microscopy Studies on <i>Candida albicans</i> .....	103
Figure 4.10: Fluorescent Microscopy Studies on <i>S. cerevisiae</i> .....	104
Figure 4.11: Phosphatidylserine Detection Assay on <i>Candida albicans</i> . ....	105
Figure 4.12: Phosphatidylserine Detection Assay on <i>S. cerevisiae</i> . ....	106
Figure 4.13: Western blot analysis .....	107
Figure 4.14: Drop assay .....	108
Figure 5.1: Derivatization and characterization of alkyne-OF.....	131
Figure 5.2: Induction of apoptosis by alkyne-OF .....	132
Figure 5.3: Determination of <i>in vivo</i> interaction of occidiofungin. ....	133
Figure 5.4: <i>In vitro</i> interaction of occidiofungin with F- and G-actin .....	134
Figure 5.5: Visualization of actin filaments .....	135
Figure 5.6: Effect of occidiofungin on actin (a) polymerization and (b) depolymerization <i>in vitro</i> .....	136
Figure 5.7: Time course analysis (A-C) and competition with native occidiofungin (D-F) in a) <i>Schizosaccharomyces pombe</i> and b) <i>Saccharomyces cerevisiae</i> . .	137
Figure 5.8: Effect of the native occidiofungin on endocytosis in fission yeast .....	138
Figure 6.1: Comparison of extraction methods of occidiofungin from plasma .....	157

Figure 6.2: Calibration curve: Standard concentrations of occidiofungin in serum. ....	158
Figure 6.3: Comparison of different routes of administration .....	159
Figure 6.4: Comparison of peak plasma concentrations between administration of free and liposomal occidiofungin via intravenous administration.....	160
Figure 6.5: Comparison of kill kinetics.....	161
Figure 6.6: Histopathology analysis of kidney tissue. ....	162
Figure 6.7: Effects of occidiofungin treatment on body weight of mice .....	163
Figure 6.8: Histopathology analysis of organs from mice treated with 2mg/kg liposomal occidiofungin every 48 hours for 28 days.....	164
Figure 6.9: Analysis of efficacy of occidiofungin <i>in vivo</i> .....	165

## LIST OF TABLES

	Page
Table 2.1: Bacterial strains and plasmids .....	34
Table 2.2: Chemical shift values for the <i>ocfC</i> mutant product.....	35
Table 2.3: Antifungal activities of the <i>ocfC</i> mutant product.....	36
Table 3.1: Chemical Shift Values for Occidiofungin Derived from the <i>ocfN</i> Mutant MS14GG88.....	59
Table 4.1: Bioactivity of Occidiofungin .....	93
Table 4.2: Occidiofungin MICs .....	94
Table 5.1: Activity of occidiofungin against filamentous and non-filamentous fungi ..	124
Table 5.2: Activity of alkyne-OF compared to native occidiofungin .....	128
Table 5.3: List of proteins pulled down exclusively by alkyne-OF using the affinity purification.....	129
Table 6.1: Activity of free and liposomal occidiofungin in serum and blood .....	156

# **1. INTRODUCTION**

## **1.1 Overview**

Fungal pathogens cause diseases in a wide variety of hosts such as plants, animals and human beings and lead to the expenditure of several billion dollars annually by way of treatment. Fungal infections in plants and livestock lead to extensive loss of crop and rapid transmission of infection in animals. In humans, fungal infections may manifest as superficial infections, such as thrush and athlete's foot or as invasive, systemic conditions which are more frequently seen in immunocompromised individuals.

Since the 1900s, several antifungals have been developed and clinically employed to combat fungal infections in different hosts. These antifungals can be classified into groups based on their mechanism of action. Since their use in clinical settings, development of resistance to each class of antifungal has been reported. This development led to an eventual lull in the antibiotic development arena and progress in further identification of bioactive antifungal compounds has been slow. More recently, interest in identifying small molecules with novel mechanisms of action has increased and several natural products are being investigated for their potential as viable treatment alternatives.

## 1.2 Classes of antifungals

Antifungal agents can be classified into various classes. The most commonly used classes of antifungal agents to treat fungal infections are the azole derivatives, polyenes, echinocandins and allylamines (Figure 1.1).

### 1.2.1 Polyenes

Polyenes are a class of natural products produced by *Streptomyces* species. They are synthesized by polyketide synthases and typically consist of a cyclic structure with multiple carbon-carbon double bonds and hydroxyl groups. The members of this class differ from each other based on the number of the double bonds and presence or absence of aromatic and aminoglycosidic groups<sup>1</sup>. Polyenes constituted the standard method of treatment of systemic fungal infections before the discovery of other classes of antifungals such as azoles<sup>2</sup>. It has been observed that a correlation exists between the amount of sterols present in the cell wall of an organism to how susceptible it is to polyene toxicity<sup>3</sup>. Polyenes interact with the sterols present in the membrane of the fungal cell. The predominant sterol found in fungal cell membranes is ergosterol and it functions the same way cholesterol does in mammalian cells. Ergosterol plays an important role in maintaining structural integrity of the fungal cell membrane<sup>4</sup>.

Based on the structures of the polyenes and their biological effects, this class of antifungals was broadly categorized into two groups by Kotler-Brajtburg *et al*<sup>5</sup>. Briefly, this study analyzed the effect of different concentrations of polyenes on *S. cerevisiae* and mouse erythrocytes. The study concluded that tri-, tetra-, penta- and hexaenes induced K<sup>+</sup> ion leakage and yeast cell death and hemolysis at a range of concentrations tested

(approximately 0.5µg/ml to 45 µg/ml) whereas heptaenes (including amphotericin B) induced K<sup>+</sup> ion leakage at lower concentrations and hemolysis only at higher concentrations. Amphotericin B, a polyene that was discovered in the 1950s, was the ‘gold standard’ to treat systemic fungal infections<sup>3</sup>. It is proposed that the antibiotic interacts with the hydrophobic leaflet of the membrane and forms a ring like structure composed of eight amphotericin B molecules. The ring like structure is formed with the hydroxyl residues of amphotericin B facing the cytoplasm of the fungal cell<sup>6,7</sup>.

Due to poor bioavailability following oral administration of polyenes, amphotericin B is administered intravenously. The major limiting factor of the clinical use of amphotericin B is the severe nephrotoxicity associated with the use of this compound. The antibiotic has been formulated in liposomes and it is believed that targeted delivery of the liposomes to the fungal cells can be achieved<sup>8</sup>. Although efficacy against systemic fungal infections did not improve with the liposomal preparation, toxicity to the host organism was highly reduced<sup>9</sup>. Liposomal amphotericin B does not induce cation efflux and cell lysis in mammalian erythrocytes, demonstrating its selectivity at the cellular level<sup>10</sup>.

Development of resistance to amphotericin B is less common than the other classes of antifungals and has been suggested to occur through multiple mechanisms. For example, alteration of cell wall composition in *Aspergillus* species<sup>11</sup>, alteration of ergosterol content and protection against oxidative damage<sup>12</sup> have been proposed as possible mechanisms by which resistance against amphotericin B occurs. Several studies have suggested that presence of sterols other than ergosterol in the cell membrane leads



to resistance to polyenes<sup>13,14</sup>. More recently, it has been suggested that *in vivo* resistance to liposomal formulations of amphotericin B possibly occurs due to the administration of lower than optimal levels of the drug<sup>15</sup>.

### 1.2.2 Azoles

Azole derivatives are synthetic antifungal compounds that were discovered in the 1960s. They are reported to be fungistatic, and are the most rapidly expanding group of antifungals. They demonstrate broad spectrum activity against yeast and filamentous fungi<sup>16</sup>. They are classified into two groups based on the number of nitrogen atoms in the azole ring. The imidazoles, such as ketoconazole and miconazole, contain two nitrogen atoms in the azole ring, whereas the triazoles, such as itraconazole and fluconazole, contain three nitrogen atoms.

Ergosterols are an important group of sterols in fungal species. They are derivatives from squalene and make up the bulk sterol in fungal membranes<sup>17</sup>. Membrane integrity requires that sterol C14 demethylation occurs without hindrance. Azoles disrupt the demethylation stage thereby causing an accumulation of lanosterols and other 14-methylated sterols. Both imidazoles and triazoles act by targeting lanosterol demethylase which is a cytochrome P-450 enzyme. The enzyme has a heme moiety in its active site<sup>18</sup>. The azoles, which carry an unhindered nitrogen atom in their ring, bind to the iron molecule in heme<sup>19</sup>. This prevents activation of oxygen that is necessary for the demethylation of lanosterol. It has also been reported that a second nitrogen atom interacts with the apoprotein of the lanosterol demethylase enzyme and the interaction is influenced by the proximity of the nitrogen atom to the apoprotein<sup>20</sup>.

The presence of methylated sterols in the plasma membrane of the fungi disrupts the stability of the membrane and cell lysis occurs. It has also been observed that some imidazoles have a direct disruptive effect on the cell membrane at higher concentrations and are seen to be fungicidal<sup>21</sup>.

The ergosterols, in addition to providing structural integrity to the fungal cell membranes, also carry out a 'sparking' function<sup>17</sup>. At low concentrations, ergosterol upon addition to other bulk sterols (such as cholesterol) induces growth of yeast cells. Sterol-starved cells undergo G1 arrest and release from such an arrest can be mediated by the addition of exogenous ergosterol<sup>22</sup>. Azoles are seen to cause loss of both types of ergosterol function<sup>22</sup>.

Azoles were some of the antifungal agents to have high bioavailability when administered orally. The conditions at which maximum availability following oral administration is achieved, differs by the type of azole in question. For example, itraconazole is best administered following consumption of food whereas voriconazole is administered on an empty stomach<sup>23,24</sup>. Fluconazole can be administered via multiple routes, including intravenous and oral. Fluconazole and oral itraconazole have relatively low *in vivo* toxicities whereas other members of the triazoles have been reported to display severe hepatotoxicity, phototoxicity and cutaneous irritation<sup>25-27</sup>.

Resistance to azoles has been observed in several isolates and multiple mechanisms of resistance have been reported. Initially, mutations in the catalytic site of the target enzyme, P450 14 $\alpha$  demethylase (ERG11), were reported to confer resistance in *S. cerevisiae* and *C. albicans*. Further, other non-catalytic site mutations that hindered

inhibition were isolated<sup>19</sup>. More recently, independent studies that analyzed clinical isolates suggested overexpression of efflux pump genes CDR1 and CDR2 in addition to mutations in ERG11 as possible mechanisms of resistance in *C. albicans*<sup>28</sup> and *C. glabrata*<sup>29</sup>.

### 1.2.3 Echinocandins

Echinocandins are lipoprotein molecules consisting of cyclic peptides which are linked to a long chain fatty acid. They are semi-synthetic compounds derived from fermentation products<sup>30-32</sup>. Three types of echinocandins have been approved for clinical use by the Food and Drug Administration (caspofungin, micafungin and anidulafungin). Though the activity of the three compounds is similar, they vary structurally. The activity of the echinocandins is attributed to the hexapeptide nucleus. Caspofungin contains a fatty acid, micafungin a complex aromatic, and anidulafungin an alkoxytriphenyl side chain<sup>33</sup>. The most recent addition to the echinocandin family is ASP9726, developed by Astellas Pharmaceuticals and currently in preclinical development<sup>34</sup>. The structures of caspofungin, micafungin and ASP9726 are depicted in Figure 1.1.

Echinocandins demonstrate antifungal activity by non-competitively inhibiting 1,3- $\beta$ -D glucan synthase which is necessary for the synthesis of 1,3- $\beta$ -D glucan, an important cell wall component. The enzyme consists of at least two subunits: Fks1p and Rho1p. Rho1p is a regulatory component, controlling the production of 1,3- $\beta$ -D glucan<sup>35</sup>. The echinocandins target *FKS1p* gene product which constitutes the active site of the enzyme, 1,3- $\beta$ -D glucan synthase<sup>36</sup>. As a result, 1,3- $\beta$ -D glucan is not produced

and the cell wall loses stability. Eventually, the fungal cell is incapable of resisting the osmotic pressure due to loss of membrane integrity leading to lysis of the fungal cells<sup>37</sup>. The activity of echinocandins against target fungal species depends on the proportion of 1,3- $\beta$ -D glucan in the cell wall. The amount of glucan varies between species and it is obvious that the species that have a lower quantity of glucan in their cell wall would not be highly susceptible to treatment by echinocandins. It has been reported that exposure of yeast cells to sub-inhibitory concentrations of echinocandins leads to a dynamic shift in the ratio of chitin to glucan in the cell walls and cell with increased amounts of chitin are resistant to echinocandins<sup>38</sup>. *Candida* species and *Aspergillus* species are seen to be highly susceptible to echinocandins. As an exception, *Cryptococcus neoformans* whose cell wall has a large amount of glucan is not very susceptible to echinocandin treatment, indicating that echinocandins may target cells by an alternative mechanism that is, as yet, unknown<sup>39</sup>. Echinocandins have also been reported to induce apoptosis in fungal cells at lower concentrations, but the intracellular component responsible for the induction is still unknown<sup>40</sup>.

Echinocandins are known to display very low drug-drug interactions. The advantage of echinocandin use is also due to the fact that human cells do not have 1,3- $\beta$ -D glucan and hence toxicity to host cells can be minimized. Echinocandins are usually formulated for administration via the intravenous route and are cleared slowly following degradation in the liver<sup>35</sup>.

Resistance to echinocandins has been widely reported. Mutations in the hotspot regions of Fks1 (HS1 and HS2) have been reported as one of the major causes of

resistance. Ghannoum *et al* report multiple studies which suggest other mechanisms of resistance. For example, over expression of chitin synthase provides additional protection against echinocandins and over expression of Sbe2, a golgi protein involved in synthesis of cell wall components has been linked with echinocandin resistance<sup>41</sup>.

#### 1.2.4 Allylamines

Allylamine derivatives are a class of chemically derived compounds that have antifungal properties. Allylamines were derived by chemically altering the structure of naftifine, an antimycotic compound. These compounds inhibit the enzyme squalene epoxidase leading to the disruption of ergosterol biosynthesis. It also leads to the buildup of squalene within the cell. This results in the cidal activity of the compounds<sup>42</sup>.

Synthetic modifications of naftifine aimed specifically at making orally bioactive compounds led to the development of several allylamines that are used in the treatment of infections caused by fungi such as *Aspergillus* species. Further, allylamines have been reported to have remarkable activity against dermatophytes such as *Trichophyton spp.* and *Epidermophyton spp.* with *in vivo* efficacy in treating these infections in a porcine model<sup>42</sup>. A liposomal formulation of terbinafine has been reported for nasal delivery to treat Aspergillosis in order to improve efficacy and bioavailability of the drug<sup>43</sup>.

Development of resistance to allylamine compounds has been reported and resistant clinical isolates have been found. Mechanisms of squalene resistance include over expression of and a single amino acid substitution in the squalene epoxidase enzyme<sup>44,45</sup>. Efflux pump mediated resistance has also been suspected to occur in *Candida albicans*<sup>46</sup>.

### *1.2.5 Nucleoside analog*

5-fluorocytosine (5-FC) is a synthetic compound that was developed in the late 1950s and adapted for use as an antimycotic agent by 1968<sup>47</sup>. 5-FC is converted to 5-fluorouracil (5-FU) following uptake by fungal cells. 5-fluorouracil is then converted to metabolites which inhibit nucleotide and protein synthesis leading to fungal cell death. The conversion of 5-FC to 5-FU involves deamidation by cysteine deamidase and the lack of this enzyme in the fungal cell leads to absence of activity against that type of fungus<sup>47</sup>. 5-FC is currently used in combination with amphotericin and azoles in the treatment of systemic fungal infections<sup>47</sup>.

Resistance to 5-FC has been widely reported and has been attributed to mechanisms such as mutations leading to reduced uptake of 5-FC, increased synthesis of pyrimidines and defective uridine monophosphate pyrophosphorylase<sup>47</sup>. Due to the extensive prevalence of resistance to 5-FC, it is not used as an antifungal agent by itself.

### **1.3 Novel antifungals that target unique cellular components**

In addition to the previously mentioned classes, several compounds with novel cellular targets are currently in clinical trials (Figure 1.2). Denning and Bromley (2015) highlight these antifungals currently being developed and point out the promise of novel antifungals in the fight against resistance<sup>48</sup>. Antifungals in pre-clinical development include [N'-(3-bromo-4-hydroxybenzylidene)-2-methylbenzohydrazide (BHBM) and its derivative, 3-bromo-N'-(3-bromo-4-hydroxybenzylidene) benzohydrazide, which were discovered in a screen that probed synthetic drugs that could target the synthesis of a sphingolipid (glucosylceramide) found in fungi. Glucosylceramide is a possible

virulence factor that is necessary for fungal cell proliferation in neutral and alkaline conditions. The compounds mentioned above inhibit transport of vesicles that carry ceramide that is essential in the synthesis of fungal glucosylceramide, thereby halting progress through the cell cycle and inhibiting cytokinesis<sup>49</sup>. Sampangine, an alkaloid compound derived from plants, is another novel antifungal that possesses broad spectrum activity against fungi, protozoans and cancer cell lines. It is believed to inhibit heme biosynthesis by hyperactivating uroporphyrinogen III synthase which is encoded by the gene *HEM4*. Due to the fact that the target is conserved in humans, this class of compounds possesses antiproliferative properties in human cancer cell lines as well<sup>50</sup>. Ilicicolin H is a non-ribosomal tetracyclic peptide which is cytotoxic to HeLa cells and also possesses antifungal activity against several fungal species. It causes cell death by inhibiting mitochondrial respiration by binding to the Qn site of the cytochrome bc(1) complex<sup>51,52</sup>. One of the antifungal compounds currently in Phase I clinical trials is biafungin that is currently being developed by Cidara Therapeutics<sup>53</sup>. Biafungin is active against *Aspergillus* species and several resistant strains of *Candida*. It is also active against caspofungin-resistant fungi and has efficacy against an *fks* mutant of *Candida albicans* in a murine model. Another antifungal in Phase I trials is VT-1129 developed by Viamet Inc. VT-1129 belongs to a new class of lanosterol 14- $\alpha$ -demethylase inhibitors that contain a tetrazole moiety that binds heme. It has been reported to be more effective against fungal enzymes compared to their human counterparts<sup>54</sup>. F901318 is an orotomide, a novel class of antifungals, which is being developed by F2G Limited and is currently in phase I trials. It has been reported that F901318 has *in vivo* efficacy

against *Aspergillus* species. Antifungals currently in Phase II trials include Nikkomycin Z, which is a nucleoside-peptide natural product developed by Valley Fever Solutions that targets chitin synthetase. Specifically, Nikkomycin acts as a competitive inhibitor of chitin synthetase and eventually leads to osmotic lysis of the cell<sup>55,56</sup>. Additionally, VT1161 (developed by Viamet Inc.) is also in Phase II and is related to the tetrazole class described above<sup>57</sup>. SCY078 (SCYNEXIS), also in Phase II trials, was developed as an orally available glucan synthase inhibitor that has been shown to reduce fungal load in a murine disseminated candidiasis model<sup>58</sup>. The development of these antifungals is encouraging since they target cellular components that are different from the common classes of antifungals.

#### **1.4 NRPS antifungal agents**

Non-ribosomal peptides are unique bioactive molecules that garner extensive interest. NRPs show a broad spectrum of biological activities and pharmaceutical applications. They can harbor antimicrobial, immunomodulator, or antitumor activities. Non-ribosomal synthesis of peptides occurs independently of messenger RNA. This method requires enzymes known as non-ribosomal peptide synthetases (NRPS). NRPS may work in conjunction with polyketide synthases (PKS). A unique property of this mechanism is that it can catalyze the production of peptides containing proteinogenic and non-proteinogenic amino acids. Some common examples of NRPs of high therapeutic importance are cyclosporine, an immunosuppressant drug, daptomycin, used in the treatment of certain infections caused by Gram-positive bacteria, aminoadipyl-cysteinyl-valine (ACV)-tripeptide, which is the precursor of cephalosporin and



penicillin<sup>59</sup> and of bleomycin<sup>60</sup>, which is used in the treatment of several cancers. Echinocandins are one of the most popular families of non-ribosomal antifungal peptides due to their prevalence and wide use. Gramicidin, a non-ribosomally synthesized antimicrobial compound has been shown to have activity against *Candida* species<sup>61</sup>. More recently, Cawoy *et al* reported the production of lipopeptide compounds in *Bacillus subtilis* that possessed bioactivity against fungal pathogens<sup>62</sup>. Pelgipeptin, a recently characterized antibacterial and antifungal compound produce by *Paenibacillus elgii*, is another non-ribosomal peptide with nine amino acids and a  $\beta$ -hydroxy fatty acid<sup>63</sup>. In addition to these, several antimicrobial, anti-tumor and immunosuppressive compounds that are non-ribosomally synthesized have been characterized and some, such as cyclosporine and daptomycin, are currently in clinical use.

The NRPS-PKS process holds immense promise for the production of bioactive compounds with novel residues that are capable of targeting new regions of the fungal cell, potentially creating new classes of antifungal compounds. One such NRP with antifungal properties that appears to target a novel cellular component as compared to the existing classes of antifungals is occidiofungin, a glycolipopeptide produced by the soil bacterium, *Burkholderia contaminans* MS14<sup>64</sup>.

## 1.5 Occidiofungin

Occidiofungin possesses antifungal properties against a host of fungal species which have been reported to have acquired resistance to antifungals such as azoles and echinocandins, making it an exciting alternative to currently available treatment options.

Structure and biosynthesis of occidiofungin:

The covalent structure of occidiofungin consists of eight amino acid residues. Occidiofungin is a cyclic compound having a base mass of 1,200 Da and composed of an asparagine in the first position, followed by a novel amino acid, a serine, a  $\beta$ -hydroxy tyrosine, a diaminobutyric acid (DABA), a glycine, another asparagine and ending with a serine. Several variants of the base compound occur naturally and the variations occur on the first residue (presence or absence of a hydroxyl group on the asparagine) and the fourth residue (presence or absence of a chlorine group on the  $\beta$ -hydroxy tyrosine). Further, the novel amino acid has a lipid chain that has a xylose attached to it. A model biosynthesis pathway for the production of occidiofungin has been suggested and the enzymes involved in the production of the antifungal have been outlined.

The gene cluster which was predicted to be responsible for the production of occidiofungin, the *ocf* cluster, was characterized and of the 16 ORFs that are present in the cluster, five (ORF5, 6, 7, 9 and 11) were predicted to be NRPS or NRPS-PKS. ORFs 4, 12, 13, 14 and 15 are involved in the modification of occidiofungin. AmbR1 and AmbR2 regulate the production of occidiofungin<sup>65</sup>.

### 1.5.1 Mechanism of action and toxicity profile of occidiofungin

Occidiofungin has a broad spectrum of activity against fungi. The activity of occidiofungin against several plant and animal pathogens was tested. Filamentous fungi such as *Rhizoctonia solani*, *Aspergillus fumigatus* and *Aspergillus niger*, were highly susceptible to occidiofungin<sup>64</sup>. The activity of occidiofungin against several yeast-like fungi was also tested. MICs done on these were according to CLSI standards. The wide range of activity of occidiofungin against several fungi suggests that the target of the antifungal is highly conserved.

In order to determine its mode of action, occidiofungin was tested against several species of fungi. The inhibition of the enzyme 1,3- $\beta$ -glucan synthase is the main pathway by which echinocandins target yeast cells and cause lysis. Fks1p/Fks2p are catalytic subunits of 1,3- $\beta$ -glucan synthase. Fks1 mutants show reduced sensitivity to echinocandins. On treating Fks1 mutants of *S. cerevisiae* with occidiofungin, no reduction in sensitivity was observed. This indicates that occidiofungin does not have a similar mode of action as echinocandins. Further, addition of ergosterol to the growth medium is seen to reduce the sensitivity of yeast cells to amphotericin B. When DOPC vesicles containing 20% ergosterol were introduced in the treatment of *C. glabrata* with amphotericin B, there was a marked decrease in sensitivity. This was not observed when the same procedure was carried out during treatment of the cells with occidiofungin, indicating that occidiofungin may not act by binding to ergosterol. Therefore occidiofungin follows an entirely different mechanism of action from the other classes of antifungals<sup>66</sup>.

Previous studies done on cells of *Rhizoctonia solani* and *Geotrichum candidum* treated with sub lethal concentrations of occidiofungin display loss in cell wall thickness. *Candida* cells that were treated with a sub lethal dose of occidiofungin displayed a visible loss of mannoproteins. TEM images also showed the presence of visible inclusion bodies in these cells. Visualization of *S. cerevisiae* cells under the microscope showed intact cells, though they were reduced in size, indicating that occidiofungin does not lyse the target cell. This phenotype was indicative of the induction of apoptosis. Apoptotic assays, such as the TUNEL assay, detection of ROS production and phosphatidylserine externalization, done on *S. cerevisiae* and *C. albicans* cells following exposure to multiple concentrations of occidiofungin indicated the occurrence of apoptosis in the fungal cells<sup>66</sup>.

*In vitro* toxicity studies of occidiofungin have been done using rat hepatoma (H4IIE) cell line and it was seen that greater than 90% cell viability was observed in all variables until a 5  $\mu$ M concentration of occidiofungin was attained. Body weight analyses have been performed in female BALB/C mice and loss of less than 15% body weight was observed in mice treated with 5 mg/kg of occidiofungin in methylcellulose<sup>67</sup>. The loss observed was transient and rapidly recovered when drug challenge was removed. Further histopathology analyses have been performed on tissues from different organs following intravenous administration of occidiofungin at doses of 5mg/kg. Tubular necrosis was seen in kidney tissue and was seen to be repaired when the treatment was stopped. All other tissues were seen to be normal<sup>68</sup>.

The toxicity profile of occidiofungin along with its broad spectrum activity against several different kinds of fungi and a potentially unique molecular target makes it a promising drug to investigate and develop for treatment against pathogenic fungi that are resistant to other classes of antifungals.

## **1.6 Conclusion**

This section provides a background for the necessity of developing novel antifungal agents and concludes with an introduction to occidiofungin. The sections that follow will discuss the merits of and challenges facing the development of occidiofungin as a viable treatment option for fungal infection. The following section will introduce and characterize one of the naturally synthesized variants of occidiofungin in an effort to understand the biosynthesis of the compound.

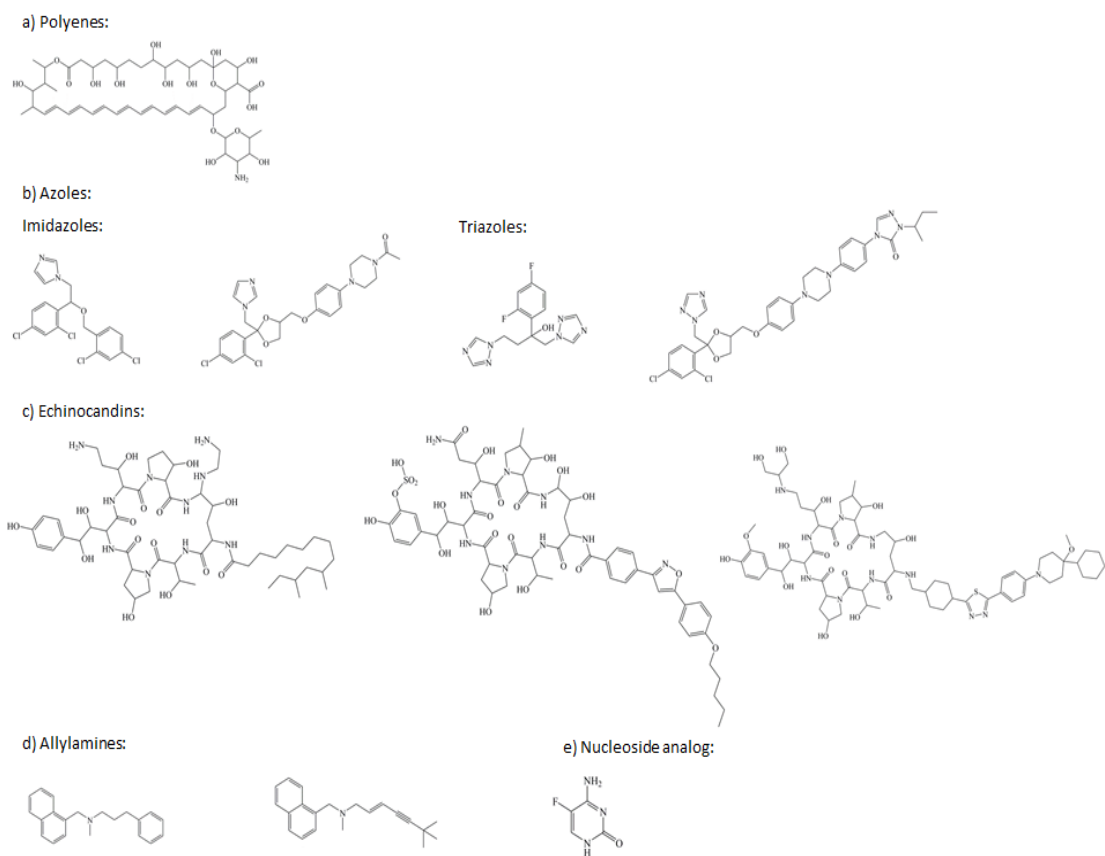


**Figure 1.1.** Structures of clinically used antifungal classes: a) Polyenes: Amphotericin B; b) Azoles: Imidazoles (left to right): Miconazole, Ketoconazole; Triazoles (left to right): Fluconazole, Itraconazole; c) Echinocandins (left to right): Caspofungin, Micafungin, ASP9726; d) Allylamines: Naftitine, Terbinafine; e) Nucleoside analog: 5-Flucytosine

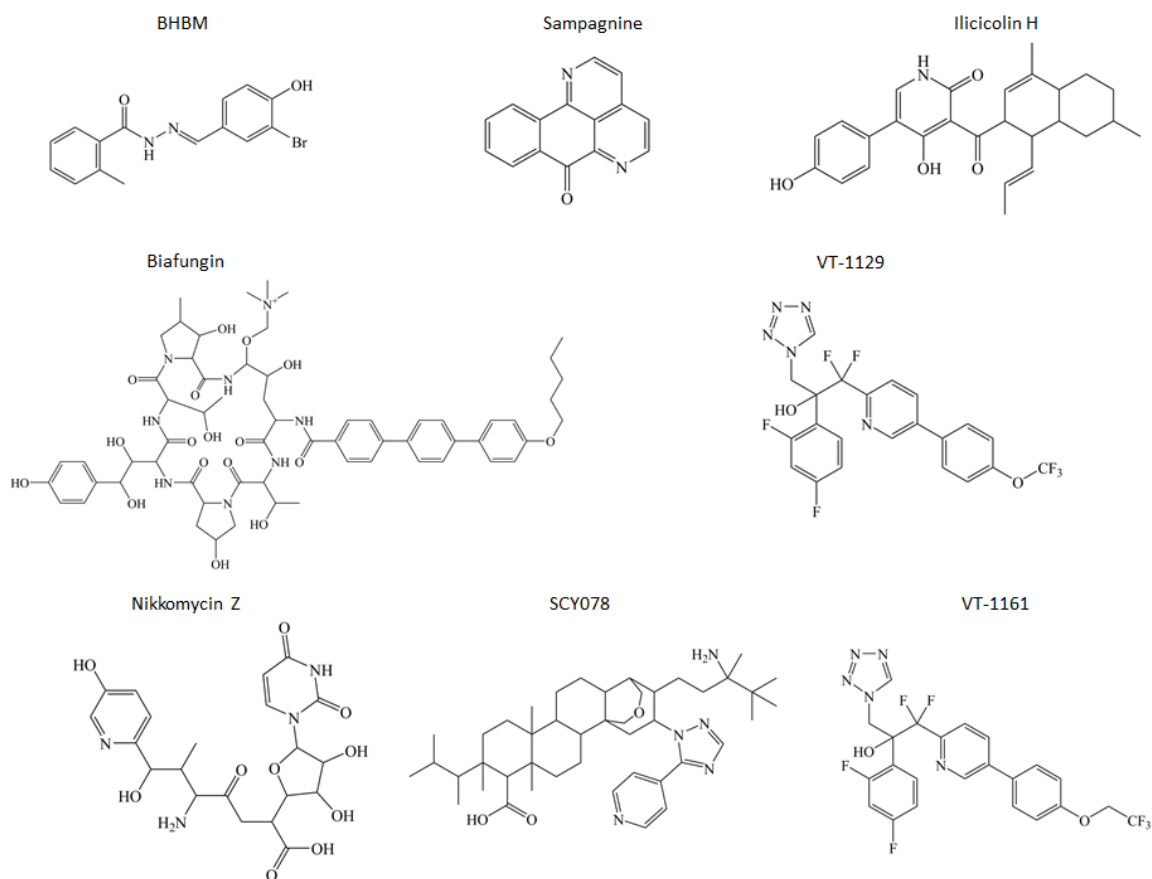


**Figure 1.2:** Antifungals in clinical development: BHBM, Sampagine and Illicicolin H are in pre-clinical development, Biafungin and VT-1129 are in Phase I trials, Nikkomycin Z, SCY078 and VT-1161 are in Phase II trials

## 2. THE OCFC GENE ENCODES A XYLOSYLTRANSFERASE FOR THE ANTIFUNGAL OCCIDIOFUNGIN PRODUCTION BY *BURKHOLDERIA CONTAMINANS* MS14\*

### 2.1 Overview

*Burkholderia contaminans* strain MS14 produces the antifungal compound occidiofungin, which is responsible for significant antifungal activities against a broad range of plant and animal fungal pathogens. Occidiofungin is a cyclic glycolipopeptide made up of eight amino acids and one xylose. A 56-kb *ocf* gene cluster was determined to be essential for occidiofungin production. In this study the *ocfC* gene, which is located downstream of *ocfD* and upstream of *ocfB* gene in the *ocf* gene cluster, was examined. Antifungal activity of the *ocfC* gene mutant MS14KC1 was reduced against the indicator fungus *Geotrichum candidum* compared with the wild-type strain. Furthermore, the analysis of the protein sequence suggests that the *ocfC* gene encodes a glycosyltransferase. Biochemical analyses using NMR and Mass spectroscopy revealed that the *ocfC* mutant produced the occidiofungin without the xylose. Purified *ocfC* mutant MS14KC1 product had similar level of bioactivity as compared to the wild-type product. The revertant MS14KC1-R of the *ocfC* mutant produced the same antifungal activity level on plate assays and the same antifungal compound based on HPLC and

---

\* Reprinted with permission from The *Burkholderia contaminans* MS14 *ocfC* Gene Encodes a Xylosyltransferase for Production of the Antifungal Occidiofungin by Akshaya Ravichandran, Kuan-Chih Chen, Adam Guerrero, Peng Deng, Sonya M. Baird, Leif Smith and Shi-En Lu. *Applied and Environmental Microbiology* 79:9. Copyright [2013] American Society for Microbiology. DOI: 10.1128/AEM.00263-13



mass spectroscopy analysis as the wild type strain MS14. Collectively, the study demonstrates the *ocfC* gene encodes a glycosyltransferase responsible to add a xylose to the occidiofungin molecule and that the presence of the xylose is not important for antifungal activity against *Candida* species. The finding provides a novel variant for future studies aimed at evaluating its use for inhibiting clinical and agricultural fungi and the finding could also simplify the chemical synthesis of occidiofungin variants.

## 2.2 Introduction

Members of the bacteria *Burkholderia* exist naturally in environments such as water, soil, and the rhizosphere of crop plants<sup>69</sup>. Some *Burkholderia* strains show striking efficacy in controlling fungal diseases of crops as biological control agents for plant disease management<sup>70</sup>. However, the use of *Burkholderia* strains is prohibited because of difficulty differentiating taxonomically these beneficial strains from the strains that are opportunistic pathogens associated with the human disease cystic fibrosis<sup>71</sup>. Understanding the molecular mechanisms of antifungal activities of the *Burkholderia* strains will provide important clues for the development of biologically based fungicides while eliminating potential health risks.

*Burkholderia contaminans* strain MS14 showed a broad range of antifungal activity to plant and human fungal pathogens<sup>64</sup>. A glycopeptide, named occidiofungin, produced by strain MS14 is responsible for its antifungal activity<sup>64,72</sup>. It is a cyclic glycopeptide made up of eight amino acids and one xylose<sup>65</sup>. Four variants, named as occidiofungin A, B, C and D have been identified from the MS14 strain culture<sup>65</sup>. Occidiofungin inhibits the growth of a broad range of fungal pathogens and it was

shown to inhibit the production of cell wall of *Geotrichum candidum*<sup>65</sup>. The compounds have shown great potential for pharmaceutical and agricultural applications<sup>67,73</sup>.

Genetic analysis revealed that a 56-kb *ocf* gene cluster is required for production of antifungal activity by *Burkholderia contaminans* strain MS14. Sixteen genes have been predicted in the *ocf* gene cluster, including the genes encoding nonribosomal peptide synthetases (*ocfD*, *ocfE*, *ocfF*, *ocfH*, and *ocfJ*), the bacterial LuxR regulatory proteins (*ambR1* and *ambR2*), and an ATP-binding cassette (*ocfA*)<sup>65</sup>. Mutagenesis and sequence analysis revealed that these genes are associated with occidiofungin production by strain MS14. Functions of a few genes in the *ocf* gene cluster, such as *ocfC*, remain to be investigated. Preliminary analysis showed the deduced protein of the *ocfC* gene shares a significant similarity to galactosyltransferases. We hypothesized that the *ocfC* gene codes for an enzyme to catalyze addition of xylose to the backbone peptide of occidiofungin. In this study, the *ocfC* gene was disrupted with an insertional mutation and effects of the mutation on occidiofungin production were evaluated. Possible functions of the *ocfC* gene are discussed.

## **2.3 Materials and methods**

### *2.3.1 Bacterial strains, plasmids and media*

Bacterial strains and plasmids used in this study are listed in Table 2.1. *Escherichia coli* JM109 (Promega, Madison, WI) was used for cloning and was cultured at 37°C on Luria-Bertani (LB) agar. Nutrient broth-yeast extract (NBY) agar media<sup>74</sup> were used to culture *Burkholderia contaminans* strain MS14 at 28°C. Potato dextrose agar (PDA) (Difco, Detroit, MI) was used for antifungal activity assays. Antibiotics

(Sigma Chemical Co., St. Louis, MO) were added to media at the following concentrations: ampicillin (100 µg/mL), kanamycin (100 µg/mL for *Escherichia coli* and 300 µg/mL for the MS14 mutants) and trimethoprim (50 µg/mL).

DNA isolation, manipulation and sequence analysis: The cetyl trimethyl ammonium bromide protocol<sup>75</sup> (10) or Wizard<sup>®</sup> Genomic DNA Purification kit (Promega Corporation, Madison, WI) was used for extraction of bacterial genomic DNA. Primers were synthesized by Integrated DNA Technologies Inc. (Coralville, IA) and Eurofins MWG Operon (Huntsville, AL). Plasmid extraction was done using the QIAprep<sup>®</sup> Spin Miniprep kit (QIAGEN Inc., Valencia, CA). Wizard<sup>®</sup> SV Gel and PCR Clean-Up System kit (Promega) was used to recover DNA fragments for cloning. Sequencing was sent to Eurofins MWG Operon. The evolutionary history of the putative *OcfC* was inferred using the Minimum Evolution method<sup>76</sup>. The evolutionary distances were computed using the Poisson correction method<sup>77</sup>. Phylogenetic analyses were conducted in MEGA4<sup>78</sup>.

### 2.3.2 Mutagenesis of the *ocfC* gene

Primers 6471R1649 (5'- GCCTACCTGCG CGTCTATCA) and 6471F137 (5'- CCATGGCGGCGATTTGCTTTGA) were designed in order to amplify the *ocfC* gene by polymerase chain reaction (PCR). The final concentrations of PCR reagents in the 50 µL reaction were: MgCl<sub>2</sub>, 2 mM; dNTPs, 0.4mM; primers, 0.6mM each; Taq DNA polymerase, 0.75 units. The PCR cycling conditions were 4 min at 95°C, then 50 s at 95°C, 50 s at 56°C and 2 min at 72°C for 30 cycles, followed by 8 min at 72°C. The PCR amplicon containing the *ocfC* gene with the flanking regions was cloned into the

vector pGEM-T Easy (Promega) to generate the plasmid pKC1. Plasmid pBSL15<sup>79</sup> was partially digested with EcoRI and then self-ligated to remove the restriction endonuclease EcoRI digestion site as described previously<sup>80</sup>. A 1.3-kb PstI fragment of the plasmid pBSL15 lacking EcoRI site and carrying the terminatorless kanamycin cassette (the *nptII* gene fragment) was cloned into the *ocfC* gene of the plasmid pKC1 using a *PstI* partial digestion strategy. The resulting plasmid pGEM-T Easy-*ocfC::nptII* was named pKC2. The *ocfC::nptII* DNA fragment was introduced to the EcoRI site of the suicide vector pBR325<sup>81</sup> for *Burkholderia* spp.<sup>82</sup> to generate plasmid pKC3. Plasmid pKC3 was electroporated into competent cells of the wild type MS14, which was prepared using the 10% glycerol-washing protocol<sup>83</sup>, for marker exchange mutagenesis (C=25μF, 200Ω, v=1.8KV, and cuvette 1mm). NBY media containing kanamycin (300μg/mL) were used for selection of the mutants. PCR amplification and sequencing were used for confirmation of double crossover mutagenesis. Plate bioassays were used to evaluate the production and biological activity of occidiofungin as described previously<sup>84</sup>.

The intact *ocfC* gene was obtained by PCR for the complementary assays. Primers *ocfC*-compF (5'- CGGAA- TTCCATGTCAATTCGTTTCTG) and *ocfC*-compR (5'- TTAAGCTTCGCTTCGAGGTCAACGGT) were designed for PCR amplification of the functional *ocfC* gene. The purpose of these two primers is to add EcoRI and HindIII sites at the both end of PCR product. The 0.8 kb PCR product was inserted into the *Burkholderia* gene expression vector pMLS7 digested with EcoRI and HindIII, to generate pKC4. Plasmid pKC4 were electroporated into cells of the mutant MS14KC1.

NBY plates with trimethoprim were used to screen the colony with pMLS7<sup>85</sup> which were confirmed by sequencing. Complementation experiments were done by the plate assay to examine the antifungal activity against *G. candidum*.

### 2.3.3 Reversion of the *ocfC* mutant into its wild genotype

To revert the *ocfC* mutant into its wild genotype, plasmid pDP12 was generated for marker exchanger gene replacement. The 1.5 Kb EcoRI fragment of pKC1 was cloned into the EcoRI site of the suicide vector pBR325. To obtain the revertants of the *ocfC* mutant MS14KC1, plasmid pDP12 was electroplated into MS14KC1 cells for marker exchange. Transformed cells were cultured in NBY broth with shaking for 4 hours. Bacterial colonies that grew on NBY supplemented with 25 µg/mL of tetracycline were used for further analysis. The colonies that were able to grow on the NBY plates supplemented with 100 µg/mL kanamycin but not 300 µg/mL were selected as candidates of the revertants. The revertants were confirmed by PCR analysis as compared with the mutant MS14KC1 and the wild type strain MS14. Verified revertant MS14KC1-R was used for further analyses of occidiofungin production.

Isolation of antifungal compound of the mutant MS14KC1 and MS14KC1-R: Isolation and purification of the occidiofungin variant produced by the *ocfC* mutant and its revertant were conducted as described previously<sup>84</sup>. In brief, the bacterial strains were incubated at 28°C for 7 days without shaking. The cell free culture extract was precipitated using ammonium sulfate (AS) (50% w/v) on ice for 2 hours. The pellet was resuspended in 1 ml of 35% acetonitrile (ACN):water (v/v) and placed in a 1.5 ml microcentrifuge tube. RP-HPLC was done using a 4.6 × 250 mm C18 column (Grace-

Vydac, catalog 201TP54) on a Bio-Rad BioLogic F10 Duo Flow with Quad Tec UV-Vis Detector system.

#### *2.3.4 In vitro susceptibility testing*

Microdilution broth susceptibility testing was performed in triplicate according to the CLSI M27-A3 method (21) in RPMI 1640 [buffered to a pH of 7.0 with MOPS (morpholinepropanesulfonic acid)] growth medium. 100X stock solutions of occidiofungin were prepared in dimethyl sulfoxide (DMSO). Minimum inhibitory concentration (MIC) endpoints for occidiofungin were determined by visual inspection and were based on the wells that had no visible growth (an optically clear well) after 24 hours of incubation. DMSO containing no antifungal agent was used as a negative control.

#### *2.3.5 NMR spectroscopy*

The same procedure for NMR analysis was used as described previously<sup>65</sup>. Occidiofungin was dissolved in deuterated dimethyl sulfoxide (DMSO-d<sub>6</sub>) and the NMR data were collected on a Bruker Avance DRX spectrometer with a CryoProbe, operating at a proton frequency of 600 MHz. The <sup>1</sup>H resonances were assigned according to standard methods<sup>86</sup> using COSY, TOCSY NOESY and <sup>13</sup>C-HSQC experiments. NMR experiments were collected at 25°C. The TOCSY experiment was acquired with a 60 ms mixing time using the Bruker DIPSI-2 spinlock sequence. The NOESY experiment was acquired with 400 ms mixing times. Phase sensitive indirect detection for NOESY, TOCSY, and COSY experiments was achieved using the standard Bruker pulse sequences. Peaks were assigned using NMRView<sup>87</sup>.

Molecular weight of the occidiofungin variant produced by MS14KC1 was measured as described previously<sup>64,84</sup>. Matrix-Assisted Laser Desorption/Ionization Mass Spectrometry — Time of Flight (MALDI-TOF, Shimadzu/Kratos) was used to determine the mass of peaks. The antifungal HPLC fraction was evaporated to dryness and was dissolved in 100  $\mu$ L of 35% acetonitrile containing 0.1% trifluoroacetic acid. From these resuspended fractions, 0.5  $\mu$ L was mixed with 0.5  $\mu$ L of  $\alpha$ -cyano-4-hydroxycinnamic acid matrix (6 mg/ml in 50% acetonitrile containing 0.1% trifluoroacetic acid) and dried on the target plate.

## 2.4 Results

### 2.4.1 Sequence analysis of the *ocfC* gene

The *ocfC* gene is located downstream of the *ocfD* gene and upstream of the *ocfB* gene in the *ocf* gene cluster (GenBank accession number: EU938698)<sup>65</sup>. No significant promoter region or terminator was identified from the 5' and 3' termini of the *ocfC* gene, suggesting the *ocfC* gene may be organized as a transcriptional operon with the downstream and upstream genes. The 657 base-paired *ocfC* gene was predicted to code for a 218-amino acid putative protein which was predicted to be the glycosyltransferase that catalyzes the transfer of a xylose to the C-7 site of occidiofungin<sup>65</sup>. Sequence analysis showed this putative protein encoded by the *ocfC* gene shared 94.0 % identity with the putative glycosyltransferase (Bamb\_6471) of *Burkholderia ambifaria* AMMD (GenBank accession number: NC\_008392). BLAST search showed there is one conserved domain from amino acid 13 to 89 on the OcfC protein, which is the signature of the Glycosyltransferase family 25<sup>88</sup>. According to the phylogenetic analysis, the OcfC

putative protein of *Burkholderia contaminans* MS14 is clustered with Bamb\_6471 of *Burkholderia ambifaria* AMMD with a bootstrap value of 100 and both were predicted to be members of the glycosyltransferase family 25. The Xcc-b100\_0220 protein for *Xanthomonas campestris* pv. *campestris* B100<sup>89</sup> and the PXO\_04234 protein of *Xanthomonas oryzae* pv. *oryzae* PXO99A<sup>90</sup> shared 55% of similarity to OcfC.

#### 2.4.2 Site-directed mutagenesis of the *ocfC* gene

A 1.5-kb PCR product was amplified using the primers 6471R1649 and 6471F137 and confirmed by sequencing to be the *ocfC* gene with its flanking regions. Sequencing further confirmed the plasmid pKC1 identity, which is the vector pGEM-T Easy carrying the *ocfC* gene. An insertional mutation was obtained by insertion of an *nptII* cassette, resulting in plasmid pKC2. The plasmid pKC3 was obtained by cloning the *nptII*- disrupted *ocfC* gene into pBR325. Introduction of pKC3 into cells of strain MS14 resulted in generations of the *ocfC* mutants MS14KC1, which was confirmed by PCR and sequencing.

#### 2.4.3 Effect of mutation in *ocfC* on antifungal activity

Mutant MS14KC1 with an insertion in the *nptII* gene cassette was evaluated for occidiofungin production by inhibitory activities against the indicator fungus *G. candidum* (Figure 2.1). The ability of MS14KC1 to inhibit the growth of the indicator fungus *G. candidum* remained with a reduced inhibitory zone ( $0.82 \pm 0.02$  cm). In contrast, the antifungal activity for wild-type strain MS14 was  $1.42 \pm 0.06$  cm in radius. The disruption of *ocfC* gene caused a 42% decrease in the antifungal activity against *G. candidum* (Figure 2.1). Based on the Fisher's least significant difference (LSD) test, this



was a significant difference ( $\alpha < 0.05$ ). As expected, the revertant strain MS14KC1-R produced the wild-type level of antifungal activity against *G. candidum*. As a negative control, the mutant MS14MT18, in which the biosynthetase gene *ocfE* is knocked out by transposon<sup>65,84</sup>, did not produce measurable antifungal activity. These results revealed the importance of *ocfC* gene for the production of the antifungal activity of strain MS14. Interestingly, no significant restoration of antifungal activity was observed when the mutant MS14KC1 harboring the intact *ocf* gene under the control of promoter *plac* in the broad-host range vector pMSL7. A significant reduction of occidiofungin production by the *ocfC* mutant was observed compared to the wild type strain. The average yield per liter of the wild-type and *ocfC* mutant product was approximately 350  $\mu\text{g/L}$  (average taken from 9 liters) and 47  $\mu\text{g/L}$  (average taken from 10.5 liters), respectively. The seven fold reduction in yield indicates that the attachment of the xylose might be important for biosynthesis or transport.

NMR analysis reveals a loss of the xylose from the wild-type product in the *ocfC* mutant (Figure 2.2A and 2.2B). Comparison of the TOCSY spectrum of the product from the *ocfC* mutant to the wild-type product reveals the loss of the proton chemical shifts for the xylose sugar. MALDI-TOF analysis also reveals the loss of the xylose sugar. The product of the *ocfC* mutant has a base mass of 1068.73 Da (Figure 2.2C), which correlates to the loss of a pentose sugar (149 Da) plus the addition of a hydroxyl group remaining on the antifungal compound. The NMR spectrum of occidiofungin has multiple spin systems for each amino acid due to different conformers on the NMR time scale. Interestingly, the spectrum is complex for a peptide that is only eight amino acids

(Figure 2.3A). The *ocfC* mutant product has a far less complex spectrum than the wild type (Figure 2.3B and Table 2.2). This is due to the loss of the bulky xylose sugar which presumably allows the compound to interchange between conformations more freely. This is reflected in the loss of conformational families in the NMR spectra for Asn1, BHY4 Gly6 and Asn7 (Figure 2.3C). The conformational families that are missing in the *ocfC* mutant have been highlighted green in the overlays of the wild-type and mutant spectrum. Cyclization of the peptide is carried out by two cyclase thioesterases that form two distinct conformational families of occidiofungin. These conformational families are visible in the *ocfC* mutant spectrum, and are easily observed by the presence of two different amide proton frequencies for Asn1 and NAA2. Therefore, the loss of the xylose sugar does not affect the formation of these two conformational groups of the antifungal compound.

#### *2.4.4 Effects of the ocfC mutation on production and antifungal activity of occidiofungin*

Occidiofungin products of the wild-type and the *ocfC* mutant MS14KC1 were purified by RP-HPLC. The *ocfC* mutant product eluted with a lower percentage of water (46%) than the wild-type product (49%) (Figure 2.4). Additionally, the *ocfC* mutant product did not elute as a doublet peak as observed in the wild-type fraction. Presumably, the observed doublet peak in the wild-type fraction is attributed to the presence of the xylose and that its presence contributes to conformational variants that have slightly different retention times. NMR analyses also revealed the loss of conformers (Figure 2.3). As expected, product isolated from *ocfC* revertant strain

(MS14 KC1-R) has the same RP-HPLC retention time and mass as the wild-type product (Figure 2.5).

MIC assay was conducted according to the CLSI M27-A3 method to determine whether the loss in activity in the *G. candidum* overlay assay was attributed to the loss of the xylose or a reduction in production. Comparing the purified wild-type and the *ocfC* mutant product on several strains of the genus *Candida*, *G. candidum* and *Saccharomyces cerevisiae* provided a quantitative assessment of the bioactivity of the mutant product. The results are listed in Table 2.2. The *ocfC* mutant product essentially had the same antifungal activity as the wild-type product in the *in vitro* assay. Presumably, the addition of the xylose may help promote solubility under normal environmental conditions. The RP-HPLC chromatograms do reveal that the *ocfC* mutant product had a longer retention time with an increased percentage of the organic solvent acetonitrile (Figure 2.4).

## 2.5 Discussion

### 2.5.1 The *ocfC* gene encodes a member of the GT25 family of glycosyltransferases

Glycosyltransferases are identified from various organisms and classified based on amino acid sequence similarity<sup>91</sup>. The GT25 family includes the known members of beta- 1,4-galactosyltransferase and lipopolysaccharide biosynthesis protein<sup>92</sup>. For *Haemophilus influenza*, glycosyltransferase LpsA is responsible for the addition of a hexose which can be either glucose or galactose<sup>93</sup>. Previous GC-MS analysis has showed that a xylose sugar is attached to the antifungal compound occidiofungin<sup>65</sup>. In this study, we hypothesized that the *ocfC* gene codes for glycosyltransferase, which was predicted

to add xylose to the oligopeptide backbone to form occidiofungin. This is proved by the sequence analysis showing that this putative protein encoded by the *ocfC* gene shared 94.0 % identity to glycosyltransferase of *B. ambifaria* AMMD in the phylogenetic tree generated. The known activities of the GT25 family include beta-1, 4-galactosyltransferase, beta-1, 3- glucosyltransferase, beta-1, 2 – glucosyltransferase and beta-1, 2- galactosyltransferase<sup>94</sup>. This study is the first evidence that xylosyltransferase is found in GT25 family. This novel glycosyltransferase has expanded the function categories of this family. Based on the evidence of this study, glycosyltransferase encoded by the *ocfC* gene should be named xylosyltransferase.

#### 2.5.2 *The ocfC gene is important for the production of occidiofungin*

The *ocfC* mutant strain MS14KC1 has approximately 42% less inhibitory activity to *G. candidum* than the wild-type strain and the occidiofungin yield of the mutant was decreased significantly compared with the wild-type strain. The revertant strain MS14KC1-R, in which the *ocfC::nptII* DNA fragment was replaced with the wild-type *ocfC* gene, restored the wild-type level of antifungal activity. More importantly, the function of the *ocfC* gene to add xylose to the occidiofungin molecule was further verified by RP-HPLC and MALDI-TOF analyses. The results further confirmed the role of *ocfC* gene in occidiofungin biosynthesis. The broad-host range vector pMLS7 was successfully used to complement the phenotype of the mutant MS14GG44 to that of the wild type strain *B. contaminans* MS14<sup>80</sup>. Surprisingly, like other studies<sup>95</sup>, a functional *ocfC* gene did not fully restore occidiofungin production of the mutant MS14KC1. The downstream genes of *ocfC* include the ABC transporter gene (*ocfB*), the hypothetical

gene (*ocfA*) and the regulator gene (*ambR2*), which have the same transcriptional orientation<sup>65</sup>. However, the mutation was made by a insertion of a terminatorless *nptIII* gene<sup>79</sup>, which should not have any polar impacts on the expression of the downstream genes<sup>96</sup>. The phenotype of the mutant MS14KC1 was resulted from the disruption of the targeted gene *ocfC*. It is speculated that the accurate balance of gene expression based on the correct genomic position and gene dosage of *ocfC* may be critical for its function.

The derivative of occidiofungin produced by the *ocfC* mutant MS14KC1 lacks xylose, which is confirmed by both NMR and MALDI-MS analysis. As noted in the TOCSY fingerprint analyses, the xylose-free occidiofungin has a far less complex spectrum than the wild type occidiofungin, which may be due to the loss of the sugar which allows the compound to interchange between conformations more freely. The two distinct conformational families of occidiofungin<sup>65</sup> carried by two cyclase thioesterases have been observed in the xylose-free occidiofungin, which suggests that the xylose sugar is not an important component for the cyclization step in occidiofungin production.

The mechanism by which the sugar xylose affects the production of occidiofungin remains to be investigated. In this study, a mutation of the *ocfC* gene results in significant reduction of occidiofungin production based on the standard plate bioassays and the yield of the xylose-free occidiofungin was decreased in the *ocfC* mutant. However, the purified xylose-free occidiofungin, which is produced by the mutant MS14KC1, showed similar antifungal activity as the wild-type occidiofungin product. Yethon et al. found that mutation of the *waaG* gene, a glycosyltransferase gene for liposaccharide (LPS), destabilized the outer membrane of *Escherichia coli*<sup>97</sup>. It was

shown that this glycosyltransferase gene, *waaG*, played an important role in stabilization of the lipopolysaccharide core protein of the outer cell membrane. We hypothesize that xylose in occidiofungin may be associated with efficient secretion or for the biosynthesis. However, sonication of the bacterial pellet did not improve the yield of the occidiofungin, which indicates the produced occidiofungin may not be significantly accumulated in bacterial cells. It is possible that the lower yield is attributed to the insertion of a terminatorless *nptII* gene, lowering the production of the downstream gene products. This is not likely given the number of reports that have shown that the cassette is non polar. Collectively, there is no significant impact of xylose on the peptide backbone and no significant effect of xylose on antifungal activity of purified occidiofungin. More investigations are needed to understand the effect of xylose on occidiofungin production.

## **2.6 Conclusion**

In conclusion, this study demonstrated that the *ocfC* gene encoding glycosyltransferase is responsible for the addition of xylose to the occidiofungin molecule. This discovery has provided important genetic and enzymatic clues for engineering new chemical variants of occidiofungin that may have applications in treating or preventing fungal infections in plants and animals.

**Table 2.1: Bacterial strains and plasmids**

Strains or plasmids	Relevant Characteristics*	Sources or reference
<b>Strains</b>		
<i>E. coli</i> JM109	<i>recA1</i> , <i>endA1</i> , <i>gyrA96</i> , <i>thi</i> , <i>hsdR17</i> , <i>supE44</i> , <i>relA1</i> , $\Delta(\text{lac-proAB})/F'[\text{traD26, rpoAB}^+, \text{lacIq}, \text{lacZ}\Delta\text{M15}]$	Promega
<i>B. contaminans</i>		
MS14	Wild type strain	(19)
MS14KC1	<i>ocfC::nptII</i> derivative of MS14; $\text{km}^r$	This study
MS14MT18	<i>ocfE::Tn5</i> derivative of MS14; $\text{km}^r$	(6)
MS14KC1-R	Revertant strain of the <i>ocfC::nptII</i> mutant	This study
<b>Plasmids</b>		
pBR325	Cloning vector; $\text{Cm}^r$ , $\text{Tc}^r$ , $\text{Ap}^r$	(16)
pMLS7	Expression vector of <i>Burkholderia</i> ; $\text{Tp}^r$	(20)
pGEM-T Easy	Cloning vector; $\text{Ap}^r$	Promega
pBSL15	Kanamycin resistance gene cassette; $\text{Km}^r$	(14)
pKC1	pGEM-T Easy carrying 1.5-kb PCR product containing the intact <i>ocfC</i> gene; $\text{Ap}^r$	This study
pKC2	pGEM-T Easy containing 2.8-kb <i>ocfC</i> and <i>nptII</i> ; $\text{Km}^r$	This study
pKC3	pBR325 carrying 2.8-kb EcoRI fragment containing the intact <i>ocfC</i> gene; $\text{Km}^r$ , $\text{Tc}^r$ , $\text{Ap}^r$	This study
pKC4	pMLS7 carrying 1.5-kb 1.5-kb PCR product containing the intact <i>ocfC</i> gene; $\text{Cm}^r$ , $\text{Tp}^r$	This study
pDP12	pBR325 carrying 1.5-kb EcoRI fragment of pKC1 containing the intact <i>ocfC</i> gene; $\text{Km}^r$ , $\text{Tc}^r$ , $\text{Ap}^r$	This study

\* $\text{Km}^r$ , kanamycin resistance;  $\text{Ap}^r$ , ampicillin resistance;  $\text{Tp}^r$ , trimethoprim resistance;  $\text{Cm}^r$ , chloramphenicol resistance

**Table 2.2: Chemical shift values for the *ocfC* mutant product**

<b>Amino acid</b>	<b>H<sup>N</sup></b>	<b>H<sup>α</sup></b>	<b>H<sup>β</sup></b>	<b>Other proton</b>
Asn1	8.13 <sup>a</sup>	4.53 [52.91]	2.58, 2.36 [40.09]	γ-NH2: 7.23, 6.84
BHN1	7.95	4.62 [58.79]	4.03 [74.94]	γ-NH2: 7.20, 6.77, β-OH: 5.71
NAA2	7.49 7.35			C2:CH2- 2.38 [39.98], C3:CH- 4.14 [47.49], C4:CH2- 1.77 [41.32] C2:CH2- 2.32 [43.78], C3:CH- 4.19 [47.49], C4:CH2- 1.39 [41.32]
Ser3	8.13 8.18	4.21 [58.90] 4.18 [58.81]		β-OH: 5.08 β-OH:5.08
BHY4	8.02	4.18 [63.07]	5.08 [73.89]	β-OH: 5.70
DABA5	7.71	4.39 [53.86]	2.11, 1.91 [32.78]	γ-H: 2.92 [32.78] NH2: 7.74
Gly6	7.93 7.85	3.81, 3.64 [45.11] 3.87, 3.65		
Asn7	8.36 8.30	4.58 [58.71] 4.56 [52.91]	2.63, 2.41 [40.09] 2.63, 2.40	γ-NH2: 7.38, 6.92 γ-NH2: 7.38, 6.92
Ser 8	7.81	4.20 [58.70]	3.62 [63.07]	β-OH: 5.69

<sup>a</sup>Proton chemical shift values are from a TOCSY and NOESY experiments. Chemical shifts in brackets are <sup>13</sup>C values from the HSQC experiment.



**Table 2.3: Antifungal activities of the *ocfC* mutant product**

<b>Strain</b>	<b>Antifungal (<math>\mu\text{g/ml}</math>)</b>	
	<b>Wild-type</b>	<b><i>ocfC</i> mutant</b>
<i>C. tropicalis</i> 66029	0.5	0.5
<i>C. glabrata</i> 66032	0.5	0.5
<i>C. albicans</i> 66027	1.0	1.0
<i>C. albicans</i> LL	0.5	0.5
<i>C. albicans</i> TE	0.5	0.5
<i>C. parapsilosis</i> 90018	1.0	1.0
<i>C. glabrata</i> TE	0.5	0.25
<i>G. candidum</i>	0.5	0.5
<i>S. cerevisiae</i> BY4741	0.06	0.06

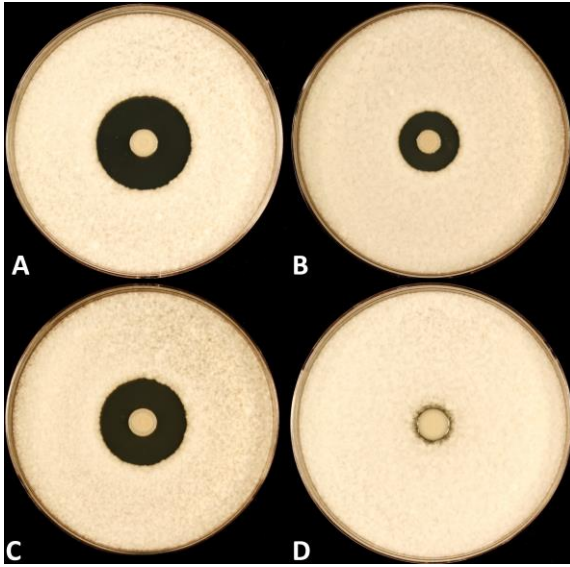


**Figure 2.1:** Plates of bioassays for antifungal activities of *Burkholderia contaminans* strains (A: The wild type strain MS14; B: MS14KC1, *ocfC::nptII*; C: MS14KC1-R, a revertant of the *ocfC* mutant; and D: MS14MT18, *ocfE::Tn5*) against indicator fungus *Geotrichum candidum*. Potato dextrose agar plates were inoculated with each strain (5  $\mu$ l containing  $\sim 10^6$  cells) and the inoculated plates were incubated at 28°C for 4 days. The plates were oversprayed with spore suspensions of the indicator fungus *G. candidum* Km and further incubated at 28°C overnight.

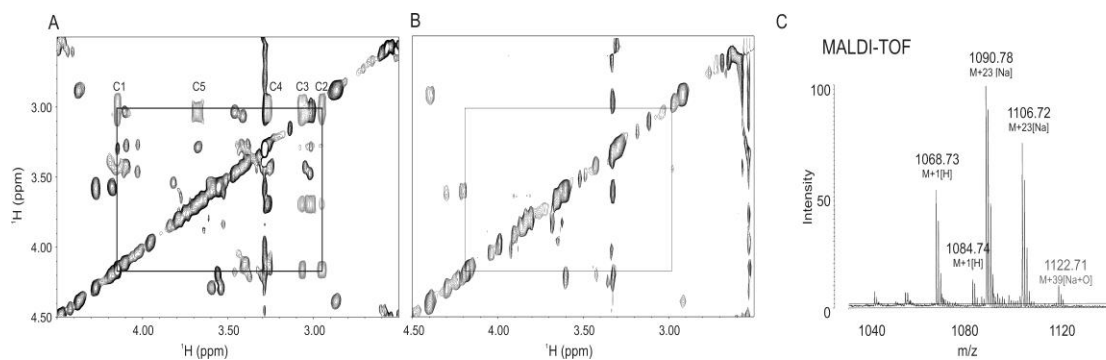


**Figure 2.2:** Absence of Xylose in the *ocfC* mutant product. A. Region of the TOCSY spectrum showing the proton chemical shifts of the xylose in the wild-type sample. B. Region of the TOCSY spectrum showing the absence of the xylose in the *ocfC* mutant product sample. C. MALDI-TOF spectrum of the *ocfC* mutant product showing a base mass of 1068 Da, which is a loss of 132 Da compared to the wild-type product mass.

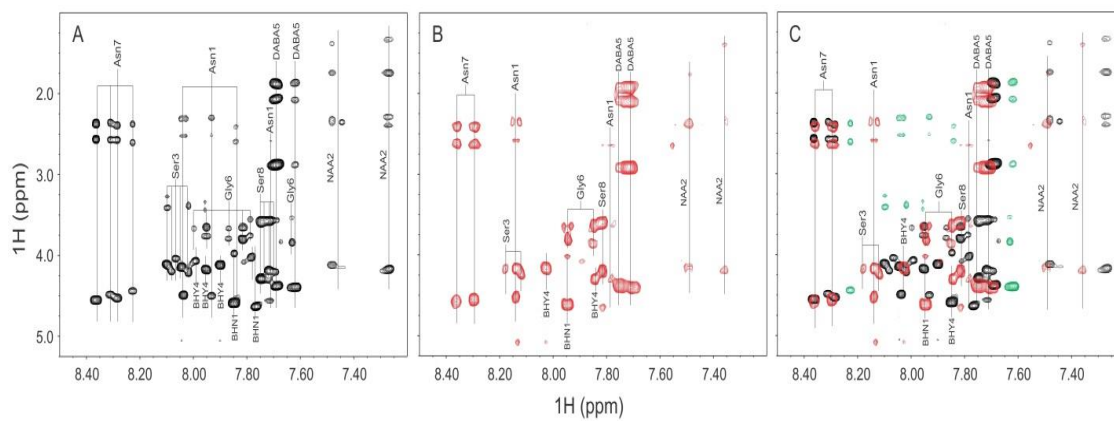


**Figure 2.3:** TOCSY fingerprint region (NH correlations). A. NH correlations in the wild-type sample. B. NH correlations in the *ocfC* mutant sample. C. Overlay of the NH correlations found in the wild-type and mutant samples. NH correlations that are not present in the *ocfC* mutant sample are colored green.

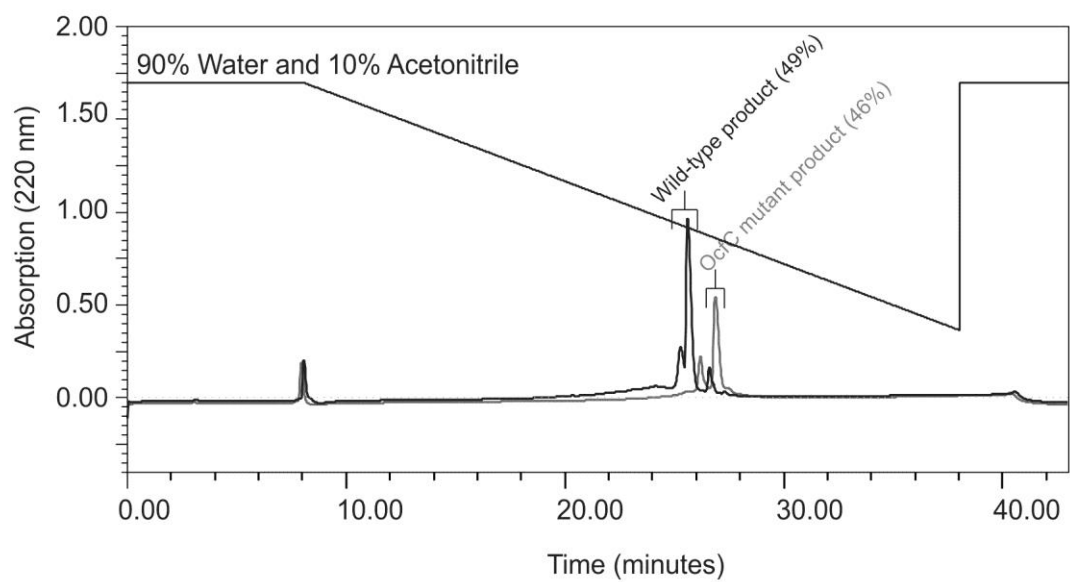


**Figure 2.4:** Overlaid RP-HPLC chromatogram obtained from the extracts of both the wild-type strain MS14 (black) and the *ocfC* mutant (grey).

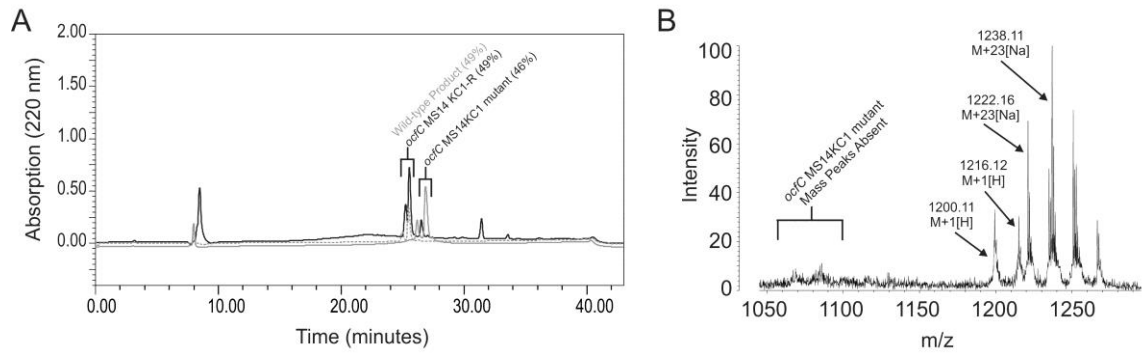


**Figure 2.5:** Product analysis of the *ocfC* mutant revertant MS14 KC1-R. A. Overlaid RP-HPLC chromatogram obtained from the extracts of the wild-type strain MS14 (grey dashed line), the *ocfC* mutant (grey) MS14 KC1, and *ocfC* revertant (black) MS14 KC1-R. B. MALDI-TOF spectrum of the *ocfC* revertant MS14 KC1-R product showing a base mass of 1200 Da and the absence of the *ocfC* mutant MS14 RC1 base mass of 1068 Da.

### 3. THE PRESENCE OF TWO CYCLASE THIOESTERASES EXPANDS THE CONFORMATIONAL FREEDOM OF THE CYCLIC PEPTIDE OCCIDIOFUNGIN\*

#### 3.1 Overview

Occidiofungin is a cyclic nonribosomally synthesized antifungal peptide with submicromolar activity produced by Gram-negative bacterium *Burkholderia contaminans*. The biosynthetic gene cluster was confirmed to contain two cyclase thioesterases. NMR analysis revealed that the presence of both thioesterases is used to increase the conformational repertoire of the cyclic peptide. The loss of the OcfN cyclic thioesterase by mutagenesis results in a reduction of conformational variants and an appreciable decrease in bioactivity against *Candida* species. Presumably, the presence of both asparagine and  $\beta$ -hydroxyasparagine variants coordinate the enzymatic function of both of the cyclase thioesterases. OcfN has presumably evolved to be part of the biosynthetic gene cluster due to its ability to produce structural variants that enhance antifungal activity against some fungi. The enhancement of the antifungal activity from the incorporation of an additional cyclase thioesterase into the biosynthetic gene cluster of occidiofungin supports the need to explore new conformational variants of other therapeutic or potentially therapeutic cyclic peptides.

---

\* Reprinted with permission from The Presence of Two Cyclase Thioesterases Expands the Conformational Freedom of the Cyclic Peptide Occidiofungin by Akshaya Ravichandran, Ganyu Gu, Jerome Escano, Shi-En Lu, and Leif Smith. *Journal of Natural Products* 76:2. Copyright [2013] American Chemical Society. DOI: 10.1021/np3005503

### 3.2 Introduction

Nonribosomal peptide synthetases (NRPSs) produce a wide array of small and structurally complex peptides that have therapeutic potential. The system enables the incorporation of nonproteinogenic amino acids into the polypeptide. Polyketide synthetases (PKSs) are a family of enzymes or enzyme complexes that produce polyketides. Integration of PKSs into the NRPSs system further increases the variety of polypeptides that can be produced by these systems. Recent studies are aimed at exploiting nonribosomal peptide synthetases (NRPSs) for producing peptide libraries that can be screened for therapeutic applications.<sup>98-105</sup>

Unlike linear peptides, cyclic peptides are restrained to fewer conformations that facilitate their interaction with their molecular target.<sup>106-114</sup> These structural constraints provide resistance to proteases, extreme pH, and temperature.<sup>106,115</sup> These attributes make them one of the most promising scaffolds for pharmacophores. Classical total synthesis of peptides by solid phase or solution phase peptide synthesis followed by subsequent cyclization reactions requires the addition and removal of protecting groups at the right stages to drive the cyclization among the correct residues.<sup>105</sup> Even with these considerations, proper cyclization is hindered by intermolecular interactions and entropically disfavored pre-cyclization conformations resulting in a vast mixture of compounds or low yields. Microorganisms ensure the formation of a functional cyclic peptide conformation by enzymatically catalyzing the cyclization and release of the peptide with regioselectivity using a cyclase thioesterase.<sup>98,104</sup> The cyclase thioesterase is



often located at the C-terminal end of the last NRPS involved in the synthesis of the peptide and is referred to as the TE domain.

The TE domain can hydrolyze the bound peptide as a linear peptide or it can catalyze an intramolecular reaction resulting in the formation of a cyclic peptide. At present, little is known about the cyclization mechanism of peptides. The crystal structure of the surfactin peptide cyclase provided the first basic understanding of its mechanism of action.<sup>116,117</sup> The peptidyl chain bound to 4-phosphopantetheine cofactor (ppan) that is attached to the thiolation (T)-domain is transferred to a serine, which is part of a catalytic triad in the adjacent TE domain. Once the peptide is transferred to the TE domain, the cyclase binding pocket enables proper orientation and cyclization of the peptide substrate. The enzyme was found to share structural homology to the  $\alpha,\beta$ -hydrolase family. The lack of water in the binding cleft of the cyclase, which prevents hydrolysis, is the significant alteration from the hydrolase family that gives the cyclase thioesterase its ability to form cyclic peptides.

Occidiofungin is a broad spectrum nonribosomally synthesized cyclic antifungal peptide that has submicro/nanomolar activity and low toxicity.<sup>64,115,118-121</sup> ESI-MS and NMR data revealed the existence of four structural variants of the antifungal peptide occidiofungin produced by the soil bacterium *Burkholderia contaminans* MS14, having a mass [M + 1] of 1,200.39, 1216.41, 1234.17, and 1250.41 Da.<sup>118</sup> The mass differences correspond to the addition of oxygen to Asparagine (Asn1) forming  $\beta$ -hydroxyasparagine (BHN1) and/or addition of chlorine to  $\beta$ -hydroxytyrosine (BHY4) forming chlor-BHY4.<sup>118</sup> NMR data sets and amino acid analysis revealed that

occidiofungin is produced via a hybrid PK-NRPS system and that the antifungal compound is composed of eight amino acids (Figure 3.1). Using NRPS-PKS web-based software and interProScan software in EMBL-EBI, predicted epimerase domains were identified in the NRPS modules for BHY4, 2,4-diaminobutyric acid (DABA5), and Ser8.<sup>118</sup> The peptide is predicted to have L-Asn1(BHN1), L-Ser3, D-BHT4, D-DABA5, L-Asn7, and D-Ser8. An interesting feature in the biosynthetic pathway of occidiofungin is the presence of two putative thioesterases. One is present as an independently expressed thioesterase, OcfN, and the other is a C-terminal TE domain of OcfD. We set out to gain a better understanding of the role of the two putative thioesterases in the biosynthetic gene cluster of occidiofungin.

We have focused our study on the last step in the formation of the cyclic NRP occidiofungin.<sup>118</sup> Here we conclusively show that the biosynthesis utilizes two distinct cyclase thioesterases to expand the formation of conformers and that the evolutionary integration of an additional cyclase thioesterase improves its bioactivity against *Candida* species. Restrictions in the conformational freedom of a peptide may facilitate the interaction of the compound with its molecular target, but there is also an inherent evolutionary constraint using an enzymatic cyclization approach. Our results suggest that when the molecular target is associated with a broad spectrum of microorganisms, the constrained conformers of a cyclic peptide may not always provide the best activity against all organisms. Our study supports the need to investigate new stereoisomers of antimicrobial cyclic peptides in an effort to identify the most effective therapeutic

compound. In addition, our study provides further understanding of the function of cyclase thioesterases.

### 3.3 Materials and methods

#### 3.3.1 Materials

Occidiofungin produced by both the wild type strain MS14 and the *ocfN* mutant MS14GG88 were purified as previously described for the wild-type sample.<sup>119</sup> Chemicals were purchased from Sigma-Aldrich (St. Louis, MO) and were the highest grade, unless otherwise stated. Media were purchased from Fisher Scientific, enzymes were purchased from New England BioLabs (Ipswich, MA), and primers were purchased from Integrated DNA Technologies (Coralville, IA) unless otherwise stated. *Candida* strains used were purchased from the ATCC biological resource center and were a gift from Thomas Edlind (Drexel University College of Medicine).

#### 3.3.2 Site directed mutagenesis

A nonpolar mutation was constructed in the open reading frame of wild-type *ocfN* by the insertion of a kanamycin resistance gene, *nptII*.<sup>79</sup> To mutate *ocfN*, a 1-kb fragment containing *ocfN* was obtained by PCR using primers MofcNF (5'-CGCCACCCGTTACGAGGATTC) and MofcNR (5'-ACGCGTCCCCTCTTCCTACG). The 1-kb PCR product was cloned into the pGEM-T Easy Vector System I (Promega Corporation, Madison, WI) resulting in plasmid pGG30. The *nptII* gene was inserted into the cloned *ocfN* at SmaI, generating plasmid pGG31. The ~2-kb EcoRI fragment of pGG31 harboring the *ocfN* gene disrupted by insertion of *nptII* was cloned into pBR325<sup>81</sup> at the EcoRI site to generate pGG32. Mutagenesis of the *ocfN* gene was

conducted via a marker exchange procedure as described previously,<sup>122</sup> to generate the mutant MS14GG88. PCR analysis and sequencing were used to verify the double crossover mutants. Production and purification of the antifungal were done as previously described.<sup>119</sup>

### 3.3.3 NMR spectroscopy

A 2 mM sample of *ocfN* thioesterase mutant fraction of occidiofungin was prepared in DMSO-*d*<sub>6</sub> (Cambridge Isotopes) and data were collected as previously described for the wild-type fraction.<sup>118</sup> The NMR data were collected on a Bruker Advance DRX spectrometer, equipped with a CryoProbe, operating at 600 MHz. The <sup>1</sup>H NMR resonances were assigned according to standard methods<sup>123</sup> using COSY, TOCSY, NOESY and HSQC experiments. NMR data were collected at 25°C. The carrier frequency was centered on the residual water resonance (3.33 ppm), which were suppressed minimally using standard presaturation methods. A 2.0 s relaxation delay was used between scans. The TOCSY experiment was acquired with a 60 ms mixing time using the Bruker DIPSI-2 spinlock sequence. The NOESY experiment was acquired with 400 ms mixing time. The parameters for collecting the HSQC spectrum were optimized to observe aliphatic and aromatic CH groups. The sweep width for the TOCSY and NOESY experiments was 11.35 ppm in both dimensions. The sweep widths for the HSQC experiments were 11.35 ppm in the proton dimensions and 0 and 85 ppm for the carbon dimension. 2D data were collected with 2048 complex points in the acquisition dimension and 256 complex points for the indirect dimensions, except for the HSQC which was collected with 2048 and 128 complex points in the direct and indirect

dimension, respectively. Phase sensitive indirect detection for NOESY, TOCSY, and COSY experiments was achieved using the standard Bruker pulse sequences.  $^1\text{H}$  NMR chemical shifts were referenced to the residual water peak (3.33 ppm). Data were processed with nmrPipe<sup>124</sup> by first removing the residual water signal by deconvolution, multiplying the data in both dimensions by a squared sinebell function with 45 or 60 degree shifts (for the  $^1\text{H}$  NMR dimension of HSQC), zerofilling once, Fourier transformation, and baseline correction. Data were analyzed with the interactive computer program NMRView.<sup>125</sup> 1D NMR temperature titrations were collected on the wild type and mutant peptides, using a Bruker AVANCE III HD 600 MHz spectrometer equipped with a cryoprobe. Eight scans were collected in each 1D experiment, using 32K points, at 298 K. The experiments were repeated using higher temperatures for both samples in 5 degrees K increments, up to a temperature of 323 K. 2D TOCSY spectra were collected at 323 K, using a mixing time of 60 milliseconds. Eight scans and 256 indirect points were used for both the wild type and mutant peptides. The 2D spectra were processed using nmrPipe, with 45 degree sinebell squared shifts in both dimensions.

#### 3.3.4 Mass spectrometry

The wild-type occidiofungin and the *ocfN* mutant sample (10  $\mu\text{g}$ ) were evaporated to dryness in a Speed Vac Concentrator (ThermoScientific, San Jose, CA) and the residue was taken up in 50  $\mu\text{L}$  MeOH and analyzed by direct infusion at 3  $\mu\text{L}/\text{minutes}$  into an LCQ DecaXP (ThermoScientific, San Jose, CA). Data were acquired over a mass range of  $m/z$  200 to 2000.

Microdilution broth susceptibility testing was performed in triplicate according to the CLSI M27-A3 method in RPMI 1640 [buffered to a pH of 7.0 with MOPS (morpholinepropanesulfonic acid)] growth medium. 100X stock solutions of occidiofungin were prepared in DMSO. MIC endpoints for occidiofungin were determined by visual inspection and were based on the wells that had no visible growth (an optically clear well) after 24 hours of incubation. DMSO containing no antifungal agent was used as a negative control. Colony forming units (CFUs) were determined in triplicate by plating 100  $\mu$ L from the MIC wells onto a Yeast Peptone Dextrose (YPD) plate as well as plating 100  $\mu$ L from 10-fold serial dilutions of the cell suspension in Yeast Peptone Dextrose (YPD) Broth. Colony counts were performed and reported as CFUs/mL. Time-kill experiments were performed as previously reported.<sup>115</sup> *C. glabrata* (ATCC 66032) colonies on 24-h-old YPD plates were suspended in 9 mL of sterile H<sub>2</sub>O. The density was adjusted to a 0.5 McFarland standard and was diluted 10-fold with RPMI 1640 medium to a final volume of 10 mL containing a final concentration of 2, 1, 0.5 and 0  $\mu$ g/mL of occidiofungin from wild type strain MS14 and the *ocfN* mutant MS14GG88. The cultures were incubated at 35°C with agitation. Samples were drawn, serially diluted, and plated on YPD medium for colony counts.

### 3.4 Results

#### 3.4.1 Proportion of occidiofungin variants in the sample

The C-terminal TE domain of OcfD and the OcfN cyclase thioesterase in the occidiofungin biosynthetic gene cluster are both predicted to be involved in the termination of synthesis and formation of the cyclic peptide. Given that the *N*-terminal

of the linear peptide is an Asn or a BHN, we hypothesized that each thioesterase was required for cyclization of the Asn1 and BHN1 variants. The Asn1 and BHN1 variants of occidiofungin are not separable by RP-HPLC, thus, both variants are present in the purified fraction (Figure 3.2). The final RP-HPLC step in the purification process reveals the presence of three peaks. Occidiofungin samples elute as a double peak before the third peak. Occidiofungin derived from the wild type strain MS14 and the *ocfN* mutant MS14GG88 have the same chromatographic profile as observed in the last purification step. Occidiofungin peaks were confirmed by MALDI-TOF and bioassays. It is important to note that the presence of the doublet peak is not associated with the presence of Asn1 or BHN1. Each peak of the double peak contains both the Asn1 and BHN1 variants.

The relative proportion of the Asn1 and BHN1 variants could not be directly compared, because direct measurement of the Asn1 peak intensities could not be done due to the peaks overlapping with Asn7. The relative proportion of the Asn1 and BHN1 variants in the wild-type fraction was determined by measuring the  $^{13}\text{C}$  NMR HSQC Ha-Ca cross peak intensities of each BHY4 peak in the data set,<sup>126,127</sup> given that each of the BHY4 peaks could be attributed to either the Asn1 or BHN1 variant. Based on the Ha-Ca cross peak intensities for BHY4 in the HSQC spectrum, the Asn1 and BHN1 variants were determined to be approximately 36 and 64% of the total amount of occidiofungin, respectively (Figure 3.3). The peaks in red and green represent the BHY4 peaks associated with BHN1 and Asn1 variants, respectively. A similar ratio was also observed in the relative abundance of each peak in the ESI-MS spectrum (Figure 3.4A).

Furthermore, the HSQC Ha-Ca cross peak intensities for the BHN1 peaks were determined to be 90.50 and 38.65, which support the intensities measured for BHY4 peaks corresponding to the BHN1 conformational variants.

Mutagenesis of the *ocfN* gene was conducted via a marker exchange procedure as described previously,<sup>118</sup> to generate the mutant MS14GG88. The percentage of Asn1 to BHN1 variants in the *ocfN* mutant MS14GG88 fraction could be determined by measuring the proportion of each BHN1 variant using the HSQC data set and by the integration of the HN of Asn1 and BHN1 in the <sup>1</sup>H NMR spectra. Asn1 and BHN1 variants are approximately 20 and 80% of the total amount of occidiofungin, respectively. The ESI-MS spectrum also shows a lower relative abundance for the Asn1 variant (1200.39 Da) compared to the BHN1 variant (1216.41 Da) (Figure 3.4B).

#### 3.4.2 Comparison of wild-type and *ocfN* mutant NMR spectra

Occidiofungin has a complex spectrum for a peptide of only eight amino acids (Figure 3.5A, Table 3.1). The NMR spectrum represents an average of the conformers on the NMR time scale. Conformers in slow exchange on the NMR time scale may result in multiple spin systems for each amino acid. In some situations, multiple conformers are known to arise for cyclic peptides due to slow interconverting conformational families.<sup>128,129</sup> Despite the conformational restrictions brought about by the cyclization, occidiofungin still has a significant amount of conformational freedom. Both Asn1 and BHN1 variants are visibly present in the wild-type fraction, which are colored red in Figure 3.5A. The TOCSY fingerprint region (NH correlations) is not as complex for the *ocfN* thioesterase MS14GG88 mutant spectra (Figure 3.5B). A



significant number of spin systems found in the wild-type spectra are absent in the *ocfN* thioesterase mutant spectra. Our experiments show that the TE domain on the C-terminal region of OcfD is able to perform the peptide macrocyclization of both the Asn1 and BHN1 variants, although there is only one amide spin system for Asn1 produced by OcfD. The loss of OcfN results in the disappearance of the other three Asn1 amide spin systems.

An overlay of the wild-type and *ocfN* mutant NMR spectra shows the amino acid spin systems in green that are absent in the mutant spectra (Figure 3.5C). These spin systems are for Asn7, Ser8, Asn1, Novel Amino Acid 2 (NAA2), Ser3, BHY4, and Gly6. The loss of these spin systems suggests that the complex spin system observed for the wild-type occidiofungin fraction is not only due to interconverting conformational families, but is the result of distinct diastereomers formed by the regiospecific activity of the OcfN cyclase and OcfD TE domain. Dramatic chemical shifts observed, such as the 2 ppm shift for HN of the NAA2, supports the formation of a structurally unique conformer of occidiofungin. A unique conformer is further supported by the subsequent loss of an NAA2 spin system in the NMR spectra of the *ocfN* mutant. Furthermore, the presence of both Asn1 and BHN1 spin systems in the mutant spectra along with the absence of the amide spin systems shown in green indicate that the additional spin systems are not due to the presence of the  $\beta$ -hydroxy group on Asn1. The additional spin systems are due to the formation of a unique diastereomer produced by OcfN cyclase thioesterase. To further test for the formation of a configurational isomer versus an interchangeable conformer, 1D NMR temperature titrations were performed. Amide

and aromatic regions revealed little change in the complexity of peaks present with the occidiofungin derived from *ocfN* mutant MS14GG88 or wild-type strain MS14 (Figure 3.6). Given that NAA2 spin systems are a good indicator for the presence of both diastereomers in the wild-type spectrum, we collected TOCSY spectra for occidiofungin derived from *ocfN* mutant MS14GG88 or wild-type strain at 50°C (Figure 3.7). There was no loss or addition of a spin system for NAA2 in the mutant spectrum. Furthermore, both spin systems for NAA2 remained in the wild-type spectrum. This data supports that the stereoisomers are non-interchangeable isomers, supporting their classification as diastereomers rather than conformers.

#### *3.4.3 Model for the coordinated function of two cyclase thioesterases*

There was no loss of an amide spin system for a BHN1 in the *ocfN* mutant NMR spectra. This suggests that *OcfN* thioesterase has a substrate requirement for the peptide containing Asn1, since there is no concomitant loss of a BHN1 spin system with the observed loss of the Asn1 spin systems. The C-terminal TE domain of *OcfD* has a preference for the peptide containing the BHN1, but is capable, albeit at a lower efficiency of cyclizing the Asn1 variant. This provides an interesting scenario for the activity of the two thioesterases (Figure 3.8). Both thioesterases contain the GX SXG motif, which is important for the catalytic transfer of the peptide from the T domain to the cyclase.<sup>130</sup> This suggests that substrate recognition occurs prior to the catalytic transfer of the peptide to the cyclase. Presumably, *OcfN* cyclase has a higher affinity or better access for the Asn1 peptide product given that the proportion of the Asn1 cyclic peptide produced by *OcfD* compared to the BHN1 product is reduced in the wild-type

fraction. Therefore the biosynthesis of occidiofungin utilizes the structural differences between Asn and BHN to increase the conformational biodiversity of occidiofungin. The increase in conformational diversity is accomplished by the regiospecific activity of each cyclase, presumably by differences in their binding clefts that helps orientate the peptide before cyclization.

#### 3.4.4 Comparison of the bioactivity of the wild-type and *ocfN* mutant product

To determine whether the increase in conformational diversity is important for bioactivity, minimum inhibitory concentrations were determined against medically relevant *Candida* species (Figure 3.9A). There was a 2-fold decrease in the MIC with the purified *ocfN* mutant product with respect to the wild-type product against *Candida albicans* LL, *C. albicans* TE, *C. glabrata* ATCC66032, *C. parapsilosis* ATCC90018, and *C. tropicalis* ATCC66029. There was no difference in the MIC for *C. albicans* ATCC66027. Colony forming units (CFUs/mL) were determined for the MIC wells of wild-type product for each *Candida* species and compared to the corresponding well containing the same concentration of the *ocfN* mutant product (Figure 3.9B). Following exposure to the same concentration of wild-type and *ocfN* mutant products, these results show a 5 to 7-log decrease in cell density of the *Candida* species treated with wild-type product. The differences in activity are also visualized by the rate of cell death. Time-kill experiments were performed against *C. glabrata* ATCC66032. There was a 10-fold difference in yeast present at 4 and 8 hours when cells were treated with 0.5  $\mu\text{g/mL}$  of occidiofungin derived from *ocfN* mutant MS14GG88 or wild-type strain (Figure 3.7). Furthermore, a slower rate of cell death was also observed for yeast treated with

occidiofungin derived from *ocfN* mutant MS14GG88 at 1.0 and 2.0  $\mu\text{g/mL}$ . Given that the cyclic occidiofungin variants produced by *OcfN* constitute less than half of the total structural variants, a 2-fold loss in activity suggests that the diastereomers synthesized by *OcfN* are 4-fold more active than the isomer produced by *OcfD* against five of the *Candida* species tested. Another possible explanation for the observed differences in activity could be attributed to possible synergism between the diastereomers produced by each cyclase thioesterase. Furthermore, the antifungal activity of the *ocfN* mutant (MS14GG88:  $8.79 \pm 0.38$  mm) was also significantly reduced ( $P < 0.05$ ) compared to wild-type activity (inhibitory zone radius  $\pm$  SEM:  $13.00 \pm 0.58$  mm) in an overlay assay against *Geotrichum candidum* (Figure 3.10).

### 3.5 Discussion

The findings from this study include experiments showing the following: the relative proportion of the Asn1 and BHN1 variants in the purified fraction; distinct differences in spin systems for the wild-type and *ocfN* mutant products; a proposed model for the coordinated function of two cyclase thioesterases; and demonstrated differences in biological activity of wild-type and *ocfN* mutant products against therapeutically relevant *Candida* species. Expanding the conformational repertoire of cyclic peptide natural products can be beneficial to microorganisms. These data suggest that the bacterium *Burkholderia contaminans* MS14 is benefited by maintaining two distinct cyclase thioesterases that improves the spectrum of activity of occidiofungin.

Our data support the observation that cyclase thioesterase substrate recognition occurs prior to the catalytic transfer of the peptide. The presence or absence of a hydroxy

group on the  $\beta$ -carbon of the *N*-terminal amino acid (Asn1) appears to be important for the substrate recognition by the two cyclase thioesterases. It has also been shown that the *N*-terminal amino acid is important for substrate recognition for other thioesterases.<sup>101,105</sup> It is possible that the presence of the hydroxy group promotes a hydrogen bond with the *ocfD* cyclase thioesterase domain or more likely promotes an interaction within the T domain of the NRPS. Different bound orientations of the peptide to the T domain would establish a basis for the coordinated function of two cyclase thioesterases.

The presence of the hydroxy group on the  $\beta$ -carbon and the bound orientation of the peptide to the T domain may prevent the interaction of the OcfN cyclase, while enabling the continued substrate recognition by the OcfD TE domain. Conformational diversity of the T domain has been shown to be important for the directed movement of the peptide substrate bound to the ppan cofactor and its interaction with externally acting enzymes.<sup>100</sup> More specifically, the active site serine of the cyclase thioesterase needs to attack the linear peptide attached by a thioester linkage to the ppan forming an acyl-O-TE intermediate. The position of the peptide bound to the ppan in the T domain will be important for bringing the peptide substrate in proximity of the appropriate cyclase thioesterase.

Furthermore, some cyclase thioesterases are capable of transacylation of the peptide to the active site serine, when the peptide is bound to a biomimetic prosthetic group.<sup>101,112</sup> However, there are several cyclase thioesterases that will not function when the product is bound to a biomimetic group. These data suggest that the interaction of the

peptide with the T domain is important for the enzymatic activity of some thioesterases and this interaction cannot be mimicked using a prosthetic group. It is conceivable that the coordinated function of the two cyclase thioesterases, involved in the synthesis of occidiofungin, utilize differences in the interaction of the ppan bound peptide within the T domain.

Presumably, *ocfN* was integrated into the occidiofungin biosynthetic gene cluster to improve its spectrum of activity against fungi. Given the broad spectrum of antifungal activity associated with occidiofungin, the molecular target is likely to be highly conserved. However, there must be some variation among fungal species to account for the differences in biological activity. Increasing the conformational repertoire must be a selective advantage to the bacterium for it to maintain the two functional cyclase thioesterases. The microbial environment is considerably different than how we intend to apply the natural products produced by microorganisms. For instance, the bacterium *Streptomyces roseosporus* is a soil saprotroph responsible for the production of daptomycin.<sup>131,132</sup> The microbial community that this bacterium encounters is far more diverse than the group of bacteria that cause human infection. Thus, evolutionary pressures that selected for the current conformers of daptomycin may not necessarily be the best conformers for treating a *Staphylococcus aureus* infection. It is very likely that the therapeutic application of daptomycin or other cyclic peptide drugs could be improved by engineering novel conformational or configurational isomers.

### 3.6 Conclusion

Creating novel diastereomers of other cyclic peptide drugs using new or engineered cyclase thioesterases may lead to improvements in their therapeutic activity against clinically relevant pathogens. This is true for occidiofungin produced by the bacterium *Burkholderia contaminans* MS14, which accomplishes this goal by the evolutionary integration of an additional cyclase thioesterase into the occidiofungin biosynthetic gene cluster. These sections conclude our analysis of naturally occurring variants of occidiofungin. In addition to better understanding the biosynthetic machinery involved in the production of occidiofungin, these studies expanded our understanding of the variants themselves. The information obtained will be utilized in future endeavors involving clinical development of occidiofungin.

Following this, we will focus on reporting the studies performed on determining the mechanism by which occidiofungin causes death in fungal cells and analyzing the specific molecular target to which occidiofungin binds, in order to achieve cell death.

**Table 3.1: Chemical Shift Values for Occidiofungin Derived from the *ocfN* Mutant MS14GG88<sup>a</sup>**

Unit	No.	$\delta_C$	$\delta_H$ ( $J_{HNH\alpha}$ in Hz)
Asn1	2	52.71, CH	4.59
	2-NH		7.75 (12.1)
	3	39.91, CH2	2.62, 2.41
	4 4-NH2	-	7.39, 6.93
BHN1	2	58.47, CH	4.66, 4.61
	2-NH		7.81, 7.9
	3	75.01, C	(8.1, 12.1)
	3-OH		3.98, 4.02
	4 4-NH2	-	4.66 7.24
NAA2	2	43.88, CH2	2.34, 2.36
	3	47.25, CH	4.23
	3-NH		7.31, 7.34
	4	41.57, CH2	(8.4, 11.4)
	5	66.36, CH	1.39, 1.76
	6	76.07, CH	3.50
	7	79.61, CH	3.08
	8	33.19, CH2	3.72
	9-17	25.14-28.02, CH2	1.54
	18	16.94, CH3	1.27 0.86
Ser3	2	58.59, CH	4.07, 4.15
	2-NH		8.11, 8.14
	3 3-OH	70.23, 64.29	(11.2, 8.0) 3.49, 3.45 4.95
BHY4	2	58.71, CH	4.06, 4.15
	2-NH		7.83, 7.94
	3	73.75, CH	(8.7, 11.7)
	3-OH		4.98, 5.08
	4	-	5.66, 5.73
	5,6	-	
	8,9	-	7.15 6.67



**Table 3.1(continued): Chemical Shift Values for Occidiofungin Derived from the *ocfN* Mutant MS14GG88<sup>a</sup>**

Unit	No.	$\delta_C$	$\delta_H$ ( $J_{HNH\alpha}$ in Hz)
DABA5	2	53.49, CH	4.43
	2-NH2		7.66 (8.5)
	3		1.88, 2.11
	4		2.92
Gly6	4, NH	39.17, CH2	7.71
	2	44.76, CH2	3.87, 3.58,
	2-NH		3.84, 3.70
			7.68, 7.85
Asn7	2	53.25, CH	4.51, 4.58
	2-NH		8.35, 8.41
	3		(9.3, 8.7)
	4		2.61, 2.38
Ser8	4-NH2	-	7.39, 6.93
	2	58.11, CH	4.33, 4.32
	2-NH		7.76, 7.78
	3		(8.2, 12.00)
3-OH	3.61, 3.62		
		64.59	4.79

<sup>a</sup> Proton chemical shift values are from a TOCSY and NOESY experiments. <sup>13</sup>C values are from the HSQC experiment.

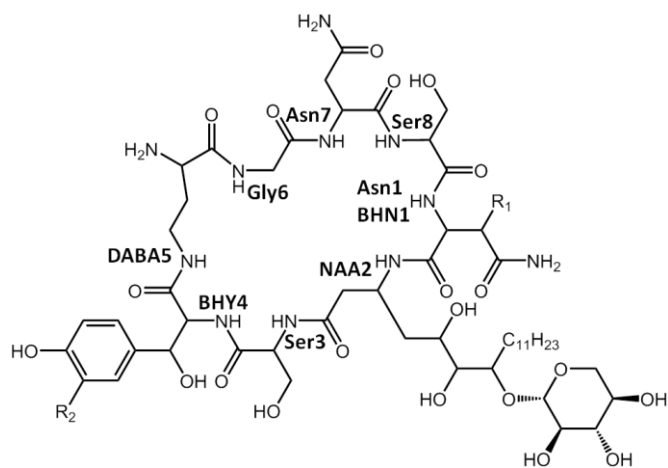


**Figure 3.1:** Covalent structure of occidiofungin. (R<sub>1</sub> = H or OH; R<sub>2</sub> = H or Cl)

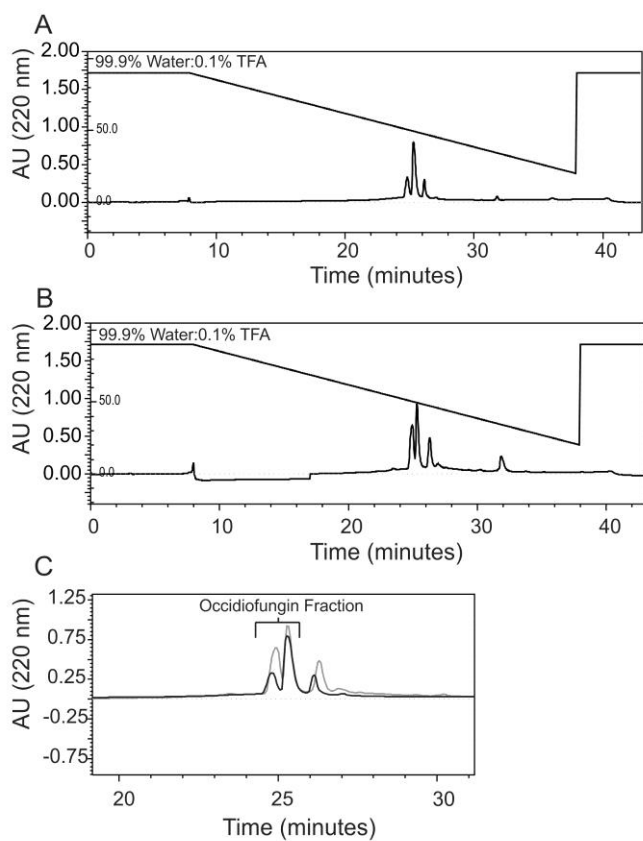


**Figure 3.2: RP-HPLC Chromatograms.** A. Chromatogram of the final purification step of the wild-type occidiofungin fraction at 220 nm using a 4.6 x 250 mm C<sub>18</sub> column. B. Chromatogram of the final purification step of *ocfN* mutant occidiofungin fraction at 220 nm using a 4.6 x 250 mm C<sub>18</sub> column. C. Overlay of the wild-type (black) and the mutant (grey) fractions of occidiofungin.

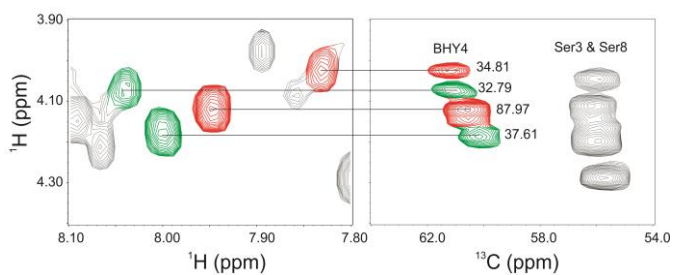


**Figure 3.3:** TOCSY (left panel) and HSQC (right panel) spectra of BHY4 in the wild-type sample. The proportions of Asn1 and BHN1 variants were determined by the measurement of the Ha-Ca cross peak intensities of BHY4 in the HSQC spectra. These values are listed next to their corresponding peaks in the right panel. The peaks in red and green represent the BHY4 peaks associated with BHN1 and Asn1 variants, respectively. Based on the calculation of their relative proportions, i.e.  $(34.81 + 87.97)$  for the BHY4 peaks found in the BHN1 conformational variants) and  $(32.79 + 37.61)$  for the BHY4 peaks found in the Asn1 conformational variants), the approximate proportion of the Asn1 variants could be calculated as  $(32.79 + 37.61)/(34.81 + 87.97) + (32.79 + 37.61)$ .

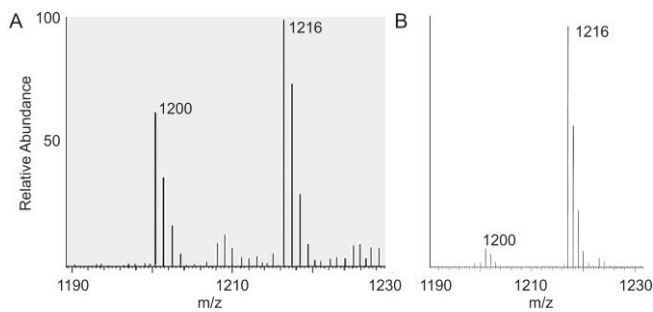


**Figure 3.4:** ESI mass spectrometry. A. ESI-MS data of purified wild-type occidiofungin fraction. B. ESI-MS data of purified *ocfN* mutant occidiofungin fraction.

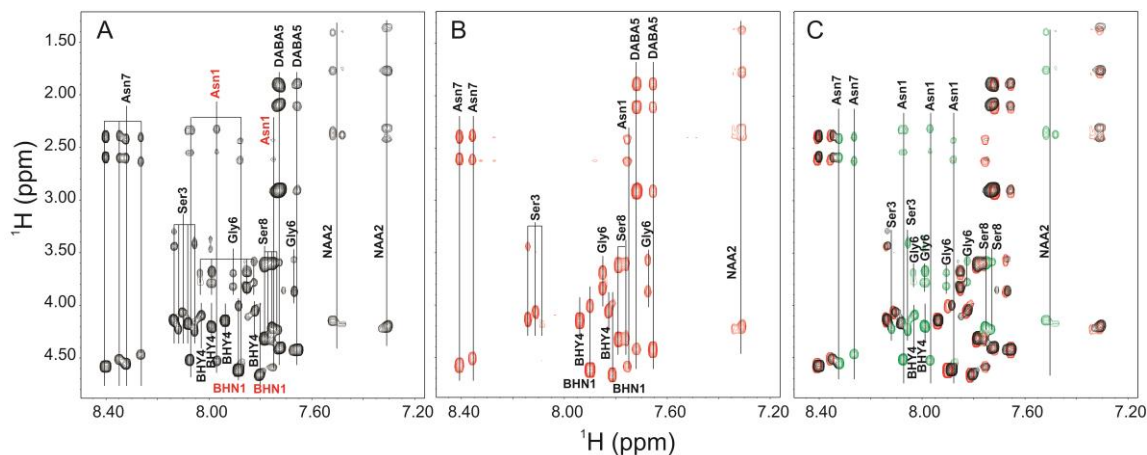


**Figure 3.5:** TOCSY fingerprint region (NH correlations). A. NH correlations in the wild-type sample. The two BHN1 and four Asn1 spin systems present in the wild-type sample are colored red. B. NH correlations in the *ocfN* mutant sample. C. Overlay of the NH correlations found in the wild-type and *ocfN* mutant samples. NH correlations that are not present in the *ocfN* mutant sample are colored green.

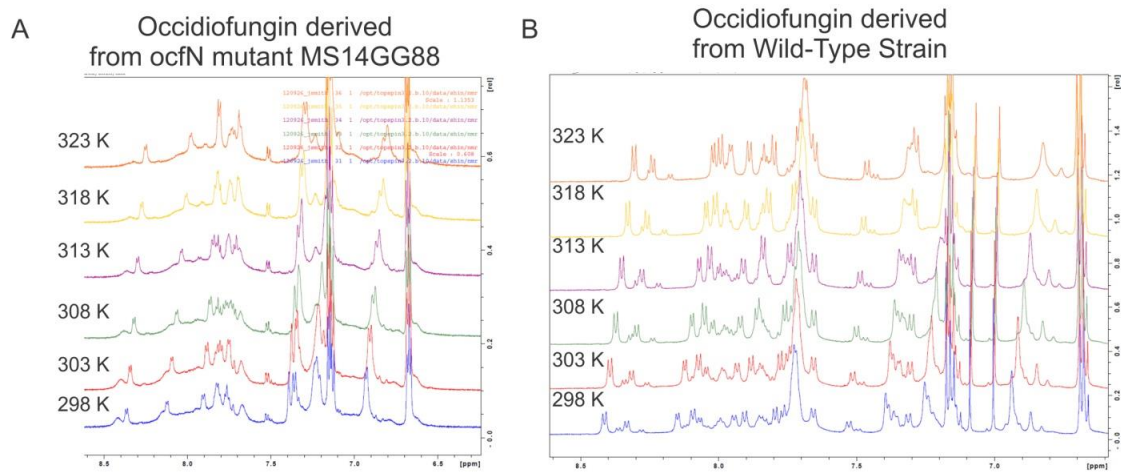


**Figure 3.6:** One-dimensional NMR temperature titration curves for occidiofungin derived from ocfN mutant MS14GG8 and wild-type strain MS14.

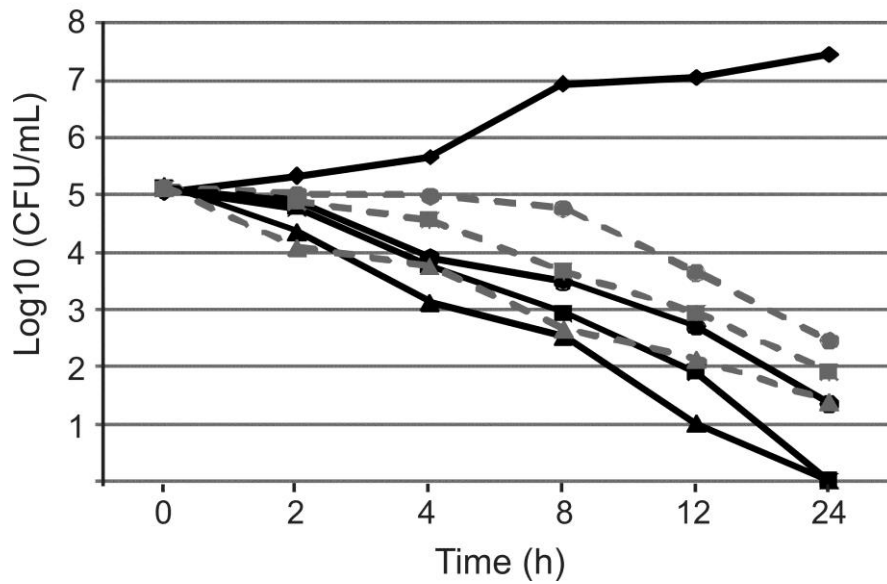


**Figure 3.7:** Time-kill experiments performed against *Candida glabrata* ATCC66032. Solid black lines and dashed grey lines correspond to samples treated with occidiofungin derived from wild-type strain MS14 and *ocfN* mutant MS14GG88, respectively. Circles, squares, and triangles represent samples treated with 0.5, 1.0, and 2.0  $\mu\text{g}/\text{mL}$  of occidiofungin, respectively. The diamonds represent the sample treated with the blank control.

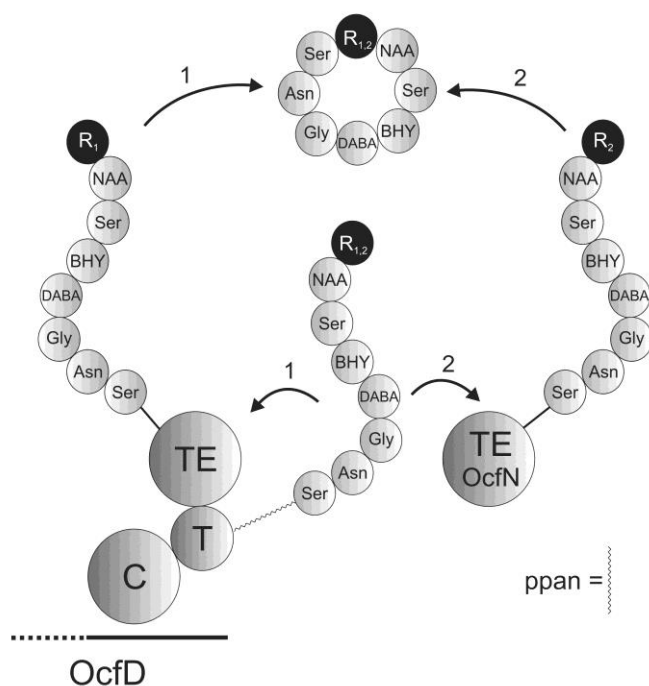


**Figure 3.8:** Schematic of occidiofungin ring closure. The completely synthesized eight amino acid linear peptide is bound by a 4-phosphopantetheine cofactor (ppan) linker to the thiolation (T) domain. The peptide varies by the presence or absence of a hydroxy group on the  $\beta$ -carbon of Asn1. The TE domain of OcfD is capable of forming the cyclic peptide of both variants in the absence of a functional OcfN cyclase thioesterase. However, it is not as efficient at producing the Asn1 cyclic peptide variant as OcfN. In the presence of a functional OcfN cyclase thioesterase, novel diastereomers of occidiofungin are formed by the selective ring closure of the Asn1 cyclic peptide. R<sub>1</sub> and R<sub>2</sub> are BHN1 and Asn1, respectively.



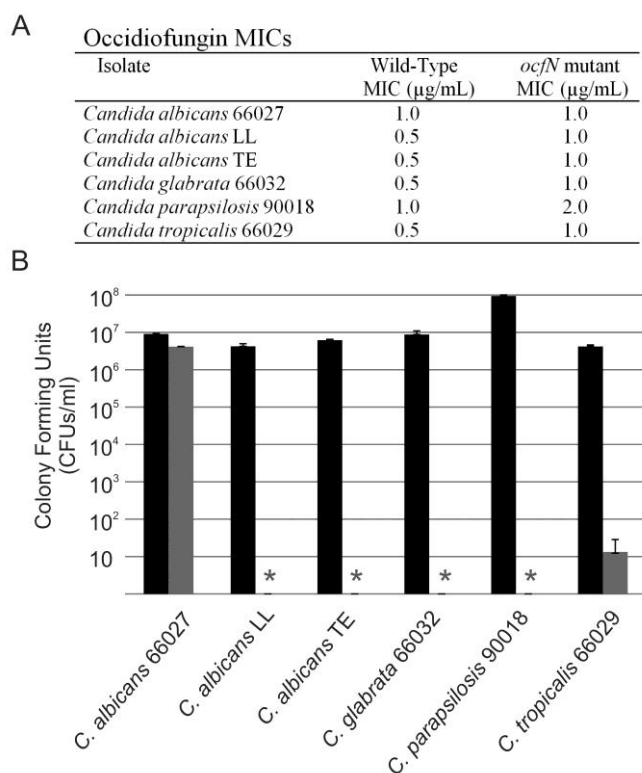


**Figure 3.9:** Comparison of the bioactivity from the wild-type and *ocfN* mutant occidiofungin fractions. A. MICs of wild-type and *ocfN* mutant fraction determined by CLSI M27-A3 method in RPMI 1640. B. Comparison of the CFUs in the MIC wells of wild-type fraction to the corresponding well having the same concentration of the *ocfN* mutant occidiofungin fraction. Asterisks represent no detectable colonies in the MIC wells of the wild-type occidiofungin fraction. Black and grey bars are *ocfN* mutant and wild-type fractions, respectively. Standard deviations for the CFU measurements are presented.

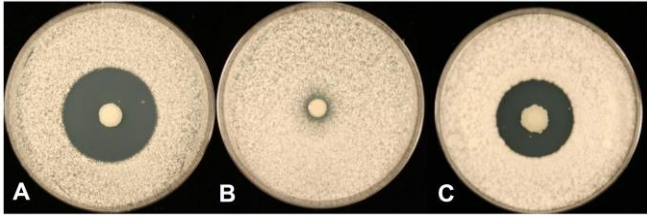


**Figure 3.10:** Potato dextrose agar plates were inoculated with each of the strains and incubated for 3 days at 28°C. The plates were oversprayed with the indicator fungus *Geotrichum candidum* and incubated overnight. A: The wild-type strain MS14; B: Negative control MS14GG78 (*ocfJ::nptII*); C: MS14GG88 (*ocfN::nptII*).

## 4. THE ANTIFUNGAL OCCIDIOFUNGIN TRIGGERS AN APOPTOTIC MECHANISM OF CELL DEATH IN YEAST\*

### 4.1 Overview

Occidiofungin is a non-ribosomally synthesized cyclic peptide having a base mass of 1200 Da. It is naturally produced by the soil bacterium *Burkholderia contaminans* MS14 and possesses potent broad-spectrum antifungal properties. The mechanism of action of occidiofungin is unknown. Viability, terminal deoxynucleotidyl transferase dUTP nick end labeling (TUNEL), reactive oxygen species (ROS) detection, membrane and cell wall stability, and membrane mimetic assays were used to characterize the effect of occidiofungin on yeast cells. Confocal and electron microscopy experiments were used to visualize morphological changes within treated cells. TUNEL and ROS detection assays revealed an increase in fluorescence with increasing concentrations of the antifungal. Yeast cells appeared to shrink in size and showed the presence of ‘dancing bodies’ at low drug concentrations (1µg/ml). A screen carried out on *Saccharomyces cerevisiae* gene deletion mutants in the apoptotic and autophagy pathways identified the apoptotic gene for YCA1, as having an important role in occidiofungin response as cells deleted for this gene exhibit a 2-fold increase in resistance. Autophagy mutants had no difference in sensitivity compared to the wild-

---

\*Reproduced with permission from ‘The antifungal occidiofungin triggers an apoptotic mechanism of cell death in yeast’ by Akshaya Ravichandran, Dayna Emrick, Jivendra Gosai, Shi-En Lu, Donna Gordon, Leif Smith. *Journal of Natural Products* **76**, 829-838. Copyright (2013) American Chemical Society. DOI: 10.1021/np300678e

type control. Results from our experiments demonstrate that the mechanism of action for occidiofungin in yeast is different from that of the common classes of antifungals used in the clinic, such as azoles, polyenes, and echinocandins. Our study also indicates that occidiofungin causes cell death in yeast through an apoptotic mechanism of action.

## **4.2 Introduction**

Discovery and implementation of novel antifungal agents are needed for more effective treatment of serious fungal infections.<sup>133</sup> Antifungals currently used in the clinic do not meet the growing needs of an increasing population of immunocompromised patients due to limitations in their spectra of activity and toxicities. Some current antifungal treatments lead to abnormal liver function test and are primarily fungistatic. Discovery of novel antifungals with a broader spectrum of activity and lower toxicity are needed. There is a significant demand for new antifungals given the prevalence of resistant fungal pathogens to conventional therapies.<sup>134,135</sup> Furthermore, identifying novel antifungals with a different mechanism of action from the current class of therapeutically used antifungals may aid in the development of new and more effective treatments.

There are three major therapeutic groups of antifungal agents used for the treatment of serious fungal infections: polyenes, azoles, and the echinocandins. The first two groups primarily target ergosterol biosynthesis or bind to ergosterol, disrupting the fungal membrane.<sup>136-138</sup> Ergosterol, much like cholesterol found in mammalian cells, is important for maintaining proper cell permeability and fluidity. These antifungals lead to an osmotic disruption of the cell membrane, leading to an efflux of essential cellular

contents resulting in cell death. Echinocandins, the third group, are the newest fungal treatment option that has fairly recently (in 2003) entered the clinic. The echinocandins are synthetically modified lipopeptides that originate from natural compounds produced by fungi and function to selectively inhibit  $\beta$ -1,3-glucan biosynthesis.<sup>139,140</sup> In fungi, covalently cross-linked polysaccharides such as  $\beta$ -1,3-glucan,  $\beta$ -1,6-glucan, and chitin form the primary scaffold that is responsible for the structural integrity and shape of the cell.<sup>141-143</sup> As non-competitive inhibitors of  $\beta$ -1,3-glucan synthase, echinocandins reduce  $\beta$ -1,3-glucan levels leading to loss of fungal cell wall integrity and osmotic disruption of the fungal cells.<sup>144-148</sup> Echinocandins are primarily used to treat *Aspergillus* spp. and *Candida* spp. infections. They are fungistatic against *Aspergillus* spp. and only moderately fungicidal against *Candida* spp.<sup>139,149-152</sup> Infections are often refractory to treatment with echinocandins due to their mechanism of action resulting in their use against a limited spectrum of fungi.<sup>153,154</sup>

Induction of apoptosis in fungal cells is an area that holds an immense opportunity for the development of new antifungals, because factors that are involved in the induction of apoptosis in yeast are different from those found in mammalian cells.<sup>155,156</sup> These differences afford an opportunity to selectively target fungal cells, while minimizing the toxicological impact the antifungal has on a patient. Cellular changes typical of mammalian cell apoptosis, such as accumulation of reactive oxygen species (ROS), fragmentation and degradation of DNA, and externalization of phosphatidylserine, occur in fungal cells.<sup>157</sup> Reports have shown that amphotericin B, a polyene antifungal drug, is capable of inducing apoptosis in fungal cells.<sup>158-160</sup> This

apoptotic response appears to occur within a narrow concentration of amphotericin B,<sup>159</sup> while a large portion of the fungal cells die from an expected necrotic mechanism attributed to its binding to ergosterol. Papiliocin, an antifungal first identified from a swallowtail butterfly, is also reported to induce apoptosis in fungal cells.<sup>161</sup> Papiliocin is believed to function in the same manner as other cationic amphipathic peptides, causing membrane disruption and leakage of cytoplasmic constituents. The peptide also has antibacterial activities associated with its broad-spectrum membrane disruptive function. Presumably, amphotericin B also contributes to a nonspecific disruption of membrane function, which triggers an apoptotic mechanism of cell death in a subset of cells.<sup>162</sup>

Occidiofungin is a cyclic glyco-lipopeptide and its complete chemical composition has been determined.<sup>64,118</sup> Its base molecular weight is 1200 Da (Figure 3.1). Occidiofungin has been demonstrated to have a broad spectrum of antifungal activity.<sup>64,115</sup> Minimum inhibitory concentrations (MICs) of occidiofungin against *Candida* species are between 0.5 and 2.0 µg/mL, which is similar in activity to echinocandins and amphotericin B.<sup>115</sup> Pharmacodynamic experiments revealed that occidiofungin's fungicidal activity against *Candida albicans* is more rapid than the fungicidal activity reported for the echinocandin caspofungin. Occidiofungin exhibited potent antifungal activity when *Candida albicans* was exposed to the antifungal for as little as one hour, suggesting that occidiofungin has a strong interaction with a cellular target.<sup>115</sup> A mouse toxicity study showed that doses higher than those commonly used to treat fungal infections did not result in mortality.<sup>163</sup> A dose as high as 20 mg/kg, resulted in no negative gross or microscopic findings in the liver or kidneys. Hematology and

serum biochemistry tests also revealed that occidiofungin does not significantly alter organ function.

Considering that the mechanism action of occidiofungin is unknown, the aim of this study was to determine the cause of fungal death following exposure to occidiofungin. We found that exposure to sublethal doses of occidiofungin leads to morphological anomalies and that exposure to lethal concentrations results in an increase in ROS, cell shrinkage, and DNA fragmentation. Overall, our study supports an apoptotic mechanism of cell death for yeast exposed to occidiofungin, which might be triggered by membrane perturbation.

### **4.3 Materials and methods**

#### *4.3.1 Antifungal preparation*

Isolation of the antifungal compound was accomplished as previously reported.<sup>119</sup> In brief, *Burkholderia contaminans* MS14 was incubated at 28°C for 7 days without shaking. The cell free culture extract was precipitated using ammonium sulfate (50% w/v) on ice for 2 hours. The pellet was resuspended in 1 ml of 35% acetonitrile (ACN):water (v/v) and placed in a 1.5 mL microcentrifuge tube. RP-HPLC was done using a 4.6 × 250 mm C18 column (Grace-Vydac, catalog 201TP54) on a Bio-Rad BioLogic F10 Duo Flow with Quad Tec UV-Vis Detector system with a 30 minute gradient from 10 to 90% (ACN):water (v/v). Purified occidiofungin elutes as a doublet peak around 45% (Figure 4.1).

#### 4.3.2 Strains, media, and plasmids

*C. albicans* (ATCC 66027), *C. glabrata* (ATCC 66032), and *S. cerevisiae* (BY4741) strains were used for all experiments described. All strains were maintained on Sabouraud dextrose (SD), yeast peptone dextrose (YPD), or synthetic selective media (-leucine) with 2% agar added for solid media. *Candida* spp. were also grown in RPMI-1640 with MOPS media where indicated. To express the human Bcl2 gene in yeast, primers were designed to amplify the Bcl2 coding sequence by PCR using pDNR-Dual-Bcl2 plasmid as the template (PMID 16512675)<sup>164</sup>. Standard molecular techniques were used to clone the resulting DNA fragment into the *LEU2*-marked pRS415 plasmid downstream of the constitutive *GAPDH* promoter and in frame with a C-terminal HA<sub>3</sub> (three haemagglutinin) epitope tag. All constructs were confirmed by sequencing before use.

#### 4.3.3 In vitro susceptibility testing

Minimal Inhibitory Concentrations (MICs) were determined using Clinical Laboratory Standards Institute (CLSI) method M27-A3. Prior to susceptibility testing, yeasts were subcultured and grown for 24 hours on fresh SD, YPD, or -leucine media. MIC endpoints were reported based on consistency in sensitivity differences from wild-type *S. cerevisiae* BY4741 after 24 and 48 hours of incubation. Susceptibility testing was done in experimental triplicate of technical duplicates. Dimethyl sulfoxide (DMSO) was used as a negative control. The strains on which the MICs were performed included haploid mutants of wild type *S. cerevisiae* BY4741 obtained from the yeast deletion



collection in which the entire open reading frame of each gene was deleted (Thermo Scientific).

Colony forming units (CFUs) were determined in duplicate by plating 100  $\mu$ L from the MIC wells following the 48 hour exposure to occidiofungin onto a YPD plate. In addition, 100  $\mu$ L from two-fold serial dilutions of the cell suspension in YPD broth were plated to aid in determining the CFUs. Deletion mutants (*apg7*, *aif1*, *csg2*, *hos3*, *nde1*, *nma1*, *nuc1*, *rny1*, *rpd3*, *vtc2*, *vtc3*, and *yca1*) that had more than a 10-fold increase or decrease in CFUs were tested by a yeast drop assay. For the drop assay, yeasts were taken from a 24 hour YPD plate and resuspended in 5 mL of YPD to an OD<sub>530</sub> of 0.095 (density of a 0.5 McFarland standard). The suspension was divided into two samples of 0.8 mL each and occidiofungin was added to one sample at 0.5 $\mu$ g/mL, which is equivalent to 0.5X MIC for this cell density. After 4hrs at 30 °C, 200  $\mu$ L aliquots were placed onto a 96-well microtiter plate and the cells were five-fold serially diluted seven times using YPD as the diluent. Then, 2  $\mu$ L from each well was spotted to YPD plates in duplicate. Photos were taken after a 72 hour incubation at 30 °C. Drop assays were carried out in duplicate.

In the sorbitol protection assay, MIC values were determined using *Candida glabrata* 66032 using the *in vitro* susceptibility assay described above except that 0.8M sorbitol was included in the suspension media. Assays were performed in duplicate and MICs were read 24 hours following incubation at 35 °C.

MIC measurements in the presence of ergosterol were performed using *C. glabrata* 66032. 1,2-Dioleoyl-sn-glycero-3-phosphocholine (DOPC) was purchased from Avanti

Polar Lipids (Alabaster, AL) and ergosterol was purchased from Sigma-Aldrich (St. Louis, MO). Vesicles were prepared using a standard sonication procedure provided by Avanti Polar Lipids in which 20 mg of DOPC with and without 2 mg of ergosterol was dissolved in 1mL of chloroform. The lipid-chloroform solution was placed in a 250 mL flask attached to a vacuum line at room temperature and dried to remove the chloroform. The dry lipid film was hydrated in 1.0 mL of RPMI 1640 media. The suspension was added to the microtiter wells yielding a final concentration of ~80 µg/mL of ergosterol. Each microtiter well contained a series of occidiofungin concentrations as described above for the *in vitro* susceptibility assay. Amphotericin B was used as a positive control, while DOPC vesicles containing no ergosterol were used as a negative control. The MICs were determined after 24 hours of incubation at 35°C.

#### *4.3.4 Monitoring cell-cycle progression*

Samples of *Candida* spp. were treated with 0, 0.5, 1, and 2 µg/ml occidiofungin over a 2.5 hour period with aliquots removed at 30 minute intervals for analysis. All cells were fixed with the addition of formaldehyde to 3.7% final and stored at 4 °C until analyzed. Cells were viewed by phase contrast microscopy (100X objective) and multiple random images were captured using a Retiga EXi Black and White CCD Camera and Image Q software. A minimum of 250 cells per time point per treatment were scored for cell cycle distribution using bud size as a marker for position within the cell cycle.

#### 4.3.5 Protein extracts and Western blot analysis

*C. albicans* (ATCC 66027) and *C. glabrata* (ATCC 66032) strains were grown in YPD at 35 °C until reaching an OD<sub>600</sub> of 0.5. The cultures were split and occidiofungin added to achieve a 2-fold series of concentrations ranging from 4 to 0.062 µg/mL. Samples were returned to 35 °C with shaking for 10 or 20 minutes. For each sample, an equivalent number of cells were isolated by centrifugation, and the resulting cell pellets stored at -20 °C. Total cellular protein was isolated by alkaline lysis,<sup>165</sup> separated by SDS polyacrylamide gel electrophoresis (PAGE), and transferred to nitrocellulose for Western blot analysis. Activation of the cell wall integrity pathway was determined using phospho-specific antibodies against p44/42 MAP kinase (Cell Signaling Technology) shown to cross react with the doubly phosphorylated form of Mkc1p from *Candida* spp.<sup>166,167</sup> Weak cross recognition of the phosphorylated form of Cek1p was also detected under some experimental conditions. Total Mkc1p was detected using anti-p44/42 antibodies (Cell Signaling Technology). A monoclonal antibody to 3-phosphoglycerate kinase (Pgk1p) was used as a loading control (Molecular Probes). Activation of Hog1p was achieved by growing cells in the presence of 1M NaCl for the time periods indicated and monitored using phospho-specific antibodies against p38 MAP kinase (Cell Signaling Technology). Autoradiographs were scanned and images analyzed using NIH Image J software. The ratio of phosphorylated Mkc1p to total Mkc1p was calculated using the intensity of each protein band taken from the same autoradiograph with the value of untreated or DMSO treated samples normalized to one.

For *S. cerevisiae* expressing plasmid-borne human Bcl2, cells were grown in -leucine synthetic media at 30 °C until an OD<sub>600</sub> of 0.5. An equivalent number of cells were isolated by centrifugation, and the resulting cell pellets stored at -20 °C. Total cellular protein was isolated by alkaline lysis,<sup>165</sup> separated by SDS PAGE, and transferred to nitrocellulose for Western blot analysis. HA<sub>3</sub> tagged Bcl2 protein was detected using anti-HA antibodies (Covance); an anti-3-phosphoglycerate kinase (Pgk1p) antibody was used as a loading control (Molecular Probes).

#### 4.3.6 Electron microscopy

For transmission electron microscopy (TEM), samples were fixed in 2.5% glutaraldehyde pH 7.2 for 2 hours at 4 °C. Specimens were rinsed in 0.1 M phosphate buffer, pH 7.2, post-fixed in 2% OsO<sub>4</sub> in 0.1 M phosphate buffer for 2 hours then rinsed in distilled water and dehydrated in a graded ethanol series. Specimens were infiltrated and embedded in Spurr's resin and polymerized at 70 °C for 15 hours. Thin sections (60-100 nm) were collected and mounted on 50 mesh grids. Samples were stained with uranyl acetate and lead citrate and were examined and photographed with a JEOL 100 CX II TEM (JEOL USA, Peabody, Massachusetts) at 80 kV.

For scanning electron microscopy (SEM), *C. albicans* was grown in RPMI to an OD<sub>600</sub> of 1.0 at which time occidiofungin was added to 2 µg/mL final concentration. After 30 minute exposure, cells were isolated by centrifugation and fixed in 2.5% glutaraldehyde in 0.1M sodium cacodylate pH 7.2. Samples were rinsed and post-fixed in osmium tetroxide in 0.1M sodium cacodylate pH 7.2. Samples were rinsed, dehydrated through a graded ethanol series and then critical point dried with a Polaron

critical point dryer (Quorum Technologies, Newhaven, UK). Dried samples were mounted on aluminum stubs using carbon tape, coated with gold/palladium using a Polaron E5100 sputter coater, and viewed on a JEOL JSM-6500 FE Scanning Electron Microscope (JEOL USA, Peabody, MA)

#### 4.3.7 Fluorescent microscopy

*C. glabrata* 66032 cells were grown at a sub-inhibitory concentration of occidiofungin (0.25 µg/mL) for 24 hours at 35 °C using the CLSI method described above. Cells were fixed with the addition of 3.7% formaldehyde to the media and stored at 4 °C until staining with Calcofluor White (Sigma; 18909) as described by the manufacturer. To visualize mannoproteins, cells were fixed for 30 minutes in 3.7% formaldehyde, washed in PBS, incubated with 0.1mg/ml Concanavalin A-FITC (Sigma; C7642) for 10 minutes at room temperature, and washed again with PBS before visualization. Stained cells were visualized using a 100X objective on a Nikon 50i fluorescent microscope. Random images were captured using a Retiga EXi Black and White CCD Camera and Image Q software.

Cell culture for fluorescent microscopy studies was prepared as follows. *S. cerevisiae* BY4741 and *C. albicans* (ATCC 66027) were grown overnight in YPD at 30 °C. The cell suspension was then diluted to 0.1 OD<sub>600</sub> with YPD and incubated at 30 °C until the culture reached an OD<sub>600</sub> between 0.6 to 0.8. The minimum inhibitory concentration of occidiofungin against *S. cerevisiae* *C. albicans* with this cell density in YPD medium is 2 µg/mL. Images were acquired using Olympus confocal microscope with a 40x/0.90 dry objective.

Viability assay using FUN-1 dye (Invitrogen) was carried out by adding 15 $\mu$ M of dye to the untreated cells and cells treated with 2 $\mu$ g/ml of occidiofungin and incubating at 30 °C for 30 minutes. The cells were mounted on a glass slide and observed using an Olympus confocal microscope. The excitation wavelength of FUN-1 is 480 nm and the emission wavelengths are 510-560 nm (green) and 560-610 nm (red). Negative control in this assay was 1.6% DMSO.

ROS detection was performed using dihydrorhodamine 123 (DHR123) (Invitrogen) which has an excitation and emission maxima of 505 nm and 534 nm, respectively.<sup>168,169</sup> The dye (25 $\mu$ g/ml) was added to cells treated with 1, 2 and 4  $\mu$ g/ml of occidiofungin for 3 hours. Terminal deoxynucleotidyl transferase dUTP nick end labeling (TUNEL) assay was carried out using the APO-BrdU TUNEL assay kit (Invitrogen).<sup>168,169</sup> The assay was performed on cells treated with 1, 4, and 8  $\mu$ g/ml of occidiofungin for 3 hours. Protoplasts of the treated cells were obtained by treatment of cells with 24  $\mu$ g/ml of zymolyase in 1.2 M sorbitol. Staining was then carried out according to the protocol outlined by APO-BrdU TUNEL assay kit (Invitrogen). The dye used in the TUNEL assay is Alexa Fluor 488 which has an excitation and emission maxima of 495 nm and 519 nm, respectively. Negative and positive controls included 1.6% DMSO and 5 mM H<sub>2</sub>O<sub>2</sub>, respectively. FITC-labeled annexin-V staining was done using Annexin-V-FLUOS kit (Roche Applied Science).<sup>168,169</sup> Cells were treated with 1 and 4  $\mu$ g/ml of occidiofungin for 3 hours and washed with PBS. The cell pellet was incubated in 100  $\mu$ L of Annexin-V-FLUOS labeling solution for 10-15 minutes at room temperatures, as specified by the manufacturer. The cells were mounted on a slide and

observed. Excitation and emission maxima for fluorescein are 488nm and 518nm respectively and for propidium iodide are 488nm and 617nm respectively.

## 4.4 Results

### 4.4.1 Membrane and cell wall stability

*Candida albicans* ATCC 66027 was used to determine whether occidiofungin activated cell wall stress following a 10 minute and 20 minute exposure to occidiofungin (Figure 4.2). The MIC value of occidiofungin in these assays was 4  $\mu\text{g}/\text{mL}$ . Phosphorylation of Mkc1p indicates the presence of oxidative stress, changes in osmotic pressure, or cell wall damage. For *C. albicans*, an increase in the phosphorylation status of this MAP kinase was observable at a dose of 250 ng/mL, which is one sixteenth less than the inhibitory concentration. A dose-dependent increase in Mkc1p phosphorylation at 10 minutes was also seen for *C. glabrata* (Figure 4.3). Mkc1p phosphorylation occurred at 125 ng/ml occidiofungin, one half of the concentration seen for *C. albicans*. Both *C. albicans* and *C. glabrata* had a maximum increase in Mkc1p phosphorylation at 1  $\mu\text{g}/\text{ml}$ . The decreased levels of Mkc1p phosphorylation at 2  $\mu\text{g}/\text{ml}$  and the absence of Mkc1p phosphorylation at 4  $\mu\text{g}/\text{ml}$  is likely due to the increased cell death occurring at these concentrations. Similarly, an increase in the level of phospho- Cek1-p indicates that occidiofungin induces cell wall stress at subinhibitory concentrations. At the higher concentrations of occidiofungin, phosphorylation of Hog1p, a MAP kinase in the osmotic stress response pathway, was also detected. Although Hog1p phosphorylation was induced by occidiofungin, the extent of activation was significantly lower than that

seen for conditions known to induce the osmotic stress response pathway (e.g. 1M NaCl).

To further analyze the impact that occidiofungin may have on cell wall integrity, MICs were determined in media supplemented with 0.8M sorbitol. Sorbitol functions as an osmotic stabilizer and would decrease the activity of occidiofungin if the antifungal targets cells by disrupting membrane stability.<sup>170</sup> MICs for *C. albicans* (ATCC 66027) in the presence and absence of sorbitol in RPMI 1640 media at 24 hours were determined to be 0.5  $\mu\text{g/mL}$  (Table 4.1). This observation suggests that osmotic disruption, which would be predicted for a cell wall biosynthesis inhibitor or a membrane disruptive compound, is not likely involved in the cidal activity of occidiofungin.

Echinocandins inhibit  $\beta$ -1,3-glucan synthase, a multi-enzyme complex composed of catalytic subunits Fks1p/Fks2p. Mutations in *FKS1* exhibit decreased sensitivity to echinocandins.<sup>144,145</sup> To determine whether occidiofungin's mode of action is similar to that of echinocandins, we compared the sensitivity of a *S. cerevisiae*  $\Delta fks1$  mutant to the wild type strain. MIC values were similar (Table 4.2), suggesting that the mechanism of action of occidiofungin differs from that of echinocandins.

Lipof ormulation of ergosterol has been used in media as a competitive inhibitor of amphotericin B.<sup>171</sup> We made 1,2-dioleoylphosphatidylcholine (DOPC) vesicles containing 20% ergosterol and added them to microtiter wells yielding a final concentration of  $\sim 80 \mu\text{g/mL}$  of ergosterol. As controls we also used DOPC vesicles with no ergosterol and vesicle free media. In these experiments we observed a 16-fold decrease in activity of amphotericin B against *C. glabrata* in the presence of DOPC



vesicles containing 20% ergosterol and a 2-fold decrease in activity in the presence of DOPC vesicles with no ergosterol (Table 4.1). There was no change in the sensitivity of *C. glabrata* treated with occidiofungin in the presence of DOPC vesicles containing 20% ergosterol or DOPC vesicles with no ergosterol as compared to the vesicle free control. These data suggest that binding of ergosterol is not an important component to the activity of occidiofungin.

#### *4.4.2 Morphological changes following subinhibitory dosing of occidiofungin*

Cell density of *C. albicans* cells exposed to a sublethal concentration of occidiofungin (0.25 µg/mL) was notably lower than that of untreated cells. To determine whether occidiofungin inhibited cell cycle progression, bud morphology of occidiofungin treated and untreated cell populations were scored. In budding yeast there is a correlation between cell growth and division such that cell cycle progression can be determined visually by simply measuring the bud size. We found that even at concentrations of occidiofungin shown to decrease cell viability; there was no difference in cell cycle distribution between the two groups (Table 4.3).

SEM and TEM were used to determine whether occidiofungin caused aberrant morphological features in *Candida* cells treated with a subinhibitory concentration of occidiofungin. Comparison of untreated cells and cells grown in subinhibitory concentrations of occidiofungin did not reveal any morphological differences by SEM (Figure 4.4). However, TEM showed a number of mild cell morphological defects in the cells grown in the presence of subinhibitory concentrations of occidiofungin. The most dramatic defect was with the organization of the coat (manno) proteins (Figure 4.5). The

coat proteins appear to be reduced (Figure 4.5B, demarcated by black arrows) compared to untreated samples. TEM results also showed the presence of intracellular inclusions (Figure 4.5B, demarcated by white arrow). Cell wall thickness was the same for treated and untreated sample supporting our Fks1 results, and suggesting that inhibition of cell wall synthesis is not involved in the mechanism of action of occidiofungin against yeast cells. Prior TEM microscopy studies with the non-yeast fungus *Geotrichum candidum* showed loss of cell wall thickness and the accumulation of intracellular inclusions.<sup>64</sup> The accumulation of intracellular inclusions appears to be the common factor between these two groups of fungi. In addition, microscopy studies using concanavalin A-FITC fluorescence against yeast cells showed no major disruption in  $\beta$ -1,3-glucan distribution (Figure 4.6). However, microscopy studies using calcofluor white, which binds to chitin, did reveal some other interesting morphological differences. Calcofluor staining of *C. glabrata* showed an enhanced distribution of chitin in daughter cells following exposure to a subinhibitory concentration of occidiofungin. Enhanced chitin localization was observed primarily at the emerging bud tips (Figure 4.7).

#### 4.4.3 Cell death experiments

Microscopy studies were carried out on *S. cerevisiae* using FUN-1 dye as a cell viability indicator. The MIC for *S. cerevisiae* in these experiments was determined to be 1  $\mu$ g/mL. FUN-1 is a membrane permeable dye with red and green emission properties. The dye accumulates within the cytosol of cells (live or dead) with an intact plasma membrane to generate a green fluorescence. In metabolically active yeast, FUN-1 is transported from the cytosol into a vacuole where it forms cylindrical intravacuolar

structures (CIVS) that fluoresce red.<sup>172</sup> The viability assay indicated that the untreated cells possessed well defined vacuoles and the presence of CIVS. However, cells exposed to 2 µg/ml of occidiofungin for 30 minutes did not possess these cylindrical structures and appeared to have lost volume (Figure 4.8). This reduction in cell size is not typical of a cell wall active antifungal which would be expected to result in swelling or lysis of the cell. These results suggest that occidiofungin does not function through a lytic pathway in *S. cerevisiae* and these results indicate the need for additional studies in non-lytic pathways of cell death.

Microscopy assays were carried out to determine whether occidiofungin-induced cell death through an apoptotic or autophagic pathway. TUNEL and ROS assays were performed to determine whether occidiofungin induced an increase in ROS and double stranded DNA breaks. In the TUNEL and ROS assays, *C. albicans* and *S. cerevisiae* cells were treated for 3 hours at 30 °C. Both assays were performed with 5mM H<sub>2</sub>O<sub>2</sub> as positive control and a solvent blank as a negative control. In the TUNEL assay, an increase in fluorescence was observed for cells exposed to H<sub>2</sub>O<sub>2</sub> but not for cells treated with the solvent blank (Figure 4.9A and Figure 4.10A). For occidiofungin treated cells, fluorescence of increasing intensity was observed with increasing concentration of occidiofungin. ROS was detected using DHR123 which is oxidized to rhodamine 123 in the presence of ROS to generate a red fluorescent signal. This experiment showed results similar to the TUNEL assay; fluorescence increased with increasing concentrations of occidiofungin (Figure 4.9B and Figure 4.10B). To determine the importance of ROS accumulation to occidiofungin mediated cell death, MIC measurements were carried out

anaerobically, conditions known to reduce ROS production.<sup>173</sup> A reduction in sensitivity to occidiofungin was observed when wild type *S. cerevisiae* BY4741 and *S. cerevisiae* BY4741 rho<sup>0</sup> were grown under anaerobic conditions (Table 4.2).

We noticed a large population of *S. cerevisiae* cells, when exposed to occidiofungin at 1 µg/mL, showed the presence of “dancing bodies” in the vacuole. These are presumably polyphosphate granules and have been shown to form prior to apoptotic cell death.<sup>174</sup> Dancing bodies are indicated by an arrow in the DIC image of cells processed for ROS detection (Figure 4.10B). As further evidence for activation of apoptosis, an increased binding of Annexin-V-Fluos to externalized phosphatidylserine was detected with increasing concentrations of occidiofungin without membrane disruption as would be observed with propidium iodide staining (Figure 4.11 and Figure 4.12).

MIC measurements of *S. cerevisiae* deletion mutants in the apoptotic and autophagic pathway were done to determine whether mutants defective in these pathways were resistant to occidiofungin (Table 4.2). Thirteen mutants involved directly or indirectly with the apoptotic pathway and seventeen autophagy mutants were evaluated. Among the apoptotic mutants, *Ande1*, which is a mutant of the gene encoding the cytosolic NADH for the mitochondrial respiratory chain, was two-fold more sensitive compared to wild-type. Deletion of *ycal*, which is the gene responsible for synthesis of a cysteine protease similar to caspase, was two-fold more resistant compared to wild type. Sensitivity of *S. cerevisiae* expressing plasmid-borne human Bcl2 was tested and there was no difference in the MICs for the plasmid-borne human

Bcl2 and empty vector, thus, Bcl2 did not have a protective role in preventing cell death. This inability to rescue occidiofungin mediated cell death was not due to lack of Bcl2 protein expression (Figure 4.13). All of the autophagy mutants tested (*Δizh2*, *Δizh3*, *Δstm1*, *Δmre11*, *Δapg12*, *Δapg5*, *Δaut7*, *Δapg7*, *Δapg10*, *Δapg3*, *Δvtc1*, *Δvtc2*, *Δvtc3*, *Δvtc4*, *Δmms22*, *Δatg14*, and *Δvps30*) had the same sensitivity profile as the wild type strain suggesting that autophagic cell death was not a central mechanism of occidiofungin action. Cell viability was tested for all the mutants by determining the colony forming units following a 48-hour incubation at the minimum inhibitory concentration. Deletion mutants (*nde1*, *yca1*, *rny1*, *rpd3*, *nma1*, *vtc2*, *vtc3*, *csg2*, *apg7*, *nucl*, *hos3*, and *aif1*) that showed at least a ten-fold higher or lower viability than wild-type after a 48 hour exposure to the MIC of occidiofungin were further analyzed by a drop assay (Figure 4.14). Deletion mutants *nde1* and *yca1*, were used as a control for an increase or decrease in sensitivity in this assay, respectively. Deletion mutants (*rpd3*, *nma1*, *apg7*, *nucl*, *hos3*, and *aif1*) that showed a difference in viability from wild-type, showed no difference in sensitivity in the drop assay. Deletion mutants (*rny1*, *csg2*, *vtc2*, *vtc3*) demonstrated resistance to occidiofungin. Gene *rny1* codes for a vacuolar RNase that promotes apoptosis under oxidative stress conditions.<sup>175,176</sup> Gene *csg2* codes for calcium regulatory protein that is involved in sphingolipid metabolism.<sup>177</sup> Genes *vtc2* and *vtc3* code for vacuolar transport chaperone proteins that are involved in polyphosphate accumulation and autophagic and non-autophagic vacuolar fusion.<sup>178,179</sup>

## 4.5 Discussion

The experimental findings from this study show that: 1) the mechanism of action for occidiofungin differs from current antifungal agents used in the clinic, 2) there are morphological changes in yeast cells exposed to sub-lethal concentrations of occidiofungin, 3) microscopy studies demonstrate that occidiofungin is rapidly fungicidal against yeast, and 4) there is a dramatic increase in ROS, double stranded DNA breakage, and externalization of phosphatidylserine, all documented indicators of apoptosis.

The yeast cell wall is composed of chitin,  $\beta$ -1,3-glucan,  $\beta$ -1,6-glucan, and mannoproteins, the organization of which is critical for cell survival under altering environmental conditions. Disruption of cell wall composition is sensed by an intracellular signaling pathway mediated by a cascade of MAP kinases. Activation of this pathway leads to the upregulation of genes whose protein products are involved in cell wall synthesis including Chs3p, the catalytic subunit of chitin synthase III (CSIII). Phosphorylation of both Mkc1p and Cek1p within a short period of time after occidiofungin addition is indicative of cell wall damage.<sup>166,167,180</sup> Further evidence for the activation of the cell wall integrity pathway comes from the microscopy studies of chitin staining using calcofluor white. Calcofluor staining of *C. glabrata* showed an enhanced distribution of chitin in daughter cells following exposure to a subinhibitory concentration of occidiofungin (Figure 4.7). Localization of chitin deposits is strictly cell cycle dependent. Fks1p localizes at the site of active cell wall growth and no cell wall material is deposited in the mother cell during bud growth.<sup>181</sup> Chs3p is primarily

responsible for the production of the chitin found in the septal ring and the majority of the cell wall. The increased chitin deposition at the site of bud growth should be the result in an upregulation of chitin synthase activity and this increase is known to occur in response to mutations resulting in cell wall weakening mutations<sup>182</sup> or hypo-osmotic stress.<sup>183</sup> Activation of the cell wall integrity pathway is not unique to occidiofungin as the echinocandin, caspofungin, has also been shown to induce both CHS expression and Mkc1p phosphorylation.<sup>184,185</sup>

These results suggest that occidiofungin does perturb the membrane integrity of yeast; however activity assays using the osmotic stabilizer sorbitol or the Fks1 mutant resulted in no change in sensitivity compared to controls. Presumably, activation of the cell wall stress pathway compensates for the effect of occidiofungin at the concentrations resulting in cell death in our study. Upregulation of Hog1p, which is an osmotic disruption indicator, was significantly lower than that seen for conditions known to induce the osmotic stress response pathway (e.g. 1M NaCl). This may be attributed to a rapidly cidal function induced by apoptosis compared to osmotic stress induced by exposure. Activation of both the Mkc1p and Hog1p MAPK pathways have been detected in cells treated with the cell wall disruption agent zymolyase and the oxidative stress inducer hydrogen peroxide suggesting that a level of coordinated regulation exists between these two signaling pathways.<sup>186,187</sup>

There were no differences in activity of occidiofungin in the ergosterol competition assay or the Fks1 deletion mutant, which are known to confer resistance to polyenes (amphotericin B) and echinocandins (caspofungin), respectively. Based on the

results of the microscopy assays and the MIC values of the selected mutants, it can be concluded that occidiofungin triggers an apoptotic pathway in the fungal cell. The apoptotic mechanism reported for amphotericin B resulted in an accumulation of cells at the G2/M phase of the cell cycle.<sup>159</sup> However, the apoptotic mechanism for occidiofungin resulted in no differences in cell cycle distribution, supporting distinct differences in the apoptotic mechanism of action for occidiofungin compared to amphotericin B. The antifungal protein osmotin also induces an apoptotic mechanism of cell death in yeast and does not arrest cell cycle progression.<sup>188</sup> Studies have shown that both apoptotic and autophagic pathways can be induced simultaneously,<sup>189,190</sup> supporting a common upstream signal in their respective pathways. VPS30 is essential for the transport of cytoplasmic material, such as large proteins and organelle material, to the lysosome under starvation conditions. Autophagy is known to be absent in null *vsp30* mutants.<sup>191</sup> Since there was no decrease in sensitivity to occidiofungin in the *S. cerevisiae*  $\Delta vsp30$  mutant, the non-lytic autophagy pathway is not likely a major component in the killing mechanism of occidiofungin. The fact that most mutants deleted for components of the autophagic pathway, except for *vtc2* and *vtc3*, did not confer any increase or decrease in sensitivity to occidiofungin suggests that autophagy is not a key pathway activated by occidiofungin and that the apoptotic pathway triggered by occidiofungin is distinctly separate from the autophagy pathway. It is likely that the non-autophagic vacuolar fusion activity of *vtc2* and *vtc3* is involved in the observed resistance of these mutants in the drop assay.



We propose that induction of apoptosis is likely the causative mechanism of cell death for cells exposed to occidiofungin. Deletion of the caspase like enzyme, Yca1p, resulted in an increase in resistance to occidiofungin, while there was a decrease in resistance with the deletion of NADH dehydrogenase (Nde1). Yca1p caspase like activity is known to contribute to the degradation of proteins under oxidative conditions and this activity contributes to apoptotic cell death.<sup>192</sup> Nde1p is known to provide cytosolic NADH to the mitochondrial respiratory chain and the decrease in respiratory chain activity should contribute to a reduction in the production of ROS that should contribute to resistance against occidiofungin. The MIC activity results for these mutants support an apoptotic mechanism of cell death. Confocal microscopy studies clearly reveal an increase in ROS and double stranded DNA breakage following a short exposure to occidiofungin. Together, the studies presented in the manuscript suggest that occidiofungin mediated cell death is primarily through apoptosis.

#### **4.6 Conclusion**

Studies aimed at understanding the apoptotic mechanism of cell death induced by occidiofungin are warranted. The specific target of occidiofungin is still unknown and the identification of the molecular target in yeast may provide an avenue for the development of antifungal agents that have reduced toxicity in mammalian cells. Occidiofungin is resistant to gastric proteases<sup>115</sup> and may provide an alternative to azoles, which are the only orally available class of antifungals. An understanding of occidiofungin's function may provide novel opportunities towards the development of other new antifungal compounds for the treatment of serious fungal disease.

**Table 4.1: Bioactivity of Occidiofungin**

Isolate	Experiment	MIC/MLC* ( $\mu\text{g/mL}$ )	Bioactivity Compared to Control
Occidiofungin			
<i>C. glabrata</i> 66032	CLSI	0.5/N.D.	-
<i>C. glabrata</i> 66032	0.8 M sorbitol	0.5/N.D.	No Change
<i>C. glabrata</i> 66032	DOPC vesicles	0.5/N.D.	No Change
<i>C. glabrata</i> 66032	DOPC vesicles:ergosterol	N.D./0.5	No Change
Amphotericin B			
<i>C. glabrata</i> 66032	CLSI	0.5/N.D.	-
<i>C. glabrata</i> 66032	DOPC vesicles	1.0/N.D.	2-Fold Decrease
<i>C. glabrata</i> 66032	DOPC vesicles:ergosterol	N.D./ > 8.0	>16-Fold Decrease

\* Only the MLC is reported, given the turbidity of the ergosterol DOPC suspension.

**Table 4.2: Occidiofungin MICs**

Isolate	MIC ( $\mu\text{g/ml}$ )
<i>S. cerevisiae</i> BY4741	0.1250
<i>S. cerevisiae</i> BY4741 Rho <sup>0</sup>	0.1250*
<i>S. cerevisiae</i> BY4741	0.2500 <sup>‡</sup>
<i>S. cerevisiae</i> BY4741 Rho <sup>0</sup>	0.2500* <sup>‡</sup>
<b>Membrane and Cell Wall Mutants</b>	
<i>S. cerevisiae</i> $\Delta\text{sur1}$	0.1250
<i>S. cerevisiae</i> $\Delta\text{ipt1}$	0.1250
<i>S. cerevisiae</i> $\Delta\text{csg2}$	0.1250
<i>S. cerevisiae</i> $\Delta\text{fks1p}$	0.1250
<b>Apoptotic Mutants</b>	
<i>S. cerevisiae</i> $\Delta\text{yca1}$	0.2500
<i>S. cerevisiae</i> $\Delta\text{nde1}$	0.0625*
<i>S. cerevisiae</i> $\Delta\text{aif1}$	0.1250
<i>S. cerevisiae</i> $\Delta\text{hos3}$	0.1250
<i>S. cerevisiae</i> $\Delta\text{uth1}$	0.1250
<i>S. cerevisiae</i> $\Delta\text{nma1}$	0.1250
<i>S. cerevisiae</i> $\Delta\text{hda1}$	0.1250
<i>S. cerevisiae</i> $\Delta\text{ste20}$	0.1250
<i>S. cerevisiae</i> $\Delta\text{rny1}$	0.1250
<i>S. cerevisiae</i> $\Delta\text{rpd3}$	0.1250
<i>S. cerevisiae</i> $\Delta\text{sir2}$	0.1250
<i>S. cerevisiae</i> $\Delta\text{nuc1}$	0.1250
<i>S. cerevisiae</i> $\Delta\text{ybh3}$	0.1250
<b>Autophagy Mutants</b>	
<i>S. cerevisiae</i> $\Delta\text{izh2}$	0.1250
<i>S. cerevisiae</i> $\Delta\text{izh3}$	0.1250
<i>S. cerevisiae</i> $\Delta\text{stm1}$	0.1250
<i>S. cerevisiae</i> $\Delta\text{mre11}$	0.1250
<i>S. cerevisiae</i> $\Delta\text{apg12}$	0.1250
<i>S. cerevisiae</i> $\Delta\text{apg5}$	0.1250
<i>S. cerevisiae</i> $\Delta\text{aut7}$	0.1250
<i>S. cerevisiae</i> $\Delta\text{apg7}$	0.1250
<i>S. cerevisiae</i> $\Delta\text{apg10}$	0.1250
<i>S. cerevisiae</i> $\Delta\text{apg3}$	0.1250
<i>S. cerevisiae</i> $\Delta\text{vtc1}$	0.1250
<i>S. cerevisiae</i> $\Delta\text{vtc2}$	0.1250
<i>S. cerevisiae</i> $\Delta\text{vtc3}$	0.1250
<i>S. cerevisiae</i> $\Delta\text{vtc4}$	0.1250
<i>S. cerevisiae</i> $\Delta\text{mms22}$	0.1250
<i>S. cerevisiae</i> $\Delta\text{atg14}$	0.1250
<i>S. cerevisiae</i> $\Delta\text{vps30}$	0.1250

\*MIC recorded at 48 hours

<sup>‡</sup>Cells were grown anaerobically

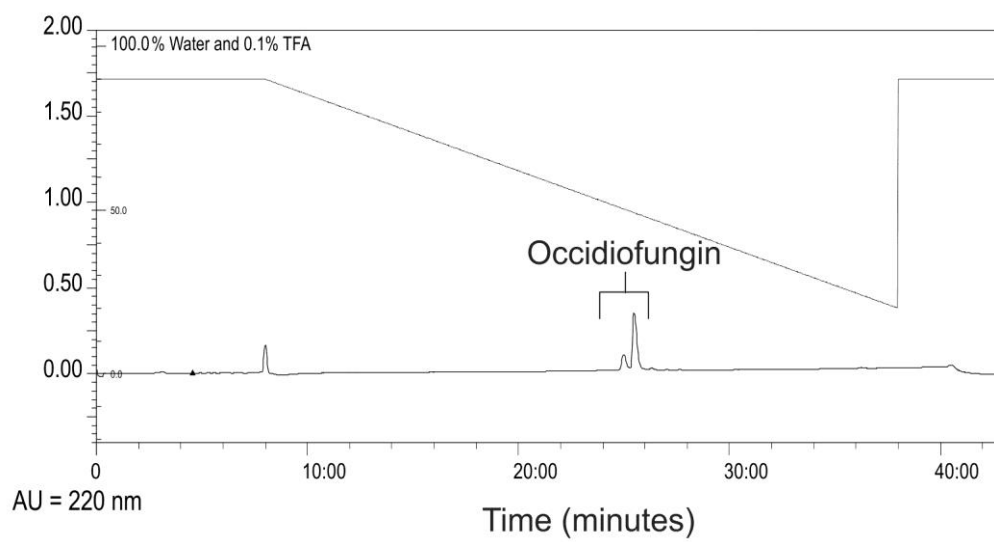


**Figure 4.1:** RP-HPLC chromatogram of 50 µg of purified occidiofungin.

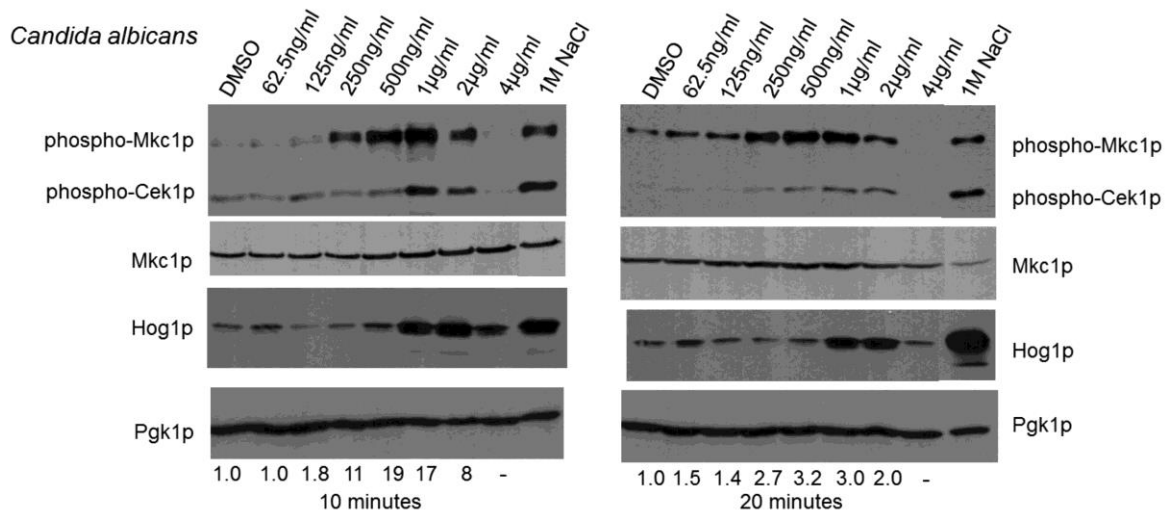


**Figure 4.2:** Western blot detection of MAPK activation. *Candida albicans* cells were treated with increasing concentrations of occidiofungin (0-4  $\mu\text{g}/\text{mL}$ ) for 10 or 20 minutes. Cell extracts were analyzed by immunoblotting with antibodies against phospho-Mkc1p, total Mkc1p, and phospho-Hog1p. Detection of phosphoglycerate kinase (Pgk1p) was used to verify equal protein loading. Cells grown in the presence of 1M NaCl were used as a positive control for Hog1p activation. The relative ratios of phosphorylated Mkc1p to total Mkc1p are indicated for each set of immunoblots with the ratio of DMSO treated cells normalized to one.

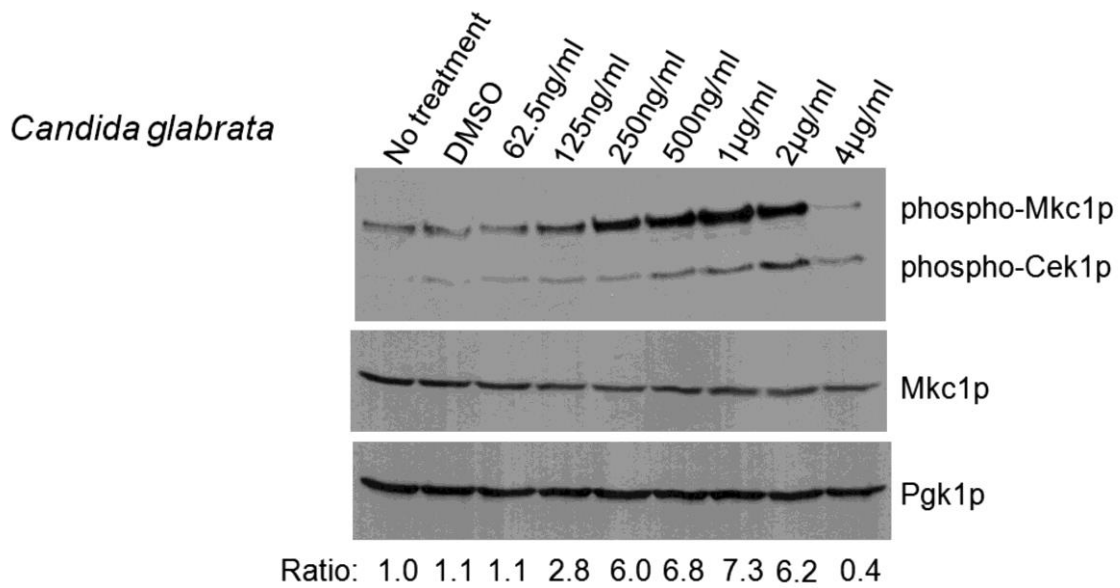


**Figure 4.3:** Western blot detection of MAPK activation in *Candida glabrata*. Cells were treated with increasing concentrations of occidiofungin (0-4 µg/mL) for 20 minutes. Cell extracts were analyzed by immunoblotting with antibodies against phospho-Mkc1p, total Mkc1p, and phospho-Hog1p. Detection of phosphoglycerate kinase (Pgk1p) was used to verify equal protein loading. The relative ratios of phosphorylated Mkc1p to total Mkc1p are indicated with the ratio obtained for untreated cells set to one.

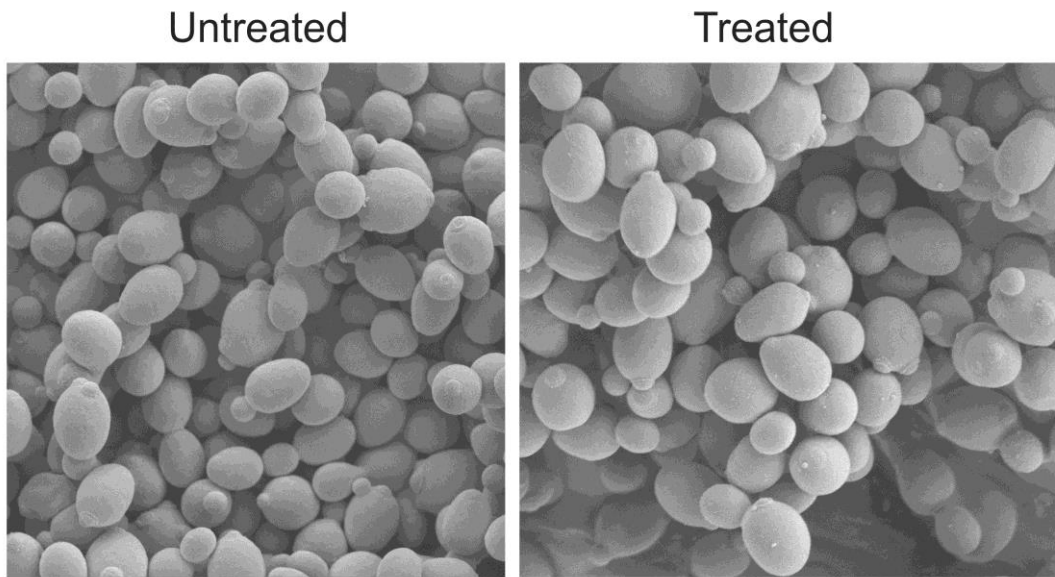


**Figure 4.4:** Scanning electron microscopy (SEM) images of *Candida albicans*: untreated (a) and occidiofungin treated (b) cells. *C. albicans* cells were propagated at 35°C in RPMI until reaching an OD<sub>600</sub> of 1.0. Occidiofungin (2 µg/mL), or an equivalent volume of DMSO, was added and cells returned to 35°C for 30 minutes. Cells were isolated by centrifugation and processed for SEM as described in Materials and Methods. 4000X magnification is shown.

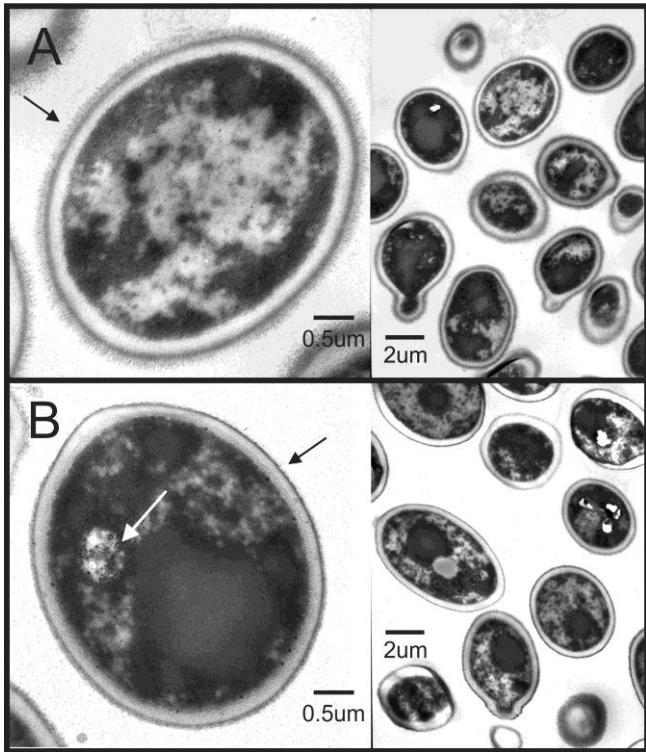


**Figure 4.5:** TEM Micrographs. (A) *Candida albicans* cells treated with the solvent blank, DMSO. (B) *Candida albicans* cells grown in a sub-lethal concentration of occidiofungin. The arrows revealed a loss of coat proteins on the surface of the cell wall as well as vesicle-like inclusions inside the cell. Side panels show an expanded region of cells having the morphological defect.



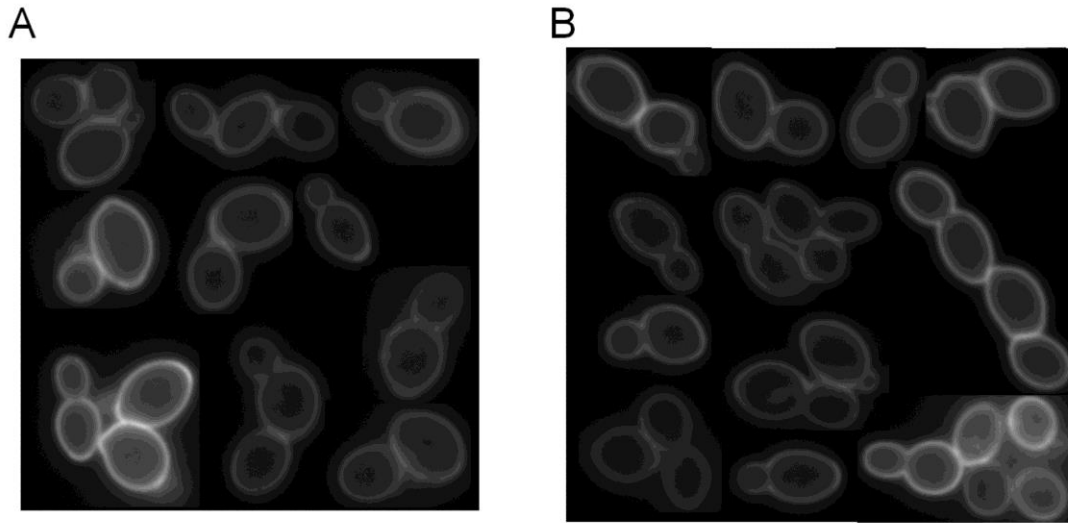


**Figure 4.6:** Cell wall mannoprotein distribution in *Candida glabrata* treated with occidiofungin remains unchanged. *C. glabrata* cells were grown for 24hr in the absence (A) or presence (B) of a sublethal concentration of occidiofungin. 1,3-b-glucan was visualized with concanavalinA-FITC staining by fluorescence microscopy. A montage of cells is shown for each treatment.

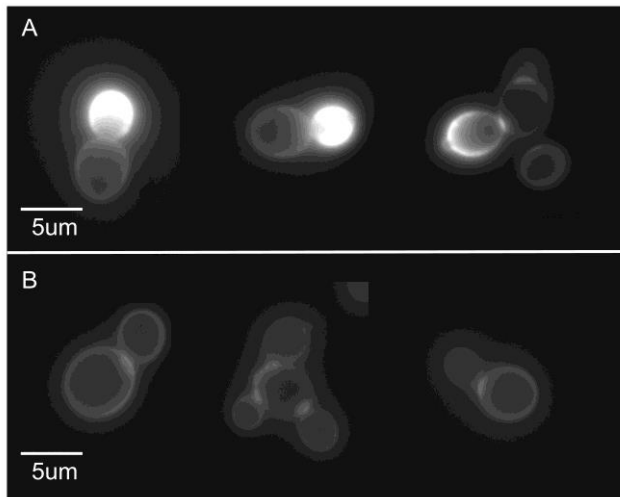


**Figure 4.7:** Chitin staining in *Candida glabrata*. Chitin staining was visualized with calcofluor white staining in live cells by fluorescence microscopy using a 100X objective and a DAPI filter set. (A) Chitin localization in cells treated with a sublethal concentration of occidiofungin. (B) Chitin localization in untreated cells. A montage of cells is shown for each.

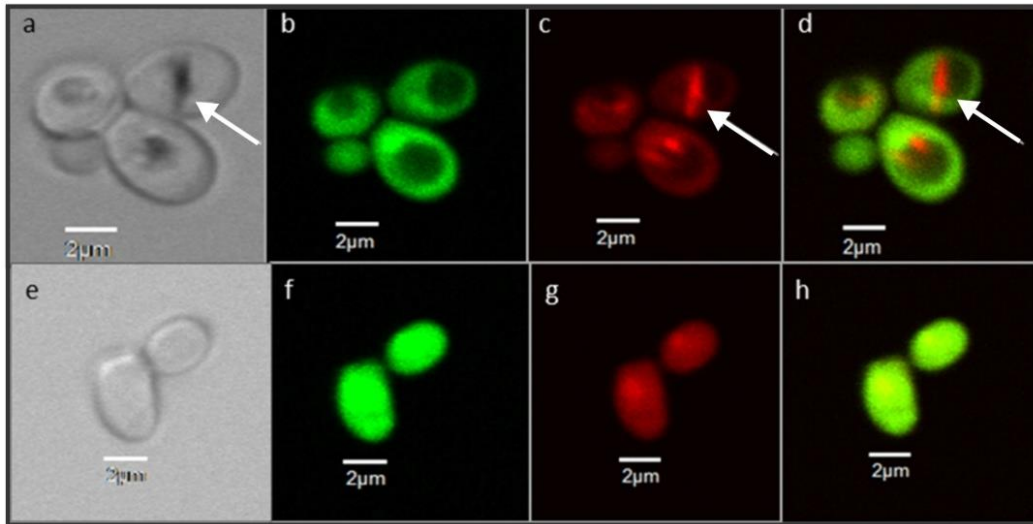


**Figure 4.8:** FUN-1 Assay. DIC and fluorescence images of yeast cells stained with FUN-1. Panels “a-d” are untreated yeast cells. CIVS stained red with FUN-1 (shown by arrows). Panels “e-h” are occidiofungin treated cells (2µg/ml). CIVS not present in cells. Panels “a” and “e” are DIC images. Panels “b” and “f” are the green emission, while “c” and “g” are the red emission channels. Panels “d” and “h” are overlays of “a-c” and “e-g”, respectively.

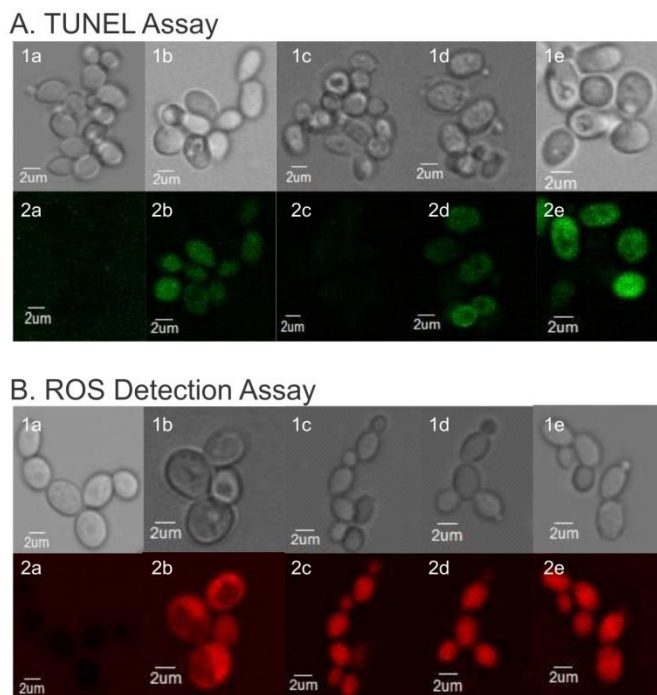
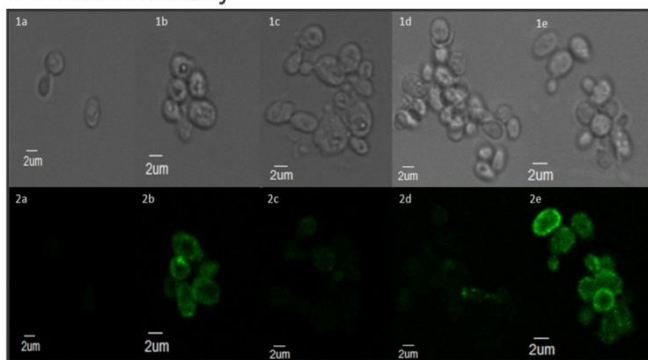


**Figure 4.9:** Fluorescent Microscopy Studies on *Candida albicans*. (A) TUNEL Assay. Rows “1” and “2” are DIC and fluorescence images, respectively. Column “a” shows cells treated with the solvent blank (DMSO with no occidiofungin), “b” shows cells treated with 5mM H<sub>2</sub>O<sub>2</sub> and “c-e” correspond to cells treated with 1 μg/ml, 4 μg/ml and 8 μg/ml of occidiofungin, respectively. (B) ROS Detection Assay. Rows “1” and “2” are DIC and fluorescence images, respectively. Column “a” corresponds to treatment with solvent blank, “b” corresponds to cells treated with 5mM H<sub>2</sub>O<sub>2</sub>, and “c-e” show cells treated with 1μg/ml, 2 μg/ml and 4 μg/ml of occidiofungin, respectively.

### A. TUNEL Assay



### B. ROS Detection Assay

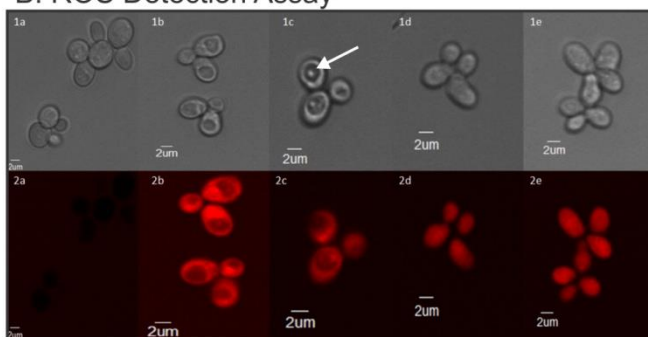


**Figure 4.10:** Fluorescent Microscopy Studies on *S. cerevisiae*. (A) TUNEL Assay. Rows “1” and “2” are DIC and fluorescence images, respectively. Column “a” shows cells treated with the solvent blank, “b” shows cells treated with 5mM H<sub>2</sub>O<sub>2</sub> and “c-e” correspond to cells treated with 1 µg/ml, 4 µg/ml and 8 µg/ml of occidiofungin, respectively. (B) ROS Detection Assay. Rows “1” and “2” are DIC and fluorescence images, respectively. Column “a” corresponds to treatment with solvent blank, “b” corresponds to cells treated with 5mM H<sub>2</sub>O<sub>2</sub>, and “c-e” show cells treated with 1µg/ml, 2 µg/ml and 4 µg/ml of occidiofungin, respectively.

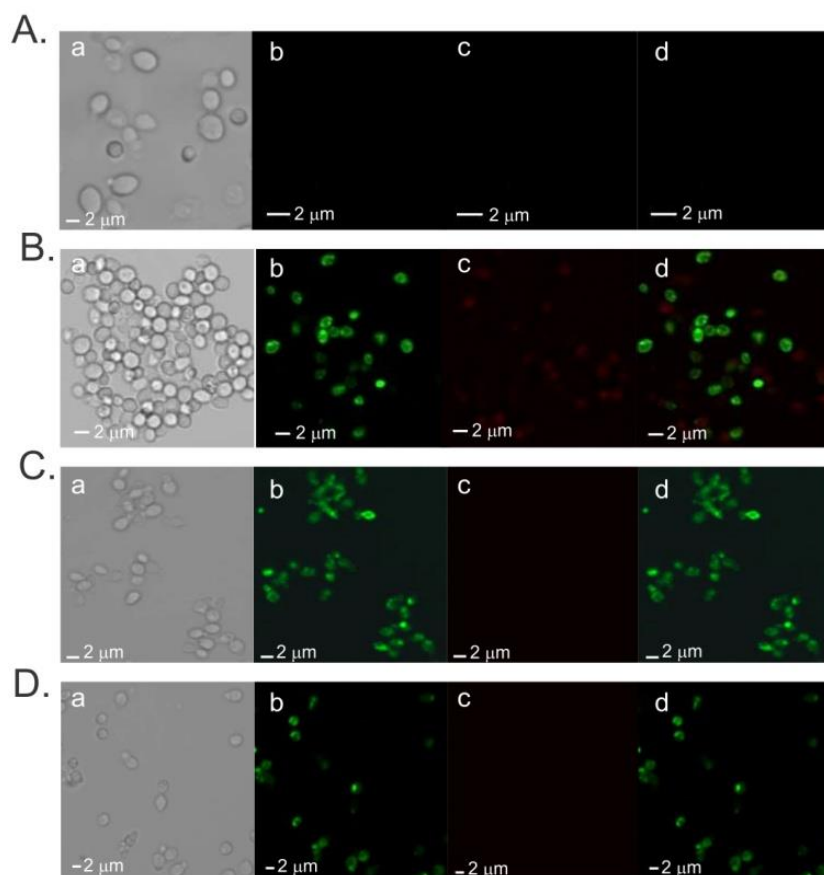


**Figure 4.11:** Phosphatidylserine Detection Assay on *Candida albicans*. Rows A-D are negative control (treatment with DMSO with no occidiofungin), positive control (5mM H<sub>2</sub>O<sub>2</sub>), cells treated with 1 µg/ml, 4 µg/ml of occidiofungin, respectively. Columns “a-d” correspond to DIC image, annexin fluorescence image, propidium iodide fluorescence image, and overlay of annexin and propidium iodide fluorescence images, respectively.

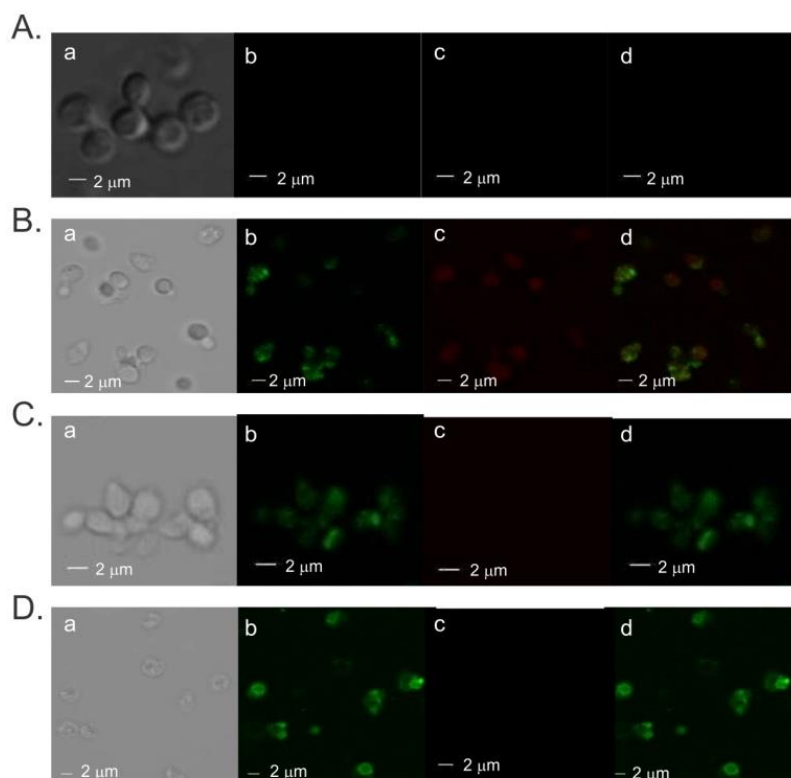


**Figure 4.12:** Phosphatidylserine Detection Assay on *S. cerevisiae*. Rows A-D are negative control (treatment with DMSO with no occidiofungin), positive control (5mM H<sub>2</sub>O<sub>2</sub>), cells treated with 1 µg/ml, 4 µg/ml of occidiofungin, respectively. Columns “a-d” correspond to DIC image, annexin fluorescence image, propidium iodide fluorescence image, and overlay of annexin and propidium iodide fluorescence images, respectively.

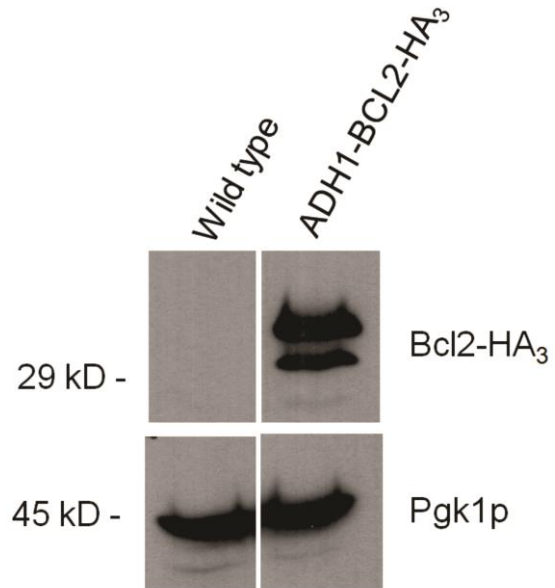


**Figure 4.13:** Western blot analysis. Constitutive expression of HA<sub>3</sub> tagged Bcl2 protein was observed. Anti-HA antibodies were used to detect HA<sub>3</sub> tagged Bcl2 protein and anti-3-phosphoglycerate kinase (Pgk1p) antibody was used as a loading control.



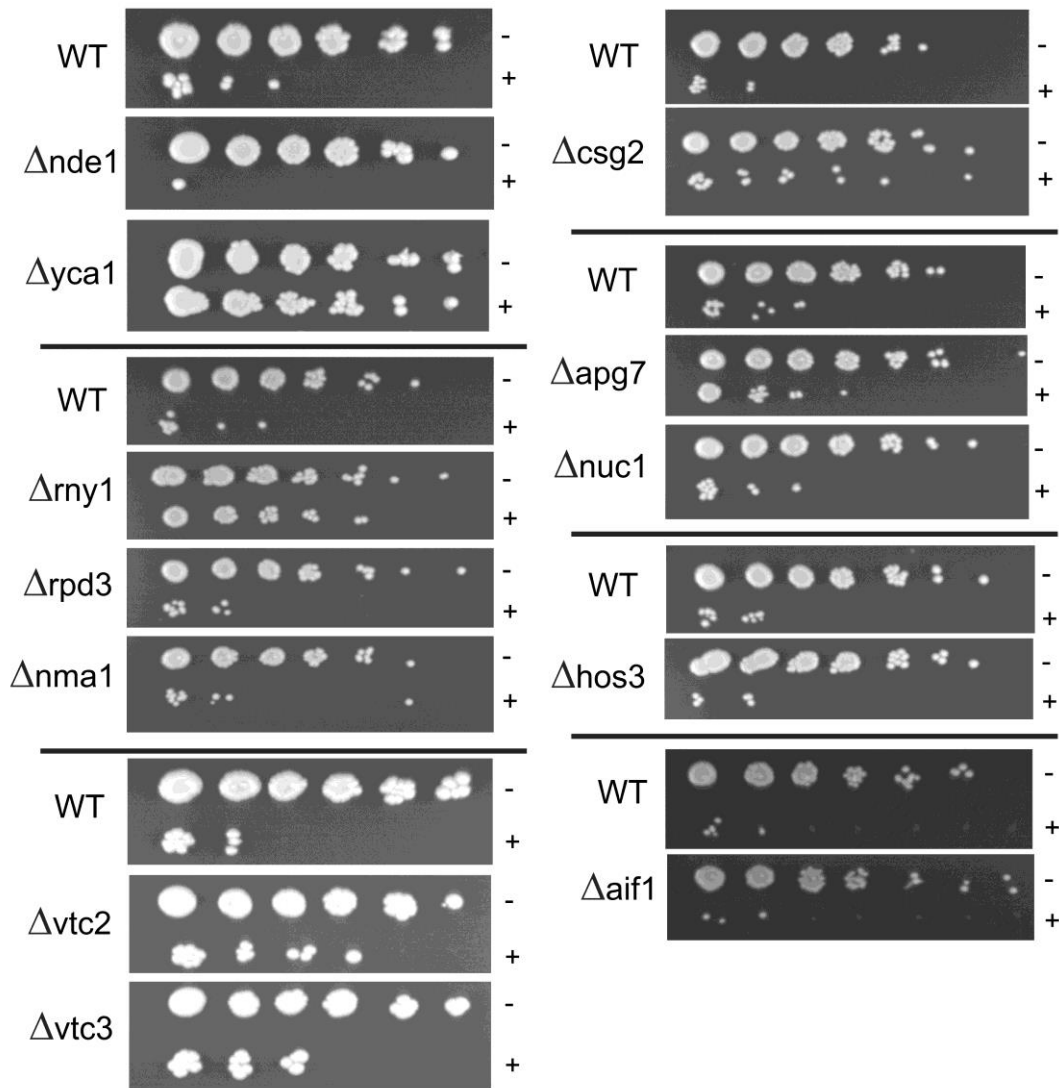


**Figure 4.14:** Drop assay. Growth sensitivity of *S. cerevisiae* deletion mutants exposed to 0.5 μg/mL occidiofungin for 4 hours was analyzed by spotting five-fold serially diluted cells to a YPD plate. The growth profile for untreated (-) or occidiofungin treated (+) cells are shown after 72 hours at 30 °C. An untreated and treated wild-type strain was included on all plates to control for experimental variations.

## 5. IDENTIFICATION OF THE CELLULAR TARGET FOR THE NOVEL ANTIFUNGAL OCCIDIOFUNGIN

### 5.1 Overview

Since the 1950s, the antifungal compounds that have been developed for clinical use fall under three broad families: azoles, polyenes and echinocandins.<sup>193,194</sup> These compounds target fungal cells by inhibiting ergosterol production, binding of ergosterol, or by disrupting cell wall biosynthesis.<sup>195-197</sup> Widespread resistance to these mechanisms of action has been reported<sup>19,28,29,198,199</sup> and this has created an urgent need to identify antifungal compounds that have new fungal cell targets.<sup>48</sup> Here, we show that a novel antifungal named occidiofungin targets actin. An alkyne functionalized variant of occidiofungin (alkyne-OF) was synthesized enabling affinity purification and confocal microscopy studies. Affinity purification assays of yeast exposed to alkyne-OF showed a high proportion of actin and actin associated proteins. Furthermore, occidiofungin was shown to bind to rabbit muscle G-actin and F-actin. Localization studies and time course experiments indicated the binding of occidiofungin to bud tips in *Saccharomyces cerevisiae* and eventual internalization into the mature cell. Similar studies in *Schizosaccharomyces pombe* demonstrated localization of occidiofungin near the poles of the cells and along the division septum, which are well-documented regions for actin patches.<sup>200</sup> These observations support the binding of occidiofungin to actin causing cell cycle arrest, starvation and death.

## 5.2 Background

Occidiofungin is a cyclic glycolipopeptide produced by a soil bacterium called *Burkholderia contaminans* MS14 and has been reported to have a wide spectrum of activity against several fungal species.<sup>64</sup> Preliminary toxicological analyses of occidiofungin using a murine model indicated that it was well tolerated at concentrations of 10 to 20 mg/kg.<sup>67</sup> Blood chemistry analyses and histopathology performed on multiple organs showed a transient non-specific stress response with no damage to organ tissues.<sup>67</sup> Taken together, the data suggest that occidiofungin is a promising candidate for development as a clinically useful antifungal agent. This study is directed towards identifying the molecular target of occidiofungin within the fungal cell to better understand how it causes fungal cell death.

## 5.3 Materials and methods

### 5.3.1 Spectrum of activity of occidiofungin

Minimum inhibitory concentration (MIC) susceptibility testing was performed according to the CLSI M27-A3 and M38-A2 standards for the susceptibility testing of yeasts and filamentous fungi, respectively. Incubation temperature was 35° C and the inoculum size was 0.5 – 2.5 x 10<sup>3</sup> colony-forming units (CFU)/mL and 0.4 - 5 x 10<sup>4</sup> conidia/mL for yeasts and filamentous fungi, respectively. Inoculum concentration for dermatophytes was 1-3x10<sup>3</sup> conidia/mL. RPMI was used throughout as the growth medium and *Cryptococcus* strains were tested in YNB. Occidiofungin MICs were recorded at 50% and 100% growth inhibition after 24 and 48 hours of incubation, with

the exception of dermatophytes which were incubated for 96 hours. Fluconazole MICs against *Candida* strains were recorded at 50% inhibition after 24 hours and against *Cryptococcus* strains after 72 hours. Voriconazole MICs were recorded at 100% inhibition after 24 hours for zygomycetes and after 48 hours for *Fusarium* and *Aspergillus* strains. Voriconazole MICs were recorded at 80% inhibition after 96 hours of incubation for dermatophytes.

### 5.3.2 Derivatization of occidiofungin

Occidiofungin was purified from a liquid culture of *Burkholderia contaminans* MS14 as previously described.<sup>84</sup> Pure occidiofungin was aliquoted into 100 µg fractions and stored dry at 4°C until use. Addition of an alkyne reactive group to the primary amine on occidiofungin was performed initially at the Texas A&M Natural Products LINCHPIN Laboratory at Texas A&M University and subsequently at the CPRIT Synthesis and Drug-Lead Discovery Laboratory at Baylor University. The reaction is depicted in Supplementary Figure 1a and the synthetic procedure employed is described below along with <sup>1</sup>H and <sup>13</sup>C NMR line listing. Spectral data (<sup>1</sup>H and <sup>13</sup>C NMR, X MHz and Y MHz, respectively) are depicted in Figure 1b. The derivatized occidiofungin was purified by Reversed-Phase High Performance Liquid Chromatography (RP-HPLC) using a 4.6- by 250-mm C18 column (Grace-Vydac; catalog no. 201TP54) on a Bio-Rad BioLogic F10 Duo Flow with Quad Tec UV-Vis detector system. The solvents used were 99.9% water (with 0.1% trifluoroacetic acid) and 99.9% acetonitrile (with 0.1% TFA). Alkyne occidiofungin (Alkyne-OF) eluted at 48% water and was collected separately and dried down. Matrix-assisted laser desorption/ionization–time of flight

mass spectrometry (MALDI-TOF MS; Shimadzu/Kratos) was used to confirm mass of the isolated peak. The fraction collected from the HPLC was evaporated to dryness and was dissolved in 100  $\mu$ L of 35% acetonitrile containing 0.1% TFA. From these resuspended fractions, 0.5  $\mu$ L was mixed with 0.5  $\mu$ L of  $\alpha$ -cyano-4-hydroxycinnamic acid matrix (6 mg/mL in 50% acetonitrile containing 0.1% TFA) and dried on the target plate.

### 5.3.3 Confirmation of activity of alkyne-OF

The activity of the purified alkyne-OF was compared to the native compound using the CLSI M27-A3 method of determination of the minimum inhibitory concentration (MIC) against yeast such as *Saccharomyces cerevisiae* BY4741 and *Schizosaccharomyces pombe* 972h (wild type), which was obtained from Dr. Susan Forsburg (Department of Biological Sciences, University of Southern California). Additionally, activity of the alkyne derivatized occidiofungin was also checked against a higher density (OD<sub>600</sub>=0.6 to 0.8) of cells of both the afore-mentioned types of yeast. In order to confirm that the alkyne-OF triggered the same response in yeast as native occidiofungin, the apoptosis assays such as the TUNEL assay (APO<sup>TM</sup>-BrdU TUNEL Assay Kit, LifeTechnologies), phosphatidylserine externalization assay (Annexin-V-Fluos staining kit, Roche) and ROS detection assay (Dihydrorhodamine 123, Sigma) were repeated as previously described<sup>(16)</sup>.

### 5.3.4 Affinity purification of proteins with alkyne-OF

An overnight culture of *S. pombe* was grown to OD<sub>600</sub> of 0.6 to 0.8. 1 mL of cells was incubated with 8  $\mu$ g/mL of alkyne-OF for 30 minutes at 30°C. The cells were spun

down and washed in PBS. The cells were then sonicated with a probe tip sonicator for 30 seconds and placed on ice for 30 seconds alternatingly to avoid overheating. The sample was then spun down at 16000x g for 10 minutes and the supernatant was removed. The Click-it protein reaction kit (Life Technologies) was used and the alkyne-OF was reacted with azide-biotin, as per the instructions on the kit. The reaction was allowed to proceed for 90 minutes at 37°C while shaking. The reacted mixture was passed through a 10 kDa cutoff filter and the proteins retained at the top of the filter were solubilized in 100 µL of 100 mM Tris HCl (pH=7.5). Streptavidin agarose beads (ThermoFisher Scientific) obtained from a 100 µL of a 50% slurry were added and the mixture was incubated at 37°C for 90 minutes. The beads were washed with 10 mL of 100 mM Tris HCl (pH=7.5) and the proteins extracted by boiling in 50 µL of 1X SDS sample loading buffer for 15 minutes. This sample was run on a 12% SDS gel until the band runs just out of the stacking phase to create a single band. The band was then cut out and used for analysis. Trypsin digestion on the band was done in the Protein Chemistry Laboratory (Texas A&M University) and subsequent LC-MS/MS analysis was performed by the Mass Spectrometry Laboratory at the University of Texas Health Science Center (San Antonio). The results were analyzed using the Scaffold software. Cells treated with DMSO and native occidiofungin were used as controls. An additional sample using cells that were lysed prior to alkyne-OF treatment was used for comparison.

### *5.3.5 Localization of alkyne-OF over a time course of exposure*

An overnight culture (*S. pombe* or *S. cerevisiae*) was grown using colonies from a freshly streaked plate to an OD<sub>600</sub> of 0.6 to 0.8. 1 mL of cells was incubated with MIC

quantities of alkyne-OF for 60 minutes at 30°C while removing 200 µL of the cell suspension at 10 minutes, 30 minutes and 60 minutes post incubation. The cells were spun down, washed in phosphate buffered saline (PBS) and fixed for 15 minutes in 3.7% formaldehyde (in PBS) at room temperature. Permeabilization of cells was done using 0.5% Triton-X (in PBS) at room temperature for 20 minutes. The cells were then washed twice using 1 mL of PBS per wash. Click reaction with azide derivatized Alexa-488 was done according to the manufacturer's protocol (Click-iT EdU Imaging kit, ThermoFisher Scientific). The cells were washed with PBS and added to the microscope slide for visualization. A competition assay was carried out by pre-treating cells with an MIC amount (0.5 µg/mL) of the native occidiofungin followed by treatment with alkyne-OF. Cells were observed using Olympus FV1000 confocal microscope with a 100x/1.4 oil immersion objective and 40x/0.9 dry objective.

#### *5.3.6 Estimation of endocytosis following occidiofungin treatment*

Three 1 mL aliquots of *S. pombe*, at a density of OD<sub>600</sub> 0.6 to 0.8, were treated with 1 µL DMSO, 0.5 µg/mL (0.5x MIC) or 1 µg/mL (1x MIC) of native occidiofungin for 30 minutes at 30°C. Cells were isolated by centrifugation at 21000x g for 2 minutes, washed thrice with PBS and resuspended in YPD containing 8 mM FM-464 (ThermoFisher Scientific). The cells were incubated in the presence of the dye for 60 minutes at 30°C, followed by two washes with PBS and then added to a microscope slide for visualization. Images were obtained using an Olympus FV1000 confocal microscope with a 40x/0.9 dry objective.

### 5.3.7 Affinity purification of actin

Purified rabbit skeletal muscle filamentous actin (Catalog no.: AKF99) and G-actin (Catalog no.: AKL95) was purchased from Cytoskeleton Inc. According to the supplier's instructions, the protein was reconstituted in Milli-Q water to achieve a stock concentration of 0.4 mg/mL. This resulted in the filaments being stored in a buffer that consisted of 5 mM Tris-HCl (pH 8.0), 0.2 mM CaCl<sub>2</sub>, 0.2 mM ATP, 2 mM MgCl<sub>2</sub> and 5% (w/v) sucrose. The solution was aliquoted into 50 µL quantities and stored at -80°C until use. Immediately before use, each aliquot was thawed by placing the tube in a 37°C water bath for 5 minutes followed by room temperature. 24 µg of F- or G-actin was then reacted with 8 µg alkyne-OF. Click chemistry was performed on this mixture to react the alkyne-OF with azide-biotin for 90 minutes as described (Click-iT protein reaction buffer kit, ThermoFisher Scientific). Unreacted reagents were removed by passing the mixture through a 10 kDa cutoff filter with 20 minutes of centrifugation at 15000x g. Proteins retained in the filter chamber were solubilized in 200 µL of 100 mM Tris-HCl (pH=7.5) and reacted with streptavidin beads as described above. The beads were washed multiple times using 100 mM Tris HCl (pH=7.5) and bound proteins eluted by boiling in 50 µL of SDS sample loading buffer. The sample was electrophoresed through a 12% SDS gel and protein bands were visualized by silver staining according to the manufacturer's protocol (Pierce Silver stain kit, ThermoFisher Scientific). F- and G-Actin treated with DMSO and native occidiofungin were used as controls.



### *5.3.8 Actin polymerization and depolymerization assays*

The effect of unmodified occidiofungin on actin polymerization and depolymerization was measured using the Actin Polymerization Biochem Kit (fluorescence format): rabbit skeletal muscle actin purchased from Cytoskeleton Inc. (Catalog no.: BK003). Occidiofungin was brought up in 1.5%  $\beta$ -cyclodextrin in PBS (pH=7.5) at a concentration of 1  $\mu\text{g}/\mu\text{L}$ . 20  $\mu\text{L}$  of this solution was used per well as described in the instructions. The same buffer without occidiofungin was used for the test buffer controls. G-buffer was made by adding 2  $\mu\text{L}$  of 100 mM ATP stock for every 1 mL of General Actin buffer prior to the start of the experiment as instructed. G-actin and F-actin stock were prepared as described in the kit to achieve stock concentrations of 0.4 mg/mL and 1 mg/mL respectively. The polymerization and depolymerization assays were then carried out as per the manufacturer's instructions.

### *5.3.9 Microscopic analysis of actin treated with occidiofungin*

Purified rabbit skeletal muscle filamentous actin (Catalog no.: AKF99, Cytoskeleton Inc.) was treated with alkyne-OF (24  $\mu\text{g}$  of F-actin to 8  $\mu\text{g}$  of alkyne-OF) as described above. The mixture was reacted with azide functionalized Alexa Fluor 488 according to the manufacturer's instructions (Click-iT EdU Imaging kit, ThermoFisher Scientific). Unbound dye was removed by overnight dialysis at 4°C against actin polymerization buffer using a 1 kDa cutoff membrane (Catalog no.: BSA02, Cytoskeleton Inc.). The actin filaments were removed, added to a slide and analyzed using an Olympus FV1000 confocal microscope 40 $\times$ /0.90 dry objective and a 100 $\times$ /1.4

oil immersion objective. A control was done using 140 nM Acti-stain 670 phalloidin (Cytoskeleton Inc.) staining of actin filaments as per instructions provided.

F-actin filaments were also reacted with different concentrations of the native occidiofungin. Approximately, molar ratios of 1:10 (24 µg actin:8 µg native occidiofungin) and 1:5 (24 µg actin:4 µg native occidiofungin) were tested. The filaments were reacted with occidiofungin for 15 minutes at room temperature. The respective mixtures were then stained with 140 nM Acti-stain 670 phalloidin for another 15 minutes at room temperature. The stained filaments were then added to a glass slide and observed on an Olympus FV1000 confocal microscope using a 100x/1.4 oil immersion objective. Untreated actin filaments were stained and observed as the control.

#### **5.4 Results and discussion**

We have previously demonstrated that the mechanism of action of occidiofungin differs from the primary mode of action of the three common classes of antifungals.<sup>66</sup> Occidiofungin has been observed to rapidly induce apoptosis in yeast cells at the minimal inhibitory concentrations.<sup>66</sup> In addition, occidiofungin was seen to have sub-micromolar activity against *Pythium* species which lacks ergosterol in the membrane and *Cryptococcus neoformans* which is resistant to echinocandins.<sup>64</sup> Several studies have reported occurrence of widespread resistance to these mechanisms of action, especially in the case of the azoles<sup>19,28,29</sup> and the echinocandins.<sup>198,199</sup> Due to its unique mechanism of action, occidiofungin has sub-micromolar activity against azole and echinocandin resistant strains of fungi. For example, several species of *Candida* that were resistant to fluconazole at high concentrations (32-64 µg/mL) were inhibited at 1-8 µg/mL of

occidiofungin. Furthermore, strains of *Candida parapsilosis* and *C. neoformans* that were resistant to treatment with caspofungin were found to be susceptible to treatment with occidiofungin. Occidiofungin was also found to have a broader spectrum of activity than clinically available antifungals and was found to be active against *Aspergillus*, *Mucor*, *Fusarium* and *Rhizopus* species. The results, as reported in Table 5.1, indicate that occidiofungin has activity against filamentous and non-filamentous fungi at sub-micromolar concentrations.

Occidiofungin was chemically modified to have a functional alkyne for Click chemistry (Sharpless-Huisgen cycloaddition) on the free amino group of the diamino butyric acid residue at position 5 (Figure 5.1). The modified occidiofungin, alkyne-OF, had an eight-fold reduction in activity with the minimum inhibitory concentration of 1 and 0.5  $\mu\text{g/mL}$  against *Saccharomyces cerevisiae* BY4741 and *Schizosaccharomyces pombe* 972 h-, respectively (Table 5.2). To determine whether alkyne-OF still had the same apoptosis inducing bioactivity as the native occidiofungin, *S. cerevisiae* was treated with alkyne-OF and apoptotic assays such as TUNEL, reactive oxygen species (ROS) detection and phosphatidylserine externalization assays were performed. Double stranded DNA breaks, the generation of ROS, and the externalization of phosphatidylserine were observed in the alkyne-OF treated cells, supporting the same mechanism of action (Figure 5.2A, 5.2B, 5.2C). Although this alkyne modification moderately reduced the inhibitory activity of the compound, the functionalized derivative has the same apoptotic bioactivity and was therefore used to identify the fungal target.

Alkyne-OF was used in a pull-down assay to identify intracellular proteins that directly or indirectly interact with the compound (Figure 5.3A). Data from multiple analyses using *S. pombe* 972h- and *S. cerevisiae* BY4741 were pooled. The resulting list of proteins obtained following LC-MS/MS analysis of bands cut from gels was distilled as follows. The proteins that were observed in the control samples (i.e. treatment with DMSO and native occidiofungin) were removed from consideration resulting in proteins that were exclusively found in the test sample (Table 5.3). The culled protein list was grouped based on gene ontology including cellular localization or molecular function. The resulting distribution is presented in Figure 5.3B. From this analysis, the majority of the proteins that were pulled down by alkyne-OF are actin or actin associated proteins, e.g. Pil1 and Cap1. In addition to the actin-related proteins, proteins involved in vesicle transport and mannosylation were found associated with alkyne-OF. The remaining proteins that were pulled down were ribosomal and mitochondrial related proteins. The data indicate that occidiofungin may play a role in binding to actin since a majority of the proteins either directly interacted with actin (such as Arp2/3 complex and myosin) or are in close proximity to actin patches within the cell.

Pull-down assay and confocal microscopy were used to confirm occidiofungin interaction with actin. Biotinylation of alkyne-OF following incubation with F- or G-actin and streptavidin agarose beads was performed to determine whether occidiofungin directly associated with purified actin *in vitro*. F- or G-actin incubated with the wild type occidiofungin and DMSO was used as a control for potential non-specific interaction of actin with the agarose beads. As shown in Figure 5.4a, the biotinylation of alkyne-OF

was required for the binding of F- or G- actin to the streptavidin beads (Lane 5 and 8). Actin was not present in the control lanes (lanes 6,7,9 and 10). The eluant from the biotinylated alkyne-OF had a single band at approximately 42 kDa which is the expected size for actin. Therefore, the affinity purification assays done with F- or G-actin confirmed that occidiofungin binds to actin. To further support this observation, confocal microscopy using the fluorophore Acti-stain 670 phalloidin was used to visualize F-actin exposed to occidiofungin or alkyne-OF. F-actin exposure to increasing concentrations of occidiofungin leads to more aggregation of actin filaments (Figure 5.4b). Using alkyne-OF labeled with azide functionalized Alexa Fluor 488 dye, occidiofungin interaction with F-actin is directly observed (Figure 5.5). In this experiment, F-actin also appears to aggregate following exposure to occidiofungin. Fluorescence visualization of this interaction following treatment with alkyne-OF and native occidiofungin demonstrated a high degree of aggregation of the filaments which could not be seen in the untreated controls. These results indicate that occidiofungin directly interacts with actin leading to the formation of aggregated filaments. However, occidiofungin association with actin was found to have no effect on its *in vitro* polymerization or depolymerization properties (Figure 5.6).

*In vivo* visualization of the localization of occidiofungin was done in intact yeast cells. Cellular localization of F-actin is well characterized in *S. pombe* and *S. cerevisiae*. Time course analysis of *S. pombe* following alkyne-OF treatment and derivatization with azide Alexa-488 showed a specific pattern of localization of the compound (Figure 5.7a). Alkyne-OF was seen to have a faint pattern of staining at the polar tips at 10

minutes post treatment, which subsequently increased in intensity at 30 minutes post treatment. Strong fluorescence was observed at the polar ends of the cell and at the septum of dividing cells. A similar assay done using *S. cerevisiae* showed localization of alkyne-OF at the bud tips at the early time points and staining throughout the parent cell at later time points (Figure 5.7b). The unique pattern formed was observed to be a combination of striated and inclusion-like structures. In both yeast systems, when the cells were pre-treated with the native occidiofungin prior to treatment with alkyne-OF, the observed cellular localization patterns disappeared (Figure 5.7a & b, panels D, E, and F). This indicates that alkyne-OF and occidiofungin compete for the same target. The vesicular pattern observed at the later time points of exposure is indicative of endocytic vesicles that are coated with actin being circulated through the cell.<sup>201</sup> Additionally, actin patches in the cells of *S. pombe* were seen at the cell tips in growing cells and at the division septum in dividing cells. Actin patches recruited to the division septum interact with myosin to form the acto-myosin ring which is instrumental in cell division.<sup>202</sup> The time course analysis in both types of fungal cells indicates localization of occidiofungin to the regions with high concentration of actin. Recent studies have shown that the dynamic nature of actin is necessary to maintain the cellular functions in which actin is involved.<sup>203</sup> The effect of native occidiofungin on endocytosis in fission yeast was evaluated by staining cells with FM-464 following treatment (Figure 5.8). Cells exposed to 0.5X MIC and 1X MIC demonstrated a concentration dependent reduction in stained endocytic vesicles. A newly formed bud has several actin patches which co-ordinate the retrograde transport of vesicles along the actin cable into the mother cell. Actin

nucleation is carried out by the Arp2/3 complex and a host of proteins including Cap1, Abp1 and Sac6 which are involved in the actin patch based transport of vesicles.<sup>200</sup> Fluorescence time course assays done on the cells of *S. cerevisiae* and *S. pombe* support this hypothesis. The early time points in *S. cerevisiae* cells show localization to bud tips with the compound eventually forming a vesicular pattern within the parent cell. Bud tips in *S. cerevisiae* are known to be rich in actin patches which are necessary to carry out cellular functions such as cell division and endocytosis.<sup>204</sup> Disruption of the dynamics of actin turnover has been reported to trigger apoptosis in yeast and mammalian cells. Specifically, clustering of actin filaments has been reported to trigger mitochondrial damage which in turn leads to release of reactive oxygen species.<sup>205</sup> In addition, caspase dependent pathways have been theorized to be induced following aggregation of actin filaments in animal cells and it is possible that a similar pathway takes place involving Yca1, the caspase found in yeast.<sup>206</sup>

## **5.5 Conclusion**

One of the challenges facing the development of antifungals is the fact that uptake of compounds into yeast cells does not occur as easily as it does in bacteria. Yeast cells have a sturdy cell wall made of several glycoproteins that make up almost one-third of the dry weight of the cell. The efficiency of antifungals relies heavily upon being able to penetrate the cell envelope. Occidiofungin has the advantage of being easily taken up by the yeast cell, as evidenced by the low MICs against several different types of fungi. Susceptibility to occidiofungin can be seen in pathogenic strains that are resistant to treatment with azoles and echinocandins (Table 5.1). Although it is now

observed that occidiofungin binds to F- and G-actin and causes aggregation of the F-actin filaments leading to apoptosis, the exact chain of events needs to be determined. Future studies aimed at understanding how occidiofungin enters the fungal cell and how this leads to the induction of apoptosis needs to be determined. Nevertheless, an actin-targeting antifungal that has a wide spectrum of activity against clinically pathogenic fungi and minimal toxicity in animal models could be the novel drug that is needed in the current antifungal arsenal to combat fungal infections.

In these sections we reported that occidiofungin rapidly induces apoptosis in fungal cells by binding to actin filaments and setting off an as yet unknown pathway of events that culminate in the apoptotic death of the cell. Knowing the target of occidiofungin is vital to the development of the compound as a clinically viable drug. In the following section, we will discuss additional findings that are vital to our understanding of how occidiofungin behaves in an animal system.



**Table 5.1: Activity of occidiofungin against filamentous and non-filamentous fungi**

Species	Occidiofungin ( $\mu\text{g/mL}$ )								Voriconazole	Fluconazole
	24 hours		48 hours		72 hours		96 hours		MIC ( $\mu\text{g/mL}$ )	MIC ( $\mu\text{g/mL}$ )
	50 %	100 %	50 %	100 %	50 %	100 %	80 %	100 %		
<i>*Trichophyton mentagrophytes</i> 10207							1	2	0.25	>16
<i>Trichophyton mentagrophytes</i> 28556							1	2	0.06	>16
<i>Trichophyton mentagrophytes</i> 28641							1	2	0.06	16
<i>&amp;Trichophyton rubrum</i> 11199							1	2	0.008	0.25
<i>Trichophyton rubrum</i> 28658							1	2	0.03	2
<i>Trichophyton rubrum</i> 28659							1	2	0.03	2
<i>Rhizopus microsporus</i> 28506	4	8	-	8					16	
<i>Rhizopus oryzae</i> 28403	4	8	-	8					>16	
<i>Rhizopus microsporus</i> 27785	2	4	-	8					>16	
<i>Mucor circinelloides</i> 19445	4	8	4	8					>16	

**Table 5.1 (continued): Activity of occidiofungin against filamentous and non-filamentous fungi**

Species	Occidiofungin ( $\mu\text{g/mL}$ )								Voriconazole	Fluconazole
	24 hours		48 hours		72 hours		96 hours		MIC ( $\mu\text{g/mL}$ )	MIC ( $\mu\text{g/mL}$ )
	50 %	100 %	50 %	100 %	50 %	100 %	80 %	100 %		
<i>Mucor racemosus</i> 27784	2	4	-	4					>16	
<i>Mucor fragilis</i> 27782	2	4	-	4					>16	
<i>Fusarium solani</i> 28386	2	4	-	4					>16	
<i>Fusarium oxysporum</i> 27718	2	4	-	4					>16	
<i>Fusarium solani</i> 18749	2	4	2	4					>16	
<i>Aspergillus flavus</i> 28517	-	4	-	4					1	
<i>Aspergillus flavus</i> 28455	2	4	-	4					2	
<i>Aspergillus flavus</i> 28445	2	4	-	4					2	
<i>Aspergillus fumigatus</i> 28434	-	4	-	4					1	
<i>Aspergillus fumigatus</i> 28435	-	2	-	2					1	
<i>Aspergillus fumigatus</i> 28436	2	4	2	4					1	
<sup>#</sup> <i>Candida albicans</i> 23512	-	1	-	2						32

**Table 5.1 (continued): Activity of occidiofungin against filamentous and non-filamentous fungi**

Species	Occidiofungin ( $\mu\text{g/mL}$ )								Voriconazole	Fluconazole
	24 hours		48 hours		72 hours		96 hours		MIC ( $\mu\text{g/mL}$ )	MIC ( $\mu\text{g/mL}$ )
	50 %	100 %	50 %	100 %	50 %	100 %	80 %	100 %		
<i>Candida albicans</i> 28200	4	8	4	8						8
<i>Candida albicans</i> 28102	-	2	-	2						0.125
<sup>#</sup> <i>Candida glabrata</i> 27243	2	4	-	4						64
<i>Candida glabrata</i> 25742	-	2	-	2						4
<i>Candida glabrata</i> 28271	4	8	4	8						>64
<i>Candida krusei</i> 9541	2	4	-	4						16
<sup>#</sup> <i>Candida krusei</i> 28415	4	8	4	8						64
<i>Candida krusei</i> 28570	4	8	4	8						16
<sup>+</sup> <i>Candida parapsilosis</i> 2006	2	4	-	4						0.125
<i>Candida parapsilosis</i> 28364	4	8	4	8						0.25
<i>Candida parapsilosis</i> 28174	-	4	-	4						0.25
<i>Candida tropicalis</i> 9624	-	2	-	2						0.25

**Table 5.1 (continued): Activity of occidiofungin against filamentous and non-filamentous fungi**

Species	Occidiofungin ( $\mu\text{g/mL}$ )								Voriconazole	Fluconazole
	24 hours		48 hours		72 hours		96 hours		MIC ( $\mu\text{g/mL}$ )	MIC ( $\mu\text{g/mL}$ )
	50 %	100 %	50 %	100 %	50 %	100 %	80 %	100 %		
<i>Candida tropicalis</i> 28272	4	8	4	8						0.125
<i>Candida tropicalis</i> 28478	4	8	4	8						0.125
<sup>+</sup> <i>Cryptococcus neoformans</i> 19526					-	2				4
<i>Cryptococcus neoformans</i> 27708					-	2				2
<i>Cryptococcus neoformans</i> 28446					-	1				4

‘-’ indicates absence of isolates with 50% inhibition endpoint.

Shaded regions indicate antifungal resistant strains: ‘\*’ indicates itraconazole resistance, ‘&’ indicates terbinafine resistance, ‘#’ indicates fluconazole resistance and ‘+’ indicates caspofungin resistance.

**Table 5.2: Activity of alkyne-OF compared to native occidiofungin**

Strain	MIC ( $\mu\text{g}/\text{mL}$ )	
	Native occidiofungin	Alkyne-OF
<i>Saccharomyces cerevisiae</i> BY4741	0.125	1
<i>Schizosaccharomyces pombe</i> 972 h	0.0625	0.5

**Table 5.3: List of proteins pulled down exclusively by alkyne-OF using the affinity purification. Proteins in the cells highlighted in green are those that were found in the pulldown assays in both *S.pombe* and *S.cerevisiae*. Proteins in the cells that are not highlighted were found in the *S.pombe* assays only.**

Standard Name	Description	Systematic Name	
		<i>S.cerevisiae</i>	<i>S.pombe</i>
Act1	Actin	YFL039C	SPBC32H8.12c
Chc1	clathrin heavy chain (predicted)	YGL206C	SPAC26A3.05
Arc5	ARP2/3 actin-organizing complex subunit	YIL062C	SPAC17G8.04c
Dpm1	dolichol-phosphate mannosyltransferase catalytic subunit	YPR183W	SPAC31G5.16c
Mpg1	mannose-1-phosphate guanyltransferase	YDL055C	SPCC1906.01
Rho1	Rho family GTPase	YPR165W	SPAC1F7.04
Sec24	COPII cargo receptor	YIL109C	SPAC22F8.08
Naa25	NatB N-acetyltransferase complex regulatory subunit	YOL076W	SPBC1215.02c
Rad25	14-3-3 protein	YIL143C	SPAC17A2.13c
Rad24	14-3-3 protein	YER173W	SPAC8E11.02c
Dis2	serine/threonine protein phosphatase PP1	YER133W	SPBC776.02c
Pr65	protein phosphatase 2A 65kD regulatory subunit (A subunit)	YAL016W	SPBC146.14c
Cka1	serine/threonine protein kinase	YIL035C	SPAC23C1.1.11
Myo1	myosin type I	YMR109W	SPBC146.13c
Pil1	fungal protein associated with endocytosis (predicted)	YGR086C	SPBC146.14c
Cap1	adenylyl cyclase-associated protein	YKL007W	SPCC306.09c
Sey1	GTP binding protein (predicted)	YOR165W	SPAC222.14c
Sfb3	vesicle component COPII-coated (predicted)	YHR098C	SPBC4.03c

**Table 5.3 (continued): List of proteins pulled down exclusively by alkyne-OF using the affinity purification. Proteins in the cells highlighted in green are those that were found in the pulldown assays in both *S.pombe* and *S.cerevisiae*. Proteins in the cells that are not highlighted were found in the *S.pombe* assays only.**

Standard Name	Description	Systematic Name	
		<i>S.cerevisiae</i>	<i>S. pombe</i>
Sar1	ADP-ribosylation factor	YPL218W	SPBC31F10.06c
Sec21	coatamer gamma subunit (predicted)	YNL287W	SPAC57A7.10c
Sec26	coatamer beta subunit (predicted)	YDR238C	SPBC146.14c
RPS002	40S ribosomal protein S0B	YLR048W	SPAPJ698.02c
RPL2002	60S ribosomal protein L20	YMR242C	SPAC26A3.04
RPS1101	ribosomal protein S11 homolog	YDR025W	SPAC31G5.03
RPP0	60S acidic ribosomal protein P0	YLR340W	SPCC18.14c
RPL1701	60S ribosomal protein L17	YKL180W	SPBC2F12.04
Cyc1	cytochrome c (predicted)	YJR048W	SPCC191.07
Tom70	mitochondrial TOM complex subunit Tom40 (predicted)	YNL121C	SPAC6B12.12
Sif2	mitochondrial conserved protein (predicted)	YBR103W	SPCC16C4.01

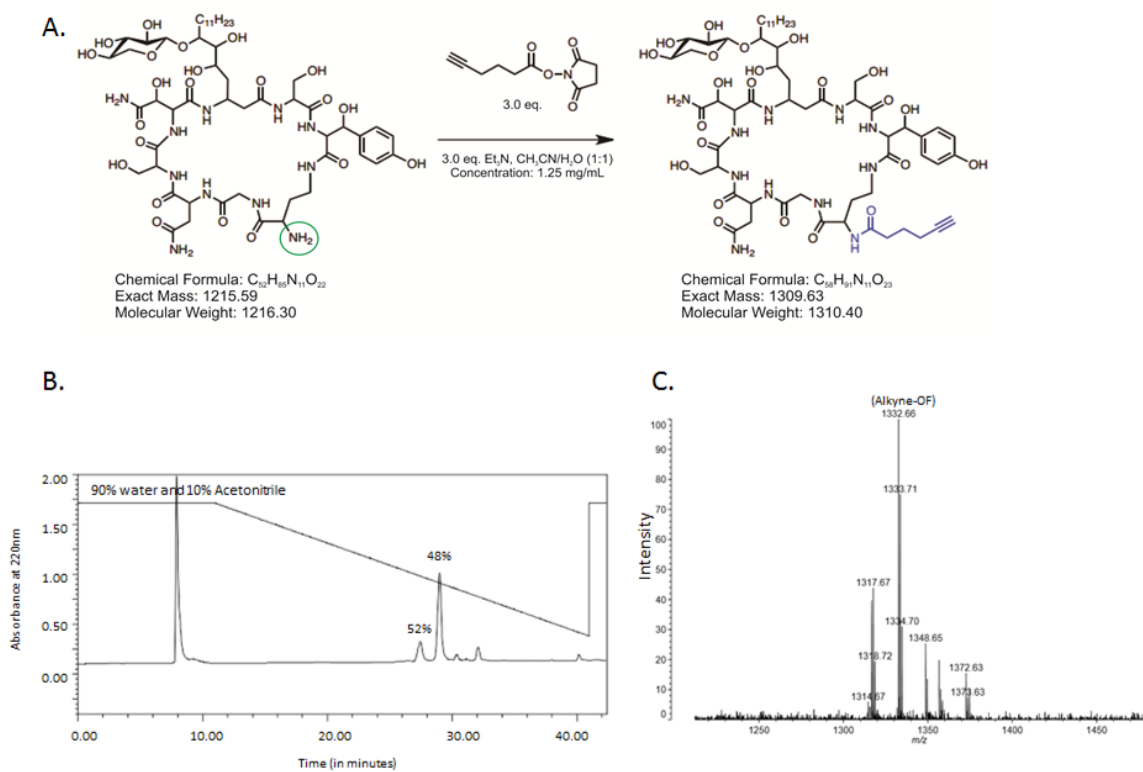


**Figure 5.1:** Derivatization and characterization of alkyne-OF. A) Chemical addition of alkyne group to occidiofungin; B) Purification of alkyne-OF by RP- HPLC; C) Confirmation of the addition of alkyne group to occidiofungin by MALDI-TOF mass spectrometry.



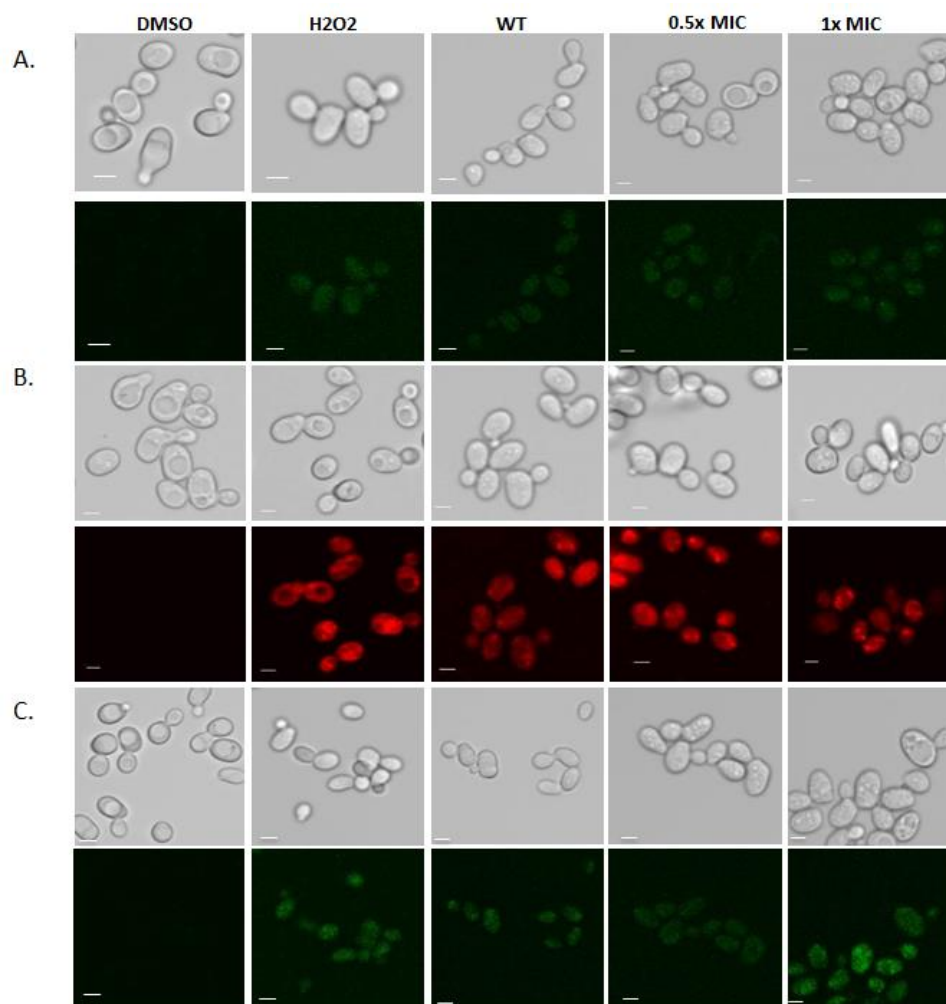


**Figure 5.2:** Induction of apoptosis by alkyne-OF. The ‘DMSO’ and ‘H<sub>2</sub>O<sub>2</sub>’ columns represent the negative and positive controls, respectively. The ‘WT’ column corresponds to cells treated with 1x MIC quantity of native occidiofungin and the last two panels represent treatment of cells with alkyne-OF at the concentration indicated. A) Externalization of phosphatidylserine demonstrated by the fluorescence of Annexin-V-Fluorescein, B) Release of reactive oxygen species indicated by the formation of rhodamine from dihydrorhodamine 123 and C) Double stranded breaks visualized by TUNEL assay, following treatment with native and alkyne-OF.

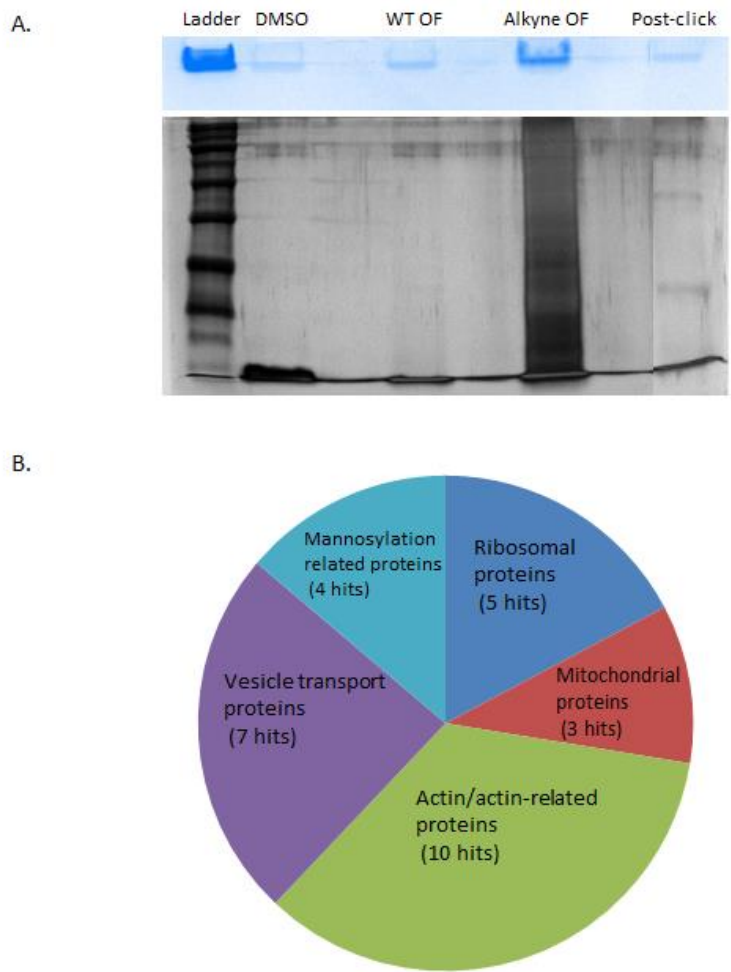


**Figure 5.3:** Determination of *in vivo* interaction of occidiofungin. A) Samples obtained following affinity purification of whole cell extracts run on 12% SDS gels and stained with Coomassie blue (top) and silver staining (bottom). The Coomassie stained gel was run only until the proteins entered the separating phase whereas the silver stained gel was allowed to run completely. The proteins from the bands in the Coomassie stained gel were determined by LC-MS/MS analysis. Broad range (10-250kDa) ladder was used on both gels; B) Cellular distribution of the results obtained following trypsin digest of the bands and LC-MS/MS analysis.

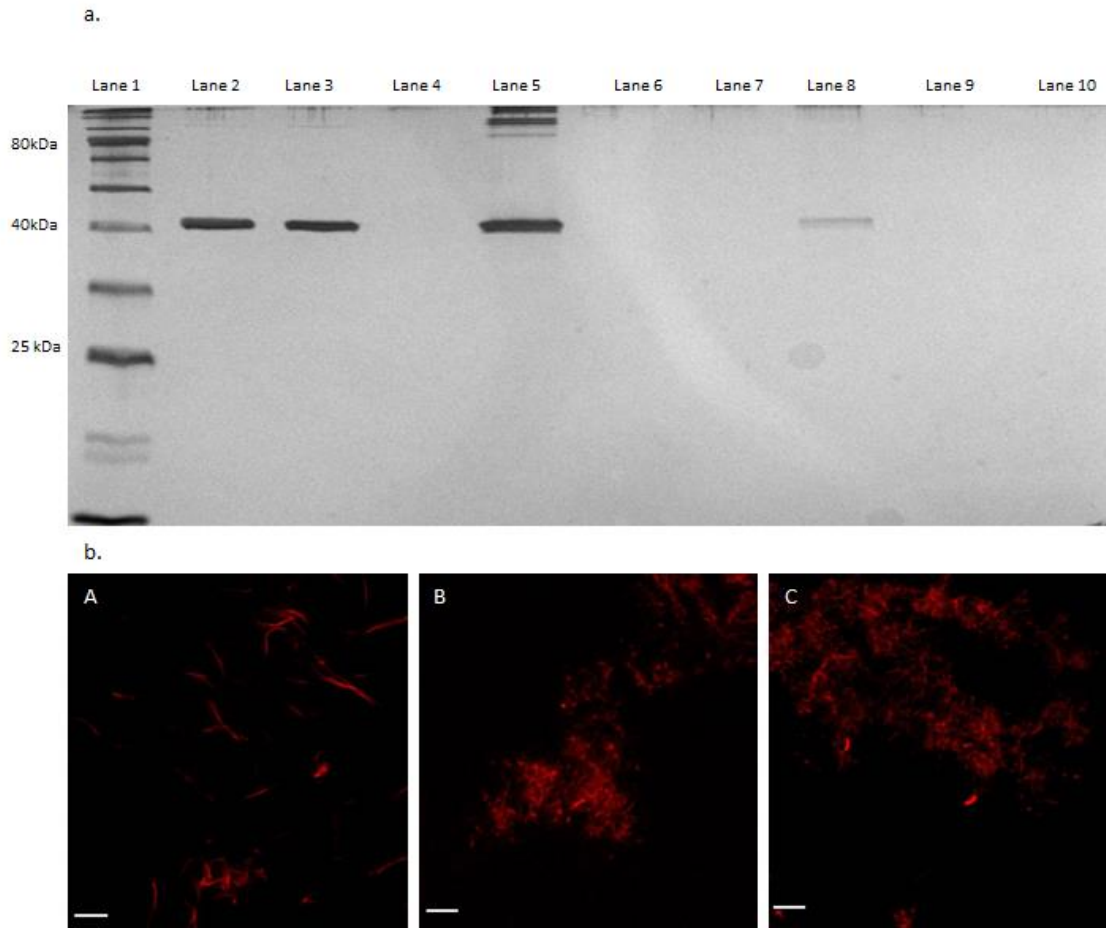


**Figure 5.4:** *In vitro* interaction of occidiofungin with F- and G-actin. a) Affinity pulldown of actin using alkyne-OF: Lane 1- Ladder, Lane 2-100 ng pure F-actin, Lane 3-100 ng pure G-actin, Lane 4-Empty, Lane 5-F-actin treated with alkyne-OF, Lane 6-F-actin treated with native occidiofungin, Lane 7-F-actin treated with DMSO, Lane 8-G-actin treated with alkyne-OF, Lane 9-G-actin treated with native occidiofungin, Lane 10-G-actin treated with DMSO; b) Fluorescence microscopy analysis of the effect of occidiofungin treatment on actin filaments: A: untreated actin filaments, B: Actin:native occidiofungin (24  $\mu$ g actin:4  $\mu$ g native occidiofungin), C: Actin:native occidiofungin (24  $\mu$ g actin:8  $\mu$ g native occidiofungin). Scale bar represents 5 $\mu$ m.

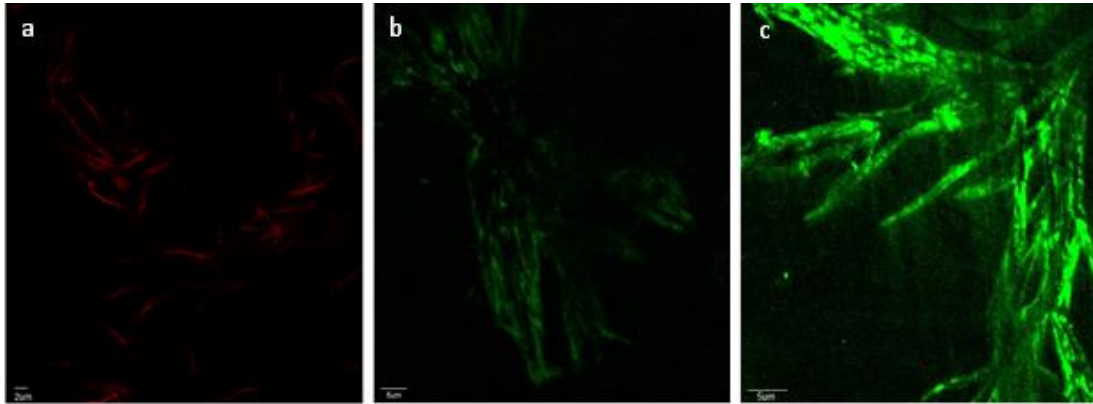


**Figure 5.5:** Visualization of actin filaments. a) Untreated F-actin filaments stained with phalloidin 670 dye; Alkyne-OF treated F-actin filaments stained with azide derivatized AlexaFluor488 [(b)- 40x; (c)- 100x]

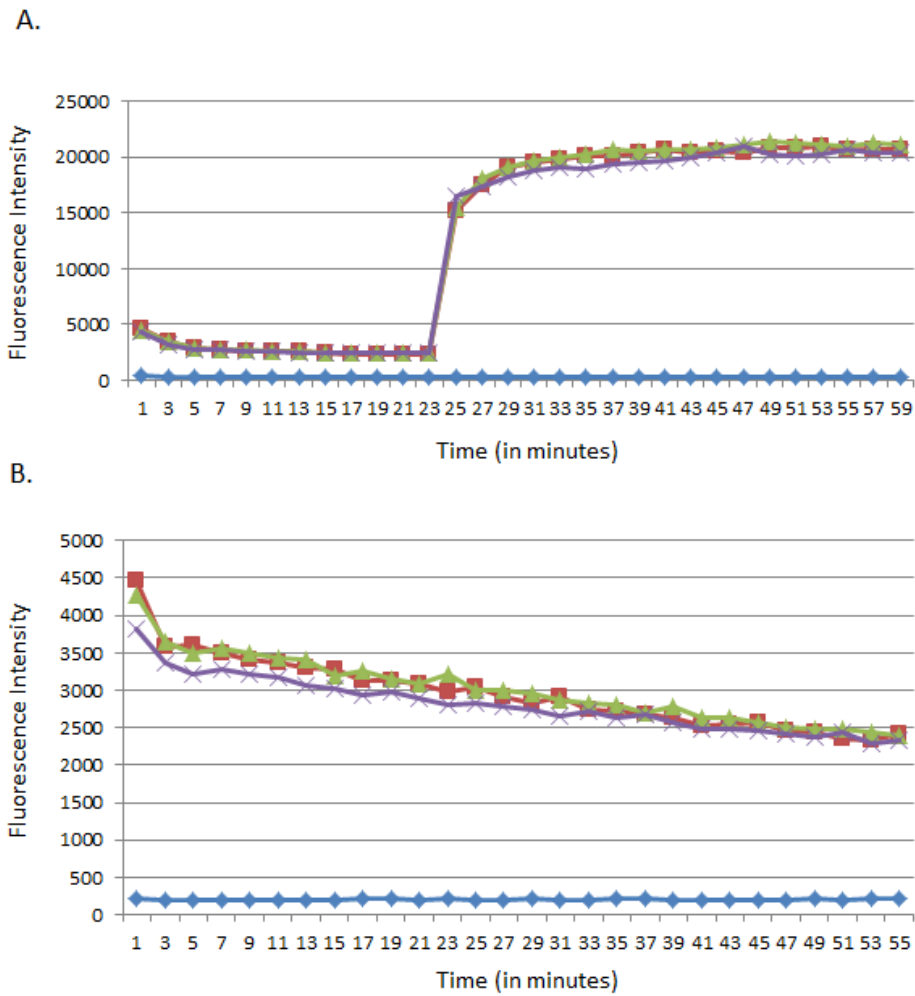


**Figure 5.6:** Effect of occidiofungin on actin (a) polymerization and (b) depolymerization *in vitro*. Symbols are as follows:  $\blacklozenge$  - G-buffer (control),  $\square$  - G-buffer and pyrene actin,  $\Delta$  - Test buffer (1.5%  $\beta$ -cyclodextrin in PBS) and pyrene actin (control),  $\times$  - 20  $\mu$ L of test buffer containing 20  $\mu$ g of occidiofungin and pyrene actin.

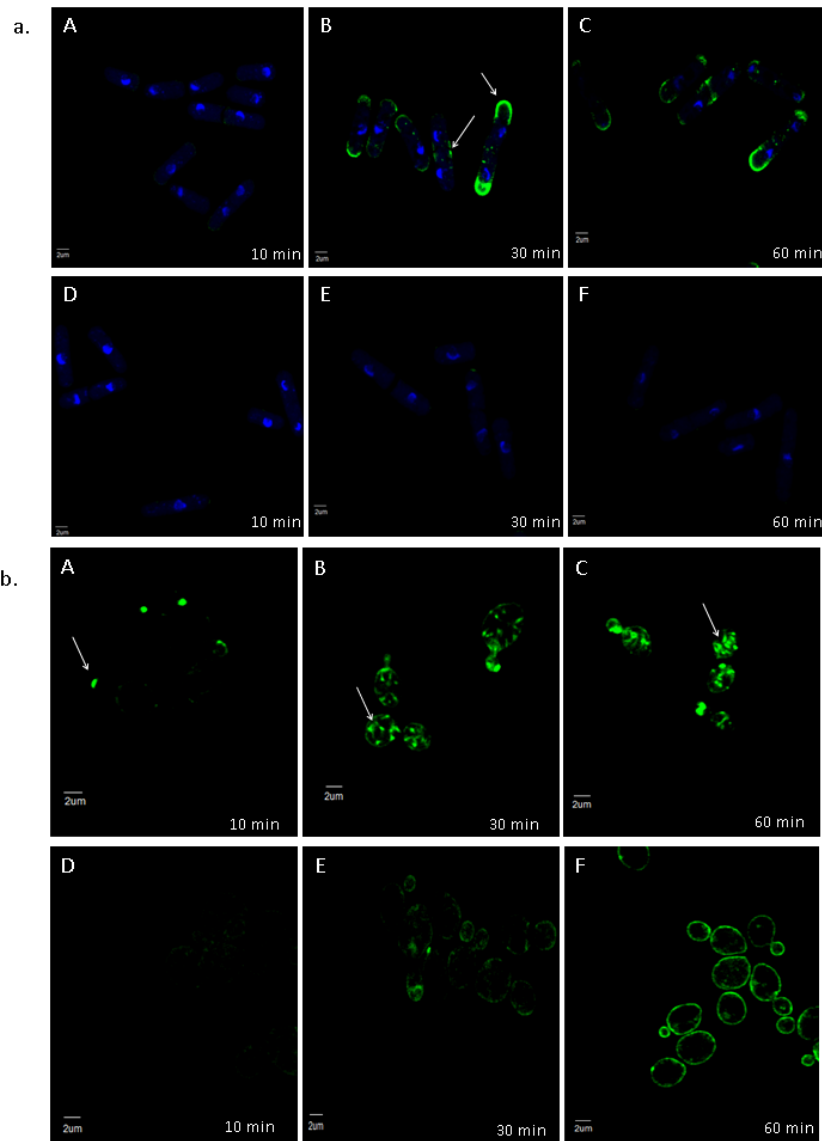


**Figure 5.7:** Time course analysis (A-C) and competition with native occidiofungin (D-F) in a) *Schizosaccharomyces pombe* and b) *Saccharomyces cerevisiae*. Arrows indicate specific localization patterns observed in each cell at 10, 30, and 60 minutes.

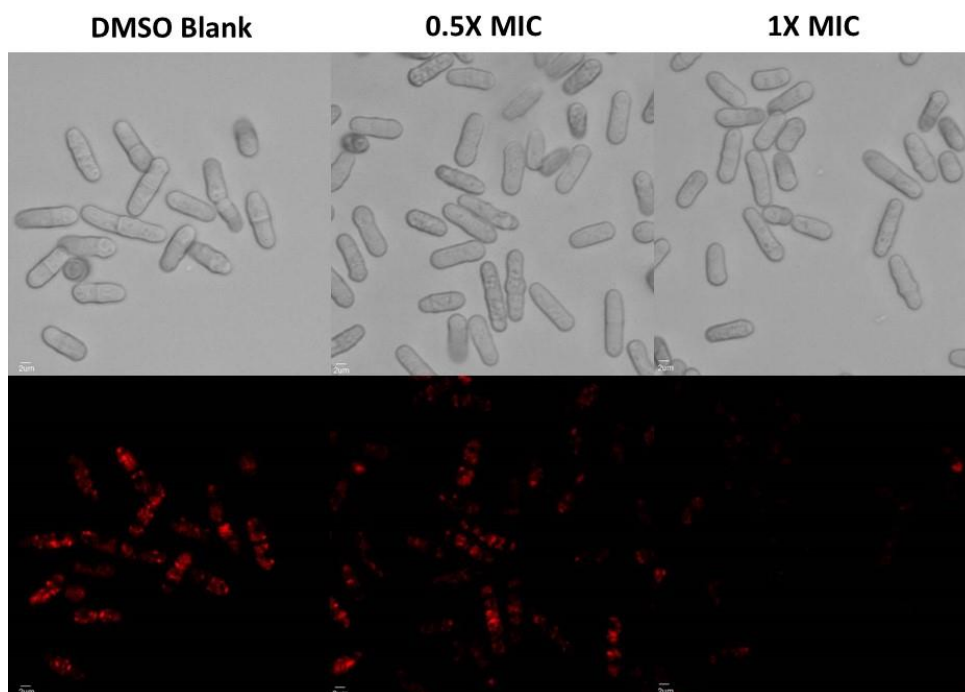


**Figure 5.8:** Effect of the native occidiofungin on endocytosis in fission yeast. DIC (top row) and fluorescence (bottom row) images of cells stained using FM-464 following treatment with sample blank (left column), 0.5x MIC of occidiofungin (middle column), and 1x MIC occidiofungin (last column). FM-464 dye uptake by endocytosis decreases in cells exposed to occidiofungin a dose dependent fashion.

**6. PHARMACOLOGICAL DEVELOPMENT OF OCCIDIOFUNGIN:  
LIPOFORMULATION, TOXICOLOGICAL ANALYSIS AND EFFICACY  
STUDIES**

**6.1 Overview**

Occidiofungin is a non-ribosomally synthesized cyclic glycolipopeptide, produced by a soil bacterium, which possesses broad spectrum antifungal properties. It has been reported to have anti-tumor properties at sub-micromolar concentrations. It has been previously shown to have minimal toxicity when administered intraperitoneally and subcutaneously at a high dose. This report explores multiple routes of administration of occidiofungin to determine the most efficient method of delivery and analyzes the toxicity associated with each route. Encapsulation of occidiofungin in lipid vesicles was done. Upon administering the liposomal occidiofungin, the peak plasma concentration was seen to increase several fold. Histopathology tests revealed mild toxicity in the kidneys, which was reversed as occidiofungin was cleared from the blood. A long duration study over 28 days, with liposomal occidiofungin administration every 48 hours, indicated absence of toxicity in organ tissues. Further, the rate of killing of yeast by liposomal occidiofungin was found to be similar to that of free occidiofungin. This provides an alternate formulation of occidiofungin with reduced organ toxicity, higher peak plasma concentration and similar rate of killing as free occidiofungin.



## 6.2 Introduction

Toxicity to host organisms is a major limiting factor in the clinical use of bioactive compounds. This is an important factor in the development of antifungal compounds for use in human beings since the fungal cells being targeted share several similar features to the host. Currently existing classes of antifungals are limited in their use by the maximum tolerated dose, especially when used against strains that have acquired resistance. Amphotericin B formulated as amphotericin deoxycholate has been associated with severe renal and hepatotoxic side effects.<sup>207,208</sup> Lipid formulations of amphotericin have been developed in order to reduce the toxicity associated with amphotericin deoxycholate. These formulations are reported to have reduced the nephrotoxic effects but appear to induce a cytokine response following administration.<sup>209,210</sup> The azole class of antifungals, by comparison, is less toxic than the polyenes. The most common side effects of azole treatment include skin sensitivity, occurrence of rashes and nausea.<sup>211</sup> Although less common, hepatotoxicity has been reported in cases with voriconazole treatment and less frequently with isaconazole and itraconazole treatment.<sup>212</sup> The risk for *in vivo* toxicity due to azoles is higher due to the occurrence of drug-drug interactions. Azoles have the highest drug-drug interactions of the three classes of antifungals and this leads to numerous side-effects.<sup>213</sup> Echinocandins are a well-tolerated class of antifungals with minimal toxicity to the host. Reports of mild side effects such as gastro-intestinal distress and elevated aminotransferase levels, which indicate liver distress, have been seen.<sup>214</sup> With the occurrence of low drug-drug

interactions, the limiting factor of the echinocandins appears to be the development of resistance in fungal strains to this class.<sup>215,216</sup>

There is an urgent need to identify antifungal compounds with novel mechanisms of action and low toxicity to the host organisms to treat infections that are resistant to currently available forms of treatment. Occidiofungin is a cyclic, non-ribosomally synthesized peptide that can be purified from a liquid culture of the soil bacterium *Burkholderia contaminans* MS14.<sup>64</sup> The covalent structure of occidiofungin has eight constituent amino acids, two of which are non-standard. One of the non-standard amino acids, NAA2 has an eighteen carbon lipid chain, to which a xylose sugar is attached.<sup>64</sup> The bacterium naturally makes several variants of the base structure of occidiofungin (1200Da) which contribute to a more varied conformational repertoire of the wild type pool of occidiofungin.<sup>217,218</sup> Occidiofungin has been reported to possess activity against a wide spectrum of fungi that are pathogenic to plants, animals and human beings.<sup>64</sup> Occidiofungin has been reported to cause cell death in fungi by triggering apoptosis in the cells. Occidiofungin does not target cell compartments that the currently available families of antifungals target i.e. cell wall and cell membrane stability.<sup>66</sup> The fact that occidiofungin targets actin, an entirely new cellular component for an antifungal, is encouraging, in the face of extensive resistance to the existing treatment options.<sup>199</sup> In order to develop occidiofungin as a clinically viable treatment option, the availability and toxicity of occidiofungin in animal models need to be determined. Previous research indicates that occidiofungin, when administered intraperitoneally and subcutaneously, was well tolerated at a dose of 20 mg/kg in 0.5% methylcellulose (constituted with 0.1%

Tween-80 in PBS), with minimal tissue toxicity. Repeated dosing, at 2 mg/kg, administered intraperitoneally for 5 days indicated up to 12% loss in body weight, which was recovered when treatment was stopped. Blood chemistry and microscopic tissue analyses indicated no severe effects on organ function and health.<sup>67</sup> Even so, questions regarding the formulation and other possible routes of administration of occidiofungin remain. In this report, we discuss alternate formulations of occidiofungin administered via multiple routes in an effort to determine the most efficient method of delivery of occidiofungin in an organism while monitoring parameters that indicate toxicity.

### **6.3 Materials and methods**

#### *6.3.1 In vitro quantification of occidiofungin in plasma*

##### 6.3.1.1 Evaluation of extraction protocols and establishment of standard curve:

In order to determine the most optimal solvent for the extraction of occidiofungin from plasma, different solvents were used. Purified occidiofungin was dissolved in phosphate buffered saline (PBS) containing 1.5% hydroxy propyl-beta-cyclodextrin and this formulation was used for all the *in vitro* and *in vivo* assays reported in this study. Occidiofungin was added to commercial BALB/c mouse plasma *in vitro* to achieve a final concentration of 2 µg/mL and multiple solvents at different concentrations were used to extract the occidiofungin out of the serum. Each solvent, at the described concentration, was added as shown in Figure 6.1 and the mixture was vortexed thoroughly. The samples were then spun down at 13000 rpm for 10 minutes and the supernatant was utilized for LC-MS/MS analysis. Azithromycin at a concentration of

100 ng/mL was used as the internal standard. Based on the comparison of the solvents, 50% methanol was found to be the most efficient method to extract the compound.

Liquid chromatography was done using Acclaim 120 C18 columns (Length: 150mm; I.D: 2.1mm; 5 $\mu$ m) to purify the occidiofungin in the sample. Occidiofungin was then subjected to MS/MS using the ThermoScientific TSQ Vantage and fragmentation of occidiofungin (parent mass 1200 m/z) was carried out. Every compound with a mass of 1200 m/z which fragmented to yield the fragment of 1068 m/z, which corresponds to occidiofungin molecule without the xylose sugar, was used for quantification of occidiofungin.

A concentration gradient of occidiofungin was set up in commercially available plasma from BALB/c mice. An initial concentration of 1000 ng/mL was setup and serial dilutions were done in plasma down to a concentration of 12.5 ng/mL. Methanol was added to each sample to reach a final concentration of 50% (v/v) and the samples were vortexed. The samples were then spun down at 13000rpm for 10 minutes and the supernatant was analyzed. Azithromycin at a concentration of 100 ng/mL was used as the internal standard.

#### 6.3.1.2 Lipof ormulation of occidiofungin:

Encapsulation of occidiofungin in vesicles using the lipids 1,2-dioleoyl-sn-glycero-3-phosphocholine (DOPC) and 1,2-dipalmitoyl-sn-glycero-3-phospho-(1'-rac-glycerol) (DPPG) was carried out. Two types of lipid formulations were tested: the first type of formulation was done by encapsulating occidiofungin in 100% DOPC whereas the second type was done by encapsulating occidiofungin in a mixture containing a 9:1

ratio of DOPC:DPPG. In each case, the appropriate amount of lipid to achieve a final concentration of 20 mg/mL was added to the bottom of an acid washed glass beaker. The lipids were vacuum dried to create a lipid cake at the bottom of the beaker. The lipids were then rehydrated using 0.5 mg/mL of occidiofungin in 1.5% hydroxy propyl-beta-cyclodextrin suspended in phosphate buffered saline. The cloudy suspension that was formed was transferred into a 1.5 mL Eppendorf tube. Sonication was carried out using a probe sonicator at 30 second on-off cycles while placing the tube on ice to minimize thermal effects. Sonication was done until the solution became translucent. The quantity of occidiofungin in the vesicles was estimated by running the vesicles made using 100 µg of occidiofungin through a gel filtration column in order to separate the encapsulated compound from free occidiofungin. The column was prepared using a bed volume of 15 mL of Sephadex G-10 beads. The void volume was estimated using Blue dextran (Sigma) as the marker. Both types of liposomal preparations containing 100 µg of occidiofungin were run on the gel filtration column and the void volume was collected. Occidiofungin from the vesicles was extracted using 50% methanol and purified by Reversed-Phase High Performance Liquid Chromatography (RP-HPLC) using a 4.6- by 250-mm C18 column (Grace-Vydac; catalog no. 201TP54) on a Bio-Rad BioLogic F10 Duo Flow with Quad Tec UV-Vis detector system. The solvents used were 99.9% water (with 0.1% trifluoroacetic acid) and 99.9% acetonitrile (with 0.1% TFA). The amount of occidiofungin extracted from the vesicles was compared to a standard run of 100 µg of occidiofungin and the difference was estimated.

#### 6.3.1.3 Comparison of bioactivity of free and liposomal occidiofungin:

Bioactivity assays were carried out using the CLSI method. The strain used to carry out the bioactivity assays was *Candida glabrata* ATCC 2001. A time course analysis of yeast cell death in YPD using free and liposomal occidiofungin was done as previously described<sup>(11)</sup>.

#### 6.3.2 *In vivo analysis of occidiofungin in a murine model*

##### 6.3.2.1 Comparison of administration routes:

Six to eight week old female BALB/c mice were used for all *in vivo* studies. In order to determine the most efficient route of administration of occidiofungin, different routes such as the oral, subcutaneous, intraperitoneal and intravenous routes were evaluated. 2.5 mg/kg of occidiofungin in 1.5% hydroxy propyl-beta-cyclodextrin suspended in PBS was administered to the mice. Four groups of nine mice were used; each group corresponding to a different route of administration. The mice were weighed prior to occidiofungin administration and changes in body weight were monitored every 24 hours. Blood draws were done by nipping the tail vein of the mice at 1, 3, 5, 7, 9, 12, 18, 24 and 48 hpi (hours post injection). Following the intravenous route of administration, blood draws were done from the lateral saphenous vein of the mouse for the initial two time points. 50µL of blood was drawn from each mouse at each time point and the samples were pooled in groups of three. 0.6% sodium citrate was used as the anticoagulant. The samples were then spun down at 13000 rpm for 10 minutes and the supernatant was removed and stored at -20°C until methanol extraction and LC-MS/MS analysis as described above.

#### 6.3.2.2 Evaluation of vesicle encapsulated occidiofungin:

Vesicle encapsulated occidiofungin was prepared as described above using DOPC and DOPC-DPPG (9:1 ratio). 2.5 mg/kg of the liposomal occidiofungin was administered to six to eight week old female BALB/c mice intravenously and blood draws were done at 1, 3, 5, 7, 9, 12, 18, 24 and 48 hpi. Occidiofungin was extracted and concentrations were estimated as described above.

#### 6.3.2.3 Toxicological evaluation:

In order to determine the toxicological effects of occidiofungin, analysis of blood components and tissue was carried out following treatment with 2.5 mg/kg (free and liposomal occidiofungin) and 5 mg/kg of free occidiofungin in a murine system. Toxicological analyses were carried out as previously described<sup>68</sup>. Briefly, occidiofungin in 1.5% hydroxy propyl-beta-cyclodextrin suspended in PBS was administered via tail vein to the mice. The mice were monitored for behavioral changes. The mice were anesthetized using isoflurane and blood draws were done from the heart for serum biochemistry assays (alkaline phosphatase, alanine aminotransferase, aspartate aminotransferase, albumin, and blood urea nitrogen) and hematology (white blood cell count and white blood cell differentiation). Body weight was measured immediately before treatment and 24 hours later before the mice were fully anesthetized and fixed in 10% neutral buffered formalin. Histological examination of each organ was done by embedding tissue in paraffin and staining with hematoxylin and eosin (H & E).

Six to eight week old mice received 2 mg/kg liposomal occidiofungin every 48 hours for 28 days, to study the effects of repeated dosing of occidiofungin. The changes in body

weight were recorded and histological analyses on tissues were carried out. A control group of three mice received empty vesicles for the same duration.

#### 6.3.2.4 Determination of efficacy of occidiofungin in a murine model of systemic candidiasis:

A group of eighteen female, six week old BALB/c mice was used to determine the efficacy of liposomal occidiofungin. Liposomal occidiofungin was prepared using a 9:1 ratio of DOPC:DPPG as described above. Neutropenia was induced in the mice by administering 150 mg/kg of cyclophosphamide in sterile PBS via the intraperitoneal route. After 72 hours, the mice were infected with  $5 \times 10^6$  CFUs of *Candida glabrata* ATCC 2001 in 100  $\mu$ L of sterile PBS intravenously. Drug treatment was carried out 24 hours following administration of *C. glabrata*. The first group of seven mice was treated with 2.5 mg/kg of liposomal occidiofungin intravenously, the second group of seven mice was treated with an equal volume of empty vesicles and the last group of four mice was treated with 5 mg/kg of caspofungin in PBS intraperitoneally<sup>219</sup>. The mice were returned to the cages and their behavior and body weight changes were monitored. The mice were sacrificed at 24 hours post drug treatment and the kidneys were removed, weighed, macerated in YPD and plated on YPD plates to determine the fungal load. The plates were incubated at 35°C before a CFU count was done on each group.

#### 6.3.3 Estimation of the activity of occidiofungin in the presence of serum

A freshly streaked plate of *Candida glabrata* ATCC 2001 was used to test the bioactivity of free and liposomal occidiofungin in the presence of 50% serum and whole blood from different animals. A culture of the yeast at an OD<sub>600</sub> of 0.13 in sterile water



was used. This was then diluted into YPD according to the CLSI M27-A3 protocol. Occidiofungin was diluted in 100 % serum or blood to achieve a starting concentration of 16 µg/mL. An equal volume of the diluted culture was overlaid and the plates were incubated overnight at 35°C. The MIC was read at 24 hours post inoculation. MLCs were estimated for the assays done in blood by plating 100µL of each well onto YPD plates and incubating at 35°C for 24 hours.

## 6.4 Results

### *6.4.1 Estimation of peak plasma concentration of non-liposomal occidiofungin by different routes of administration*

In order to determine the most efficient method of delivery of occidiofungin, four different routes of delivery were compared. Prior to the *in vivo* aspect of this assay, occidiofungin was added to commercial mouse plasma *in vitro* and an extraction protocol was developed. Several different solvents at different concentrations were tested and the results are listed in Figure 6.1. The table shows the peaks obtained when extraction was carried out with each solvent and detection for the parent mass of occidiofungin (1200 Da) with a signature fragment of mass 1068 Da (indicating loss of sugar due to fragmentation) was performed. An accompanying peak for the detection of the internal standard, azithromycin, is also represented. Of the multiple solvents tested, 50% methanol was found to be best suited to extract occidiofungin from plasma. All further extractions of occidiofungin from plasma were carried out using 50% methanol. With this established extraction protocol, a standard curve was constructed using known concentrations of occidiofungin added to plasma. The standard curve, as represented in

Figure 6.2, was seen to have an  $R^2$  value of 0.9957. As a result, the reliable limit of quantification of occidiofungin by this process was determined to be 50 ng/mL and the limit of detection was seen to be 10 ng/mL. The comparison of the different routes of administration yielded important information regarding the retention of the parent form of occidiofungin (1200 Da) in the bloodstream, following an injection of 2.5 mg/kg of occidiofungin in 1.5% hydroxy propyl-beta-cyclodextrin by oral, subcutaneous, intraperitoneal and intravenous routes of administration (Figure 6.3). The oral and subcutaneous routes of administration yielded peak plasma concentrations below the limit of quantification. Furthermore, the intraperitoneal route yielded a peak plasma concentration of 200 ng/mL at 9-12 hpi. Occidiofungin appears to be cleared from the bloodstream at 48 hpi. Intravenous route of administration appeared to yield the highest peak plasma concentration: 390 ng/mL at 1 hpi. The compound was eliminated gradually from the bloodstream by 24 hpi with a half-life of approximately 14 hours.

#### *6.4.2 Determination of peak plasma concentration following liposomal occidiofungin administration*

Liposomal formulation of occidiofungin was done to improve the peak plasma concentration of occidiofungin, since the above mentioned concentrations are not sufficient to effect inhibition of fungal load in a murine model. Administration of 2.5 mg/kg of DOPC vesicles intravenously resulted in higher peak plasma concentration of occidiofungin as can be seen in Figure 6.4A. At 1 hpi, the concentration of occidiofungin in plasma was seen to reach 1800 ng/mL following which it gradually reduced and was eventually cleared out of the system at 48 hpi. In comparison, plasma concentration of

occidiofungin following administration of vesicles made out of 9 parts DOPC and 1 part DPPG containing 2.5 mg/kg of occidiofungin was seen to be approximately 7500 ng/mL at 1 hpi (Figure 6.4B). The half-life in both cases was seen to be around 14.6 hours.

#### *6.4.3 Comparison of pharmacodynamics between free and liposomal occidiofungin*

The *in vitro* analysis to estimate the kill kinetics of purified liposomal occidiofungin indicated no significant differences in the rate of killing of yeast by purified liposomal occidiofungin compared to free occidiofungin. The comparison of different concentrations of free and liposomal occidiofungin can be seen in Figure 6.5. Ten-fold changes in CFUs between the free and liposomal occidiofungin was observed at 4 to 12 hours post antibiotic administration at 0.5x MIC. Similar differences were also observed at 1x MIC. Even though differences in CFUs were seen between free and liposomal occidiofungin, the rate of killing between free and liposomal occidiofungin were found to be consistent over a 12 hour period of time.

#### *6.4.4 Toxicology and histopathology analysis*

Hematology and serum biochemistry assays done on the blood from the mice used for comparison of different routes of administration of free occidiofungin indicated that there were no significant differences between the treated mice and the control mice for all parameters except levels of alanine transaminase (ALT). ALT levels in the mice that received occidiofungin intraperitoneally and intravenously were significantly higher than the controls<sup>68</sup>. Further, histopathology analyses conducted on the organs of these mice indicated that no significant differences between the treated and the control mice were seen, except in the renal medulla of the mice treated intravenously, and in some

cases, intraperitoneally. The renal medullary findings included scattered minimal to occasionally mild small foci interpreted as acute tubular necrosis with minimal granular casts (Figure 6.6). This effect has been reported to be transient as it is not seen at 48 hpi following treatment at a higher dose (5 mg/kg)<sup>68</sup>.

The changes in body weight of mice that were repeatedly dosed with 2 mg/kg liposomal occidiofungin every 48 hours for 28 days indicated that weight lost following administration of occidiofungin was recovered when the challenge was removed (Figure 6.7). Furthermore, the histopathology report on these mice indicated no prolonged effects on the organ tissues (Figure 6.8). Sections of lung, thyroid, trachea, small intestine, thymus, esophagus, stomach, brain, colon, adrenal gland and heart were analyzed microscopically for abnormalities. They were found to be histologically within normal limits compared to the controls, suggesting that repeated dosing for a long duration did not have lasting effects on the organ tissues.

#### *6.4.5 Efficacy analysis of liposomal occidiofungin*

Comparison of fungal load in the kidneys of mice treated with 5 mg/kg of liposomal occidiofungin with the control indicated that no significant reduction occurred. The mice treated with 5 mg/kg of caspofungin demonstrated several fold reduction in the number of CFUs compared to the controls, as seen in Figure 6.9.

#### *6.4.6 Activity of occidiofungin in the presence of serum*

When activity of occidiofungin against *C. glabrata* ATCC 2001 was determined in the presence of 50% serum, the activity of occidiofungin was significantly less when compared to its effectiveness in YPD (Table 6.1). MIC of free and liposomal

occidiofungin in the presence of mouse, rat and porcine serum was seen to be greater than 16 µg/mL. When the mouse serum was heat inactivated and when esterase inhibitors were added, the activity of free and liposomal occidiofungin was seen to be greater than 16 µg/mL. When the assay was carried out using human serum, the MIC was seen to be 8 µg/mL. When purified liposomal occidiofungin was used in the place of free occidiofungin in human serum, activity was seen to improve two-fold. The same two-fold difference was observed in MLCs when the assay was done using 50% human whole blood instead of serum. When the activity of free and purified liposomal occidiofungin was tested in hamster and guinea pig blood, the MLCs were seen to be greater than 16 µg/mL. Liposomal occidiofungin demonstrated an MLC of 16 µg/mL in beagle and rhesus monkey blood whereas the MLC of free occidiofungin was greater than 16 µg/mL. Liposomal occidiofungin has increased activity in human blood with an MLC of 8 µg/mL whereas free occidiofungin has activity at 16 µg/mL.

## **6.5 Discussion**

Occidiofungin has a wide spectrum of activity against several types of fungi that are resistant to the commonly used classes of antifungals. In addition to being active against resistant strains of fungi, occidiofungin is also active against *Pythium* species and filamentous fungi. Preliminary toxicological evaluations done on occidiofungin indicated that a transient allergy response, indicated by an increase in neutrophils, occurred following administration<sup>68</sup>. Body weight changes observed were within normal limits and tubular necrosis seen in the kidney tissue was found to be transient<sup>68</sup>. This study focuses on determining the most effective formulation of occidiofungin to

minimize toxicity in the animal system while increasing peak plasma concentration of occidiofungin in an effort to demonstrate efficacy in reducing fungal load in a murine model.

Following the evaluation of four different routes of administration of occidiofungin formulated in 1.5% hydroxy propyl-beta-cyclodextrin, we were able to demonstrate that intravenous administration of occidiofungin yielded the greatest peak plasma concentration. Even so, peak plasma concentration of approximately 390 ng/mL following a 2.5 mg/kg intravenous administration would be insufficient to cause a significant reduction in the fungal load in organs. Lipoformulation of occidiofungin was attempted using two different combinations of lipids to boost the amount of occidiofungin that could be recovered from the blood. Lipoformulation has the advantage of not only limiting interaction of the drug with other components of blood but also reducing toxicity to organs. Following encapsulation of occidiofungin using DOPC and a 9:1 mixture of DOPC:DPPG, a marked increase in the peak plasma concentration of occidiofungin via intravenous administration was seen for both formulations. Between the two, the combinations of the two lipids yielded a peak plasma concentration of about 7000ng/ml on average compared to an average of 1500 ng/mL with the pure DOPC formulation. Therefore, the DOPC:DPPG (9:1) lipoformulation of occidiofungin was used for further studies.

Tolerability analysis of the lipoformulation by administration of 2 mg/kg of DOPC:DPPG-OF every 48 hours for 28 days showed that fluctuations in body weight occurred when each dose was administered but recovery was rapid. No significant

behavioral changes could be seen following administration. Histopathology assays done on multiple organs at the end of 28 days suggested that no significant toxicity could be observed following repeated dosing. In addition to being well-tolerated by the mice, the lipof ormulation of occidiofungin demonstrated similar pharmacodynamics to free occidiofungin. Kill curve assays done on free and liposomal occidiofungin demonstrated that the rate of killing between the two formulations was not significantly different. Therefore, by encapsulating occidiofungin in lipid vesicles we were able to improve the formulation of occidiofungin that resulted in a higher peak plasma concentration. In addition, the formulation had a reduction in toxicity, while having a similar activity against fungi *in vitro*.

Efficacy study done in a murine model of systemic candidiasis using 2.5 mg/kg of liposomal occidiofungin in comparison with empty vesicle control indicated that there was no significant difference in the fungal load in the kidneys of the treated group. A positive control group of mice that received 5 mg/kg caspofungin had greater than a log reduction in CFU count compared to the negative control. This indicated that even though there was enough occidiofungin in the plasma to cause reduction in fungal load following administration, efficacy could not be observed. This suggests that occidiofungin is not bioavailable *in vivo* possibly due to binding to serum proteins. This was confirmed by bioactivity assays done using 50% serum and blood from different animals that could be used as model systems. Interestingly, activity can be seen in human blood and serum with both liposomal and free occidiofungin. Liposomal occidiofungin was consistently more active in the presence of different sera and blood

compared to free occidiofungin. Chemical modification of the base structure of occidiofungin or development of alternative formulation needs to be done in order to reverse the binding of occidiofungin to proteins in serum.

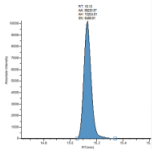
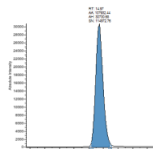
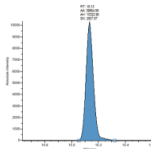
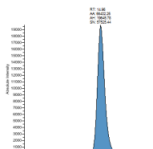
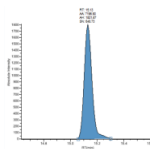
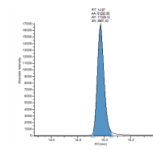
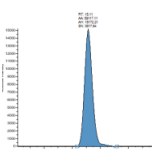
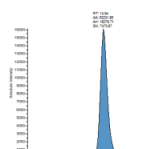
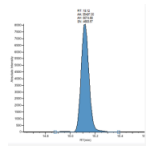
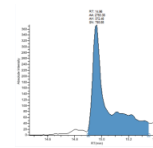
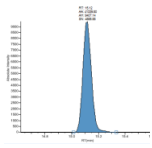
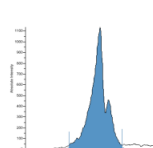
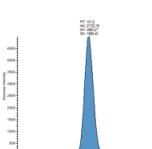
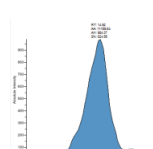
## **6.6 Conclusion**

One of the common problems associated with treatment with antifungals such as amphotericin B or caspofungin is the toxicity associated with the drugs. We have been able to demonstrate a formulation of occidiofungin that is taken up by a wide spectrum of fungal cells and is well tolerated at doses that are capable of controlling fungal infection. This opens avenues for the development of occidiofungin as a treatment alternative with lower toxicity and histopathological side effects than the antifungals currently in use.<sup>8,220</sup> Additionally, we have reported sub-micromolar activity of occidiofungin against multiple cancer cell lines in the presence of serum. Given that occidiofungin binds to actin to cause cell death, it may be possible that occidiofungin has greater activity against actively growing cells. Further studies will be aimed at understanding the reduction in activity of occidiofungin in blood and development of ways to combat the problem to demonstrate efficacy in treating systemic candidiasis.



**Table 6.1: Activity of free and liposomal occidiofungin in serum and blood**

<b>Medium</b>	<b>Minimum Inhibitory Concentration (µg/mL)</b>		<b>Minimum Lethal Concentration (µg/mL)</b>	
	Free occidiofungin	Liposomal occidiofungin	Free occidiofungin	Liposomal occidiofungin
<b>YPD</b>	0.5	0.5		
<b>Mouse serum</b>	>16	>16		
<b>Mouse serum (Heat inactivated)</b>	>16	>16		
<b>Mouse serum (w/ esterase inhibitors)</b>	>16	>16		
<b>Rat serum</b>	>16	>16		
<b>Human serum</b>	8	4		
<b>Porcine serum</b>	>16	16		
<b>Hamster whole blood</b>			>16	>16
<b>Guinea pig whole blood</b>			>16	>16
<b>Beagle whole blood</b>			>16	16
<b>Rhesus monkey whole blood</b>			>16	16
<b>Human whole blood</b>			16	8

Solvent	Occidiofungin	Internal standard
80% Methanol		
70% Methanol		
50% Methanol		
70% Methanol with 0.1% Acetic acid		
70% Methanol with 2N HCl		
70% Acetonitrile with 0.1% acetic acid		
70% Acetonitrile with 2N HCl		

**Figure 6.1:** Comparison of extraction methods of occidiofungin from plasma

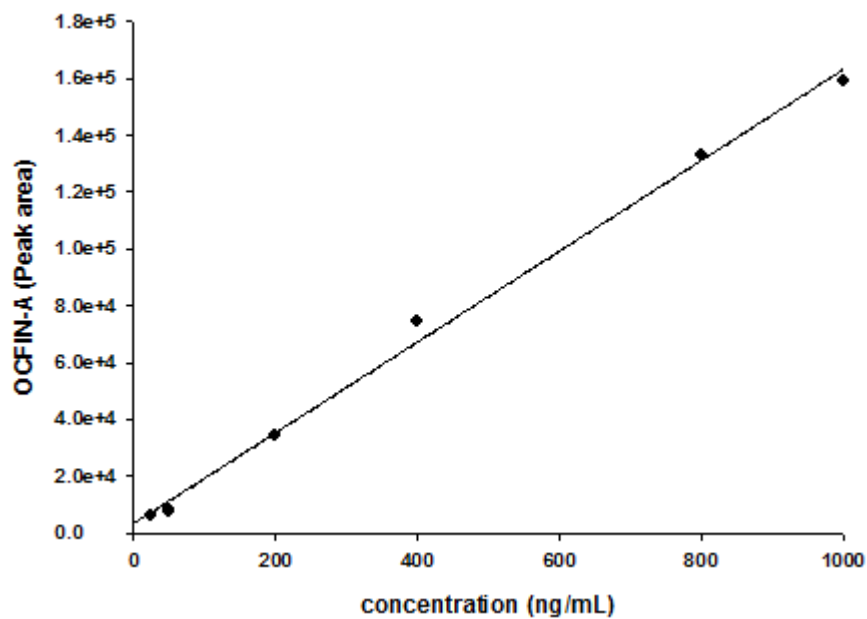


**Figure 6.2:** Calibration curve. Standard concentrations of occidiofungin in serum.  $r^2=0.9957$ ;  $y=-159.8398x+3152.4367$

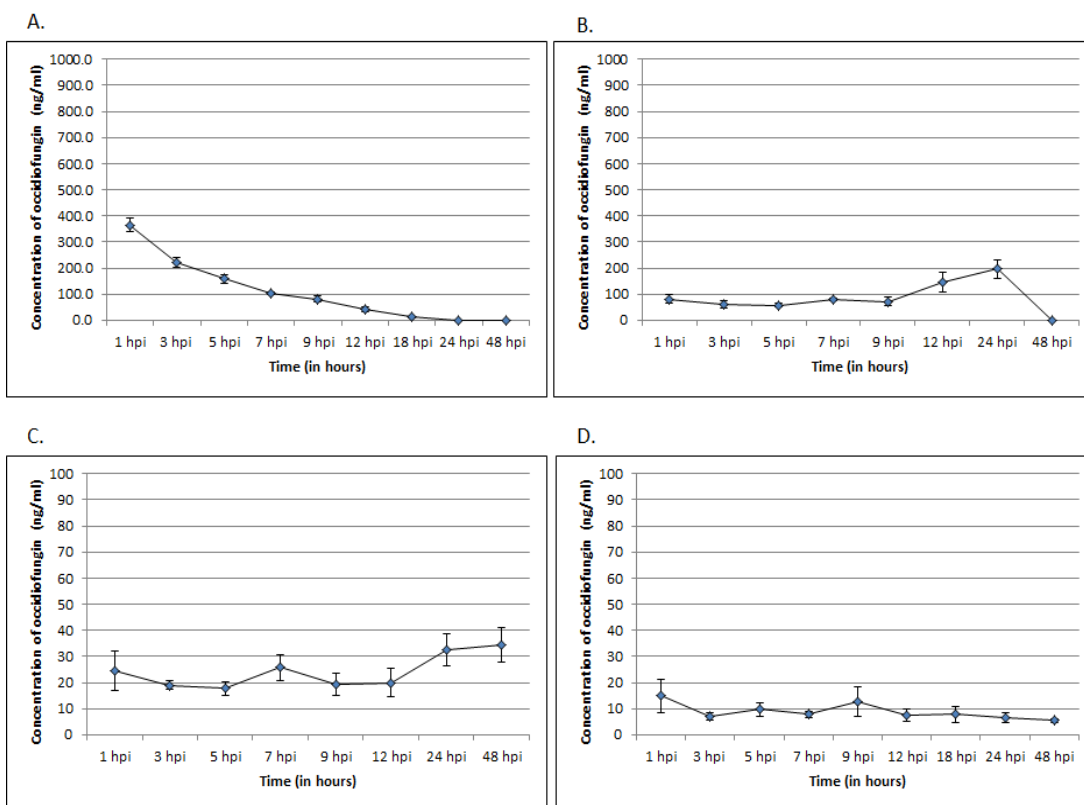


**Figure 6.3:** Comparison of different routes of administration. The plots demonstrate occidiofungin extracted from the plasma of mice treated with 2.5 mg/kg of occidiofungin via A) Intravenous route, B) Intraperitoneal route, C) Sub-cutaneous route and D) Oral route. Error bars indicate standard error of the mean (S.E.M)

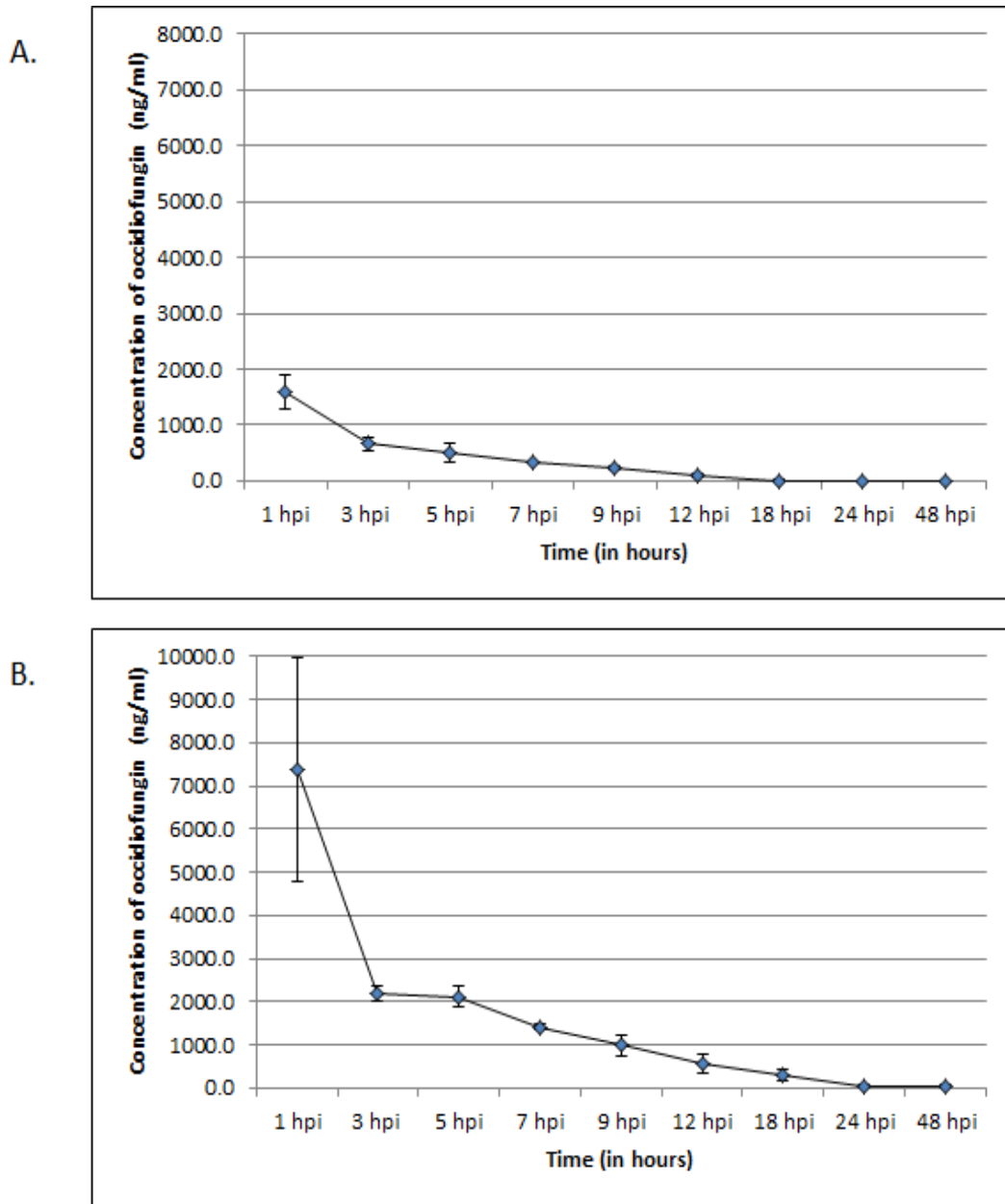


**Figure 6.4:** Comparison of peak plasma concentrations between administration of free and liposomal occidiofungin via intravenous administration. A) DOPC vesicles, B) DOPC:DPPG (9:1) vesicles. Error bars indicate S.E.M.

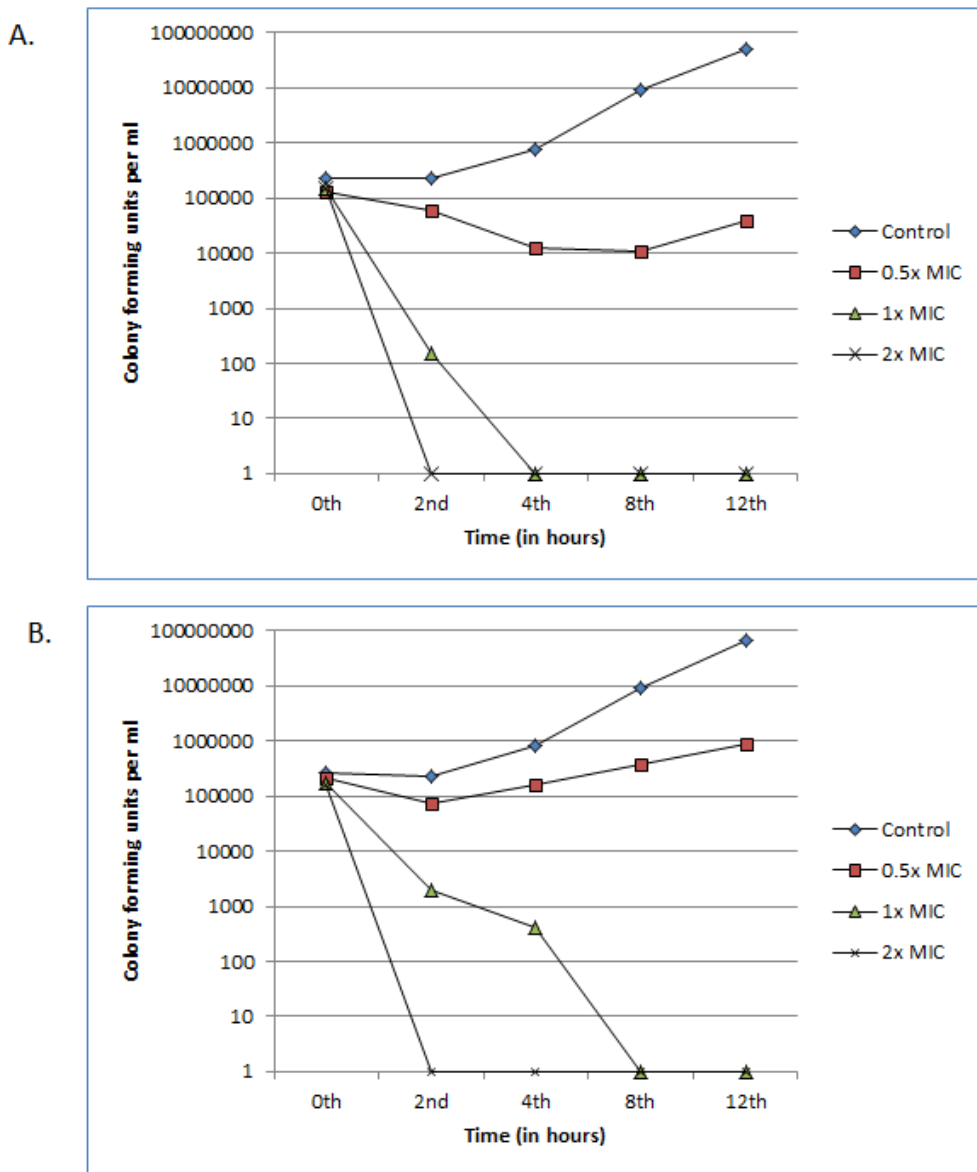


**Figure 6.5:** Comparison of kill kinetics. The effects of A) free and B) liposomal occidiofungin against *Candida glabrata* ATCC 2001 are represented. Figure legends are denoted adjacent to each graph.

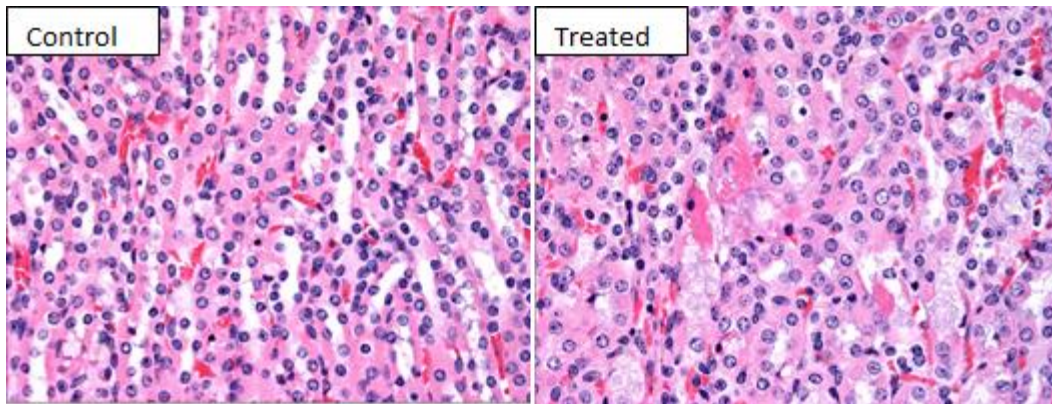


**Figure 6.6:** Histopathology analysis of kidney tissue. Images showing tubular necrosis in kidney tissue following treatment with 2.5 mg/kg of occidiofungin for 24 hours by i.v (right). Tissue from the control group that did not receive occidiofungin (left) demonstrates the normal state. Images are at 40x magnification.

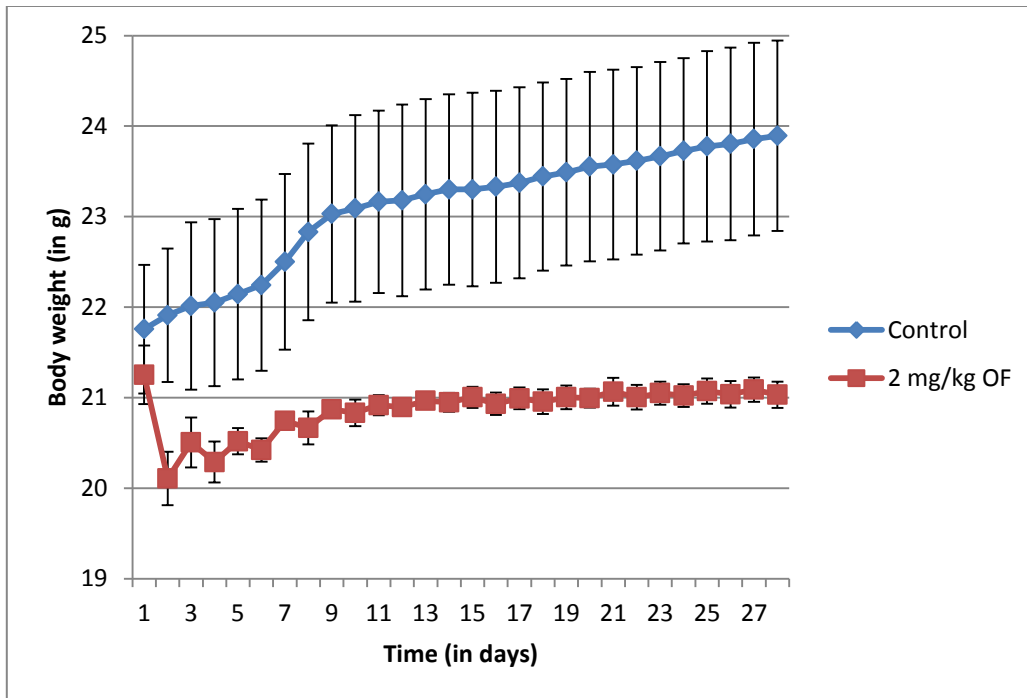


**Figure 6.7:** Effects of occidiofungin treatment on body weight of mice. The trendlines denote body weight changes in mice treated with 2 mg/kg liposomal occidiofungin for 28 days compared with a control group that received empty vesicles for the same duration. Error bars indicate standard deviation.



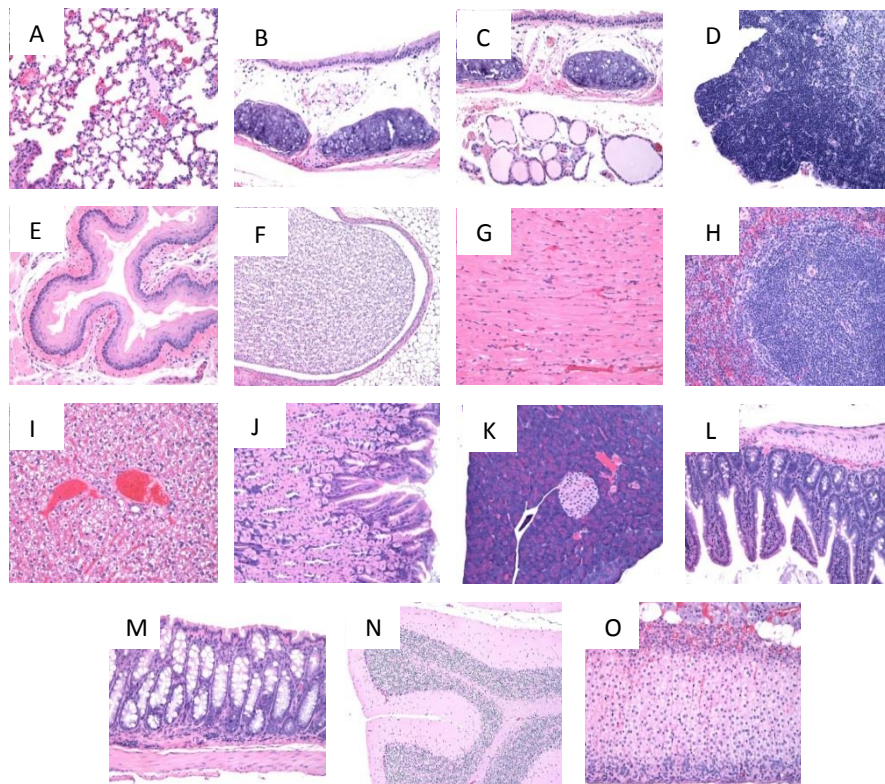


**Figure 6.8:** Histopathology analysis of organs from mice treated with 2mg/kg liposomal occidiofungin every 48 hours for 28 days. A) Lung (20x), B) Trachea (20x), C) Thyroid (20x), D) Thymus (20x), E) Esophagus (20x), F) Kidney (20x), G) Heart (20x), H) Spleen (20x), I) Liver (20x), J) Stomach (20x), K) Pancreas (20x), L) Small intestine (20x), M) Colon (20x), N) Brain (10x), O) Adrenal gland (20x). All tissues were found to be normal.

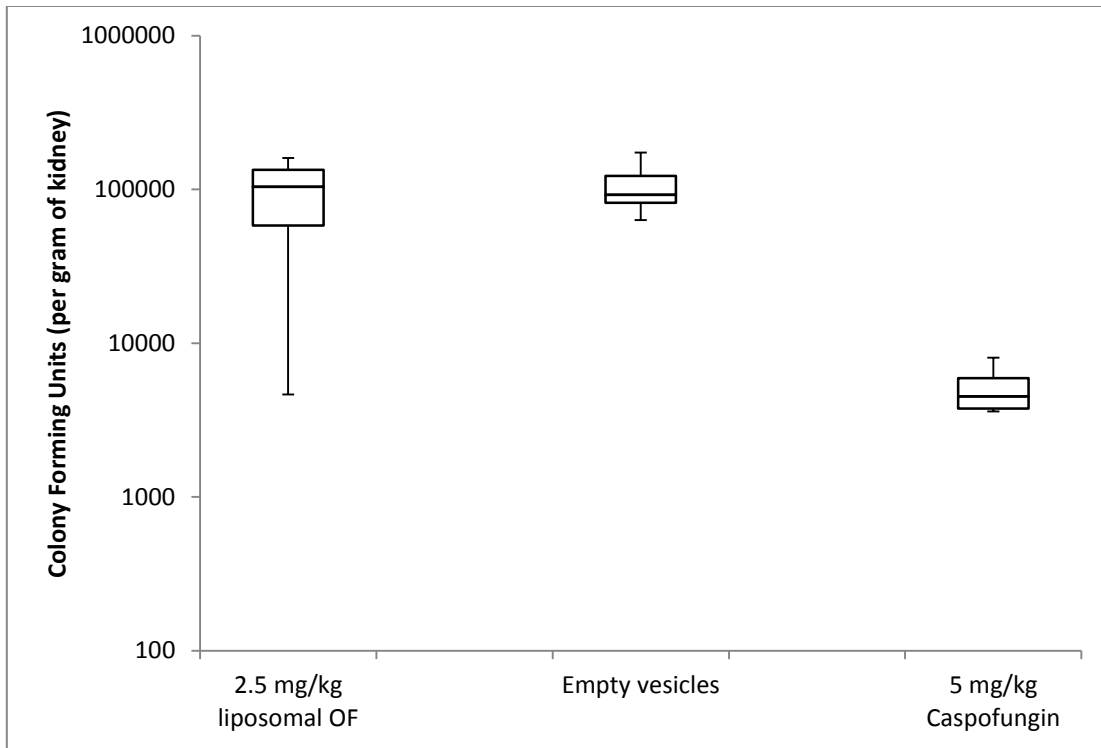


**Figure 6.9:** Analysis of efficacy of occidiofungin *in vivo*. Efficacy analysis of liposomal occidiofungin in a murine model of systemic candidiasis. No statistically significant reduction in fungal load was observed following occidiofungin treatment. Error bars denote deviation from the mean.

## 7. CONCLUSION

Major breakthroughs in the development of antifungals to treat systemic fungal infections have been few and far between since the discovery of amphotericin. The mechanisms of action of those classes of antifungals cluster around cell wall and cell membrane biosynthesis, leading to the development of resistance. Widespread resistance to the antifungals in use has created an urgent necessity for the identification and development of antifungals with novel targets. Such antifungals have a better chance of working against fungal infections that are resistant to the currently available antifungals. Our research suggests that occidiofungin holds promise to be developed as a clinically useful alternative to treat systemic fungal infections.

This dissertation is a compilation of studies that have expanded our understanding of occidiofungin. We report findings that suggest occidiofungin has multiple advantages over other antifungals. One such advantage is derived from the fact that the bacterium produces a pool of variants of the base structure of occidiofungin. Sections two and three discuss the structural and functional characterization of two such variants. We were able to characterize a variant of occidiofungin that retained activity without the xylose sugar that is found attached to the base structure. The advantage lies in the fact that future development of this variant could further minimize toxicity in an animal system since xylose is a sugar that is alien to higher vertebrates. In addition, we discovered that an additional thioesterase that was evolutionarily incorporated into the biosynthetic pathway of occidiofungin added unique diastereomers of the compound to

the wild type pool. This could potentially be advantageous against other microbes that the bacterium naturally encounters in its surroundings. These studies aided in improving our understanding of the biosynthetic machinery of occidiofungin and the benefits of these structural variants.

One of the most important advantages of occidiofungin lies in the fact that the mechanism of action and the molecular target are unique. Sections four and five discuss the induction of apoptosis, possibly as a result of the perturbation of actin dynamics in yeast. Although other actin binding compounds such as jasplakinolide have antifungal properties<sup>221</sup>, occidiofungin is taken up much more efficiently by fungal cells at a much lower concentration. Its activity against caspofungin and fluconazole resistant strains of fungi is possibly due to its unique target. We observed that occidiofungin binds to actin, as a result of affinity purification assays. Further, filaments of F-actin were seen to clump together following occidiofungin treatment. This could lead to induction of apoptosis resulting in cell death. Discovery of the molecular target of occidiofungin is important for pre-clinical development of the drug.

This dissertation also reports formulation of occidiofungin in lipid vesicles to improve plasma concentration and mitigate toxicity effects. Toxicity analysis of occidiofungin reported in section six of this dissertation suggests that liposomal occidiofungin is well-tolerated in murine models. Histopathology studies on multiple organs showed that exposure of occidiofungin over a long period of time to mice did not cause toxic effects. Although occidiofungin could be recovered from the plasma, it was found to be unavailable to reduce fungal load in select organs in mice. This effect was

observed in the *in vitro* bioactivity assays done in serum. This suggests strong, irreversible binding of occidiofungin with serum proteins. Our findings from our experiments identify areas where further development of occidiofungin can be done to improve availability and effect activity in the presence of animal serum.

One of the ways that the problem of binding to serum can be overcome is by chemically modifying the structure of occidiofungin to achieve improved bioavailability while retaining fungicidal activity in an animal model. We have already reported a xylose-free variant of occidiofungin that retains activity. Further experiments in modifying this variant for use in animal systems could lead to potential alternatives. In addition, other formulations of occidiofungin could be attempted in order to minimize interaction with proteins. Another area which requires focus is the subsequent process that is triggered following the binding of occidiofungin to actin leading up to apoptosis. Research in this area could also open up new avenues that could be potential target for antifungals. We believe this research could broaden the field of antifungals leading to the development of a successful, novel compound that could be used to treat invasive fungal infections.

## REFERENCES

1. Volpon, L. & Lancelin, J. M. Solution NMR structure of five representative glycosylated polyene macrolide antibiotics with a sterol-dependent antifungal activity. *European journal of biochemistry / FEBS* **269**, 4533-4541 (2002).
2. Graybill, J. R. New antifungal agents. *European journal of clinical microbiology & infectious diseases: official publication of the European Society of Clinical Microbiology* **8**, 402-412 (1989).
3. Donovick, R., Gold, W., Pagano, J. F. & Stout, H. A. Amphotericins A and B, antifungal antibiotics produced by a streptomycete. I. *In vitro* studies. *Antibiotics annual* **3**, 579-586 (1955).
4. Gary-Bobo, C. M. Polyene--sterol interaction and selective toxicity. *Biochimie* **71**, 37-47 (1989).
5. Kotler-Brajtburg, J. et al. Classification of Polyene Antibiotics According to Chemical Structure and Biological Effects. *Antimicrob. Agents Chemother.* **15**, 716-722 (1979).
6. de Kruijff, B. & Demel, R. A. Polyene antibiotic-sterol interactions in membranes of *Acholeplasma laidlawii* cells and lecithin liposomes. 3. Molecular structure of the polyene antibiotic-cholesterol complexes. *Biochimica et biophysica acta* **339**, 57-70 (1974).

7. Surarit, R. & Shepherd, M. G. The effects of azole and polyene antifungals on the plasma membrane enzymes of *Candida albicans*. *Journal of medical and veterinary mycology* **25**, 403-413 (1987).
8. Juliano, R. L., Grant, C. W., Barber, K. R. & Kalp, M. A. Mechanism of the selective toxicity of amphotericin B incorporated into liposomes. *Molecular pharmacology* **31**, 1-11 (1987).
9. Deray, G. Amphotericin B nephrotoxicity. *The Journal of antimicrobial chemotherapy* **49**, 37-41 (2002).
10. Johnson, P. C. et al. Safety and efficacy of liposomal amphotericin B compared with conventional amphotericin B for induction therapy of histoplasmosis in patients with AIDS. *Annals of internal medicine* **137**, 105-109 (2002).
11. Seo, K., Akiyoshi, H. & Ohnishi, Y. Alteration of cell wall composition leads to amphotericin B resistance in *Aspergillus flavus*. *Microbiology and immunology* **43**, 1017-1025 (1999).
12. Sokol-Anderson, M. L., Brajtburg, J. & Medoff, G. Amphotericin B-induced oxidative damage and killing of *Candida albicans*. *The Journal of infectious diseases* **154**, 76-83 (1986).
13. Čapek, A., Šimek, A., Brůna, L., Šváb, A. & Buděšínský, Z. Antimicrobial agents. *Folia Microbiologica* **19**, 169-171 (1974).
14. Dick, J. D., Merz, W. G. & Saral, R. Incidence of polyene-resistant yeasts recovered from clinical specimens. *Antimicrob. Agents Chemother.* **18**, 158-163 (1980).

15. Teixeira-Santos, R. et al. New Insights Regarding Yeast Survival following Exposure to Liposomal Amphotericin B. *Antimicrob. Agents Chemother.* **59**, 6181-6187 (2015).
16. Nes, W. D., Janssen, G. G., Crumley, F. G., Kalinowska, M. & Akihisa, T. The structural requirements of sterols for membrane function in *Saccharomyces cerevisiae*. *Archives of biochemistry and biophysics* **300**, 724-733 (1993).
17. Parks, L. W., Lorenz, R. T. & Casey, W. M. in *Emerging Targets in Antibacterial and Antifungal Chemotherapy* (Sutcliffe, J. & Georgopapadakou, N. ed.) 393-409 (Springer, 1992).
18. Hitchcock, C. A. Cytochrome P-450-dependent 14 alpha-sterol demethylase of *Candida albicans* and its interaction with azole antifungals. *Biochemical Society transactions* **19**, 782-787 (1991).
19. Joseph-Horne, T. & Hollomon, D. W. Molecular mechanisms of azole resistance in fungi. *FEMS microbiology letters* **149**, 141-149 (1997).
20. Vanden Bossche, H. in *Candida Albicans: Cellular and Molecular Biology* (Prasad, R. ed.) 239-257 (Springer, 1991).
21. Georgopapadakou, N. H., Dix, B. A., Smith, S. A., Freudenberger, J. & Funke, P. T. Effect of antifungal agents on lipid biosynthesis and membrane integrity in *Candida albicans*. *Antimicrob. Agents Chemother.* **31**, 46-51 (1987).
22. Lorenz, R. T., Casey, W. M. & Parks, L. W. Structural discrimination in the sparking function of sterols in the yeast *Saccharomyces cerevisiae*. *Journal of bacteriology* **171**, 6169-6173 (1989).



23. Barone, J. A. et al. Food interaction and steady-state pharmacokinetics of itraconazole oral solution in healthy volunteers. *Pharmacotherapy* **18**, 295-301 (1998).
24. Van Peer, A., Woestenborghs, R., Heykants, J., Gasparini, R. & Gauwenbergh, G. The effects of food and dose on the oral systemic availability of itraconazole in healthy subjects. *European Journal of Clinical Pharmacology* **36**, 423-426 (1989).
25. Purkins, L. et al. Pharmacokinetics and safety of voriconazole following intravenous- to oral-dose escalation regimens. *Antimicrobial Agents Chemotherapy* **46**, 2546-2553 (2002).
26. Pappas, P. G. et al. Alopecia associated with fluconazole therapy. *Annals of internal medicine* **123**, 354-357 (1995).
27. Ashley, E. S. D., Lewis, R., Lewis, J. S., Martin, C. & Andes, D. Pharmacology of systemic antifungal agents. *Clinical Infectious Diseases* **43**, S28-S39 (2006).
28. Rosana, Y., Yasmon, A. & Lestari, D. C. Overexpression and mutation as a genetic mechanism of fluconazole resistance in *Candida albicans* isolated from human immunodeficiency virus patients in Indonesia. *Journal of medical microbiology* **64**, 1046-1052 (2015).
29. Sanguinetti, M. et al. Mechanisms of azole resistance in clinical isolates of *Candida glabrata* collected during a hospital survey of antifungal resistance. *Antimicrob. Agents Chemother.* **49**, 668-679 (2005).

30. Nyfeler, R. & Keller-Schierlein, W. Metabolites of microorganisms. 143. Echinocandin B, a novel polypeptide-antibiotic from *Aspergillus nidulans* var. *echinulatus*: isolation and structural components. *Helvetica chimica acta* **57**, 2459-2477 (1974).
31. Masurekar, P. S., Fountoulakis, J. M., Hallada, T. C., Sosa, M. S. & Kaplan, L. Pneumocandins from *Zalerion arboricola*. II. Modification of product spectrum by mutation and medium manipulation. *The Journal of antibiotics* **45**, 1867-1874 (1992).
32. Iwamoto, T. et al. WF11899A, B and C, novel antifungal lipopeptides. I. Taxonomy, fermentation, isolation and physico-chemical properties. *The Journal of antibiotics* **47**, 1084-1091 (1994).
33. Chen, S. C.-A., Slavin, M. A. & Sorrell, T. C. Echinocandin antifungal drugs in fungal infections. *Drugs* **71**, 11-41 (2011).
34. Morikawa, H. et al. Synthesis and antifungal activity of ASP9726, a novel echinocandin with potent *Aspergillus* hyphal growth inhibition. *Bioorganic & medicinal chemistry letters* **24**, 1172-1175 (2014).
35. Denning, D. W. Echinocandin antifungal drugs. *Lancet* **362**, 1142-1151 (2003).
36. Garcia-Effron, G., Park, S. & Perlin, D. S. Correlating echinocandin MIC and kinetic inhibition of *fkp1* mutant glucan synthases for *Candida albicans*: implications for interpretive breakpoints. *Antimicrobial Agents Chemotherapy* **53**, 112-122 (2009).

37. Wiederhold, N. P. & Lewis, J. S. The echinocandin micafungin: a review of the pharmacology, spectrum of activity, clinical efficacy and safety. *Expert opinion on pharmacotherapy* **8**, 1155-1166 (2007).
38. Munro, C. A. Chitin and glucan, the yin and yang of the fungal cell wall, implications for antifungal drug discovery and therapy. *Advances in applied microbiology* **83**, 145-172 (2013).
39. Maligie, M. A. & Selitrennikoff, C. P. *Cryptococcus neoformans* resistance to echinocandins: (1,3) $\beta$ -glucan synthase activity is sensitive to echinocandins. *Antimicrob. Agents Chemother.* **49**, 2851-2856 (2005).
40. Hao, B., Cheng, S., Clancy, C. J. & Nguyen, M. H. Caspofungin kills *Candida albicans* by causing both cellular apoptosis and necrosis. *Antimicrob. Agents Chemother.* **57**, 326-332 (2013).
41. Wormser, G. P. & Kan, V. L. Antifungal Therapy. *Clinical Infectious Diseases* **51**, 483 (2010).
42. Petranyi, G., Ryder, N. S. & Stutz, A. Allylamine derivatives: new class of synthetic antifungal agents inhibiting fungal squalene epoxidase. *Science* **224**, 1239-1241 (1984).
43. Ozer, K. O. & Tanriverdi, S. T. Design of terbinafine hydrochloride loaded liposome included pullulan film system for unguinal treatment of onychomycosis (2014).

44. Osborne, C. S. et al. Biological, biochemical, and molecular characterization of a new clinical *Trichophyton rubrum* isolate resistant to terbinafine. *Antimicrob. Agents Chemother.* **50**, 2234-2236 (2006).
45. Cannon, R. D. et al. Efflux-mediated antifungal drug resistance. *Clinical microbiology reviews* **22**, 291-321 (2009).
46. Odds, F. C. In *Candida albicans*, resistance to flucytosine and terbinafine is linked to MAT locus homozygosity and multilocus sequence typing clade 1. *FEMS yeast research* **9**, 1091-1101 (2009).
47. Vermes, A., Guchelaar, H. J. & Dankert, J. Flucytosine: a review of its pharmacology, clinical indications, pharmacokinetics, toxicity and drug interactions. *The Journal of antimicrobial chemotherapy* **46**, 171-179 (2000).
48. Denning, D. W. & Bromley, M. J. How to bolster the antifungal pipeline. *Science* **347**, 1414-1416 (2015).
49. Mor, V. et al. Identification of a new class of antifungals targeting the synthesis of fungal sphingolipids. *mBio* **6**, 7-15 (2015).
50. Huang, Z. et al. Sampangine inhibits heme biosynthesis in both yeast and human. *Eukaryotic cell* **10**, 1536-1544 (2011).
51. Singh, S. B. et al. Antifungal Spectrum. *ACS Medicinal Chemistry Letters* **3**, 814-817 (2012).
52. Gutierrez-Cirlos, E. B., Merbitz-Zahradnik, T. & Trumpower, B. L. Inhibition of the yeast cytochrome bc1 complex by ilicicolin H, a novel inhibitor that acts at

- the Qn site of the bc1 complex. *The Journal of biological chemistry* **279**, 8708-8714 (2004).
53. Zhao Y, Perez WB, Jiménez-Ortigosa C, Hough G, Locke JB, Ong V, Bartizal K, Perlin DS. CD101: a novel long-acting echinocandin. *Cellular microbiology* (2016). (Ahead of print)
54. Lockhart, S. R. et al. The investigational fungal cyp51 inhibitor VT-1129 demonstrates potent *in vitro* activity against *Cryptococcus neoformans* and *Cryptococcus gattii*. *Antimicrob. Agents Chemother.* **60**, 2528-2531 (2016).
55. Cabib, E. Differential inhibition of chitin synthetases 1 and 2 from *Saccharomyces cerevisiae* by polyoxin D and nikkomycins. *Antimicrob. Agents Chemother.* **35**, 170-173 (1991).
56. Gaughran, J. P., Lai, M. H., Kirsch, D. R. & Silverman, S. J. Nikkomycin Z is a specific inhibitor of *Saccharomyces cerevisiae* chitin synthase isozyme Chs3 *in vitro* and *in vivo*. *Journal of bacteriology* **176**, 5857-5860 (1994).
57. Warrilow, A. G. S. et al. The clinical candidate VT-1161 is a highly potent inhibitor of candida albicans cyp51 but fails to bind the human enzyme. *Antimicrob. Agents Chemother.* **58**, 7121-7127 (2014).
58. Lepak, A. J., Marchillo, K. & Andes, D. R. Pharmacodynamic target evaluation of a novel oral glucan synthase inhibitor, SCY-078 (MK-3118), using an *in vivo* murine invasive candidiasis model. *Antimicrob. Agents Chemother.* **59**, 1265-1272 (2015).

59. Kallow, W., Neuhof, T., Arezi, B., Jungblut, P. & von Dohren, H. Penicillin biosynthesis: intermediates of biosynthesis of delta-L-alpha-aminoadipyl-L-cysteinyl-D-valine formed by ACV synthetase from *Acremonium chrysogenum*. *FEBS letters* **414**, 74-78 (1997).
60. Shen, B. et al. The biosynthetic gene cluster for the anticancer drug bleomycin from *Streptomyces verticillus* ATCC15003 as a model for hybrid peptide-polyketide natural product biosynthesis. *Journal of industrial microbiology & biotechnology* **27**, 378-385 (2001).
61. Kondejewski, L. H., Farmer, S. W., Wishart, D. S., Hancock, R. E. & Hodges, R. S. Gramicidin S is active against both gram-positive and gram-negative bacteria. *International journal of peptide and protein research* **47**, 460-466 (1996).
62. Cawoy, H. et al. Lipopeptides as main ingredients for inhibition of fungal phytopathogens by *Bacillus subtilis/amyloliquefaciens*. *Microbial biotechnology* **8**, 281-295 (2015).
63. Qian, C.-D. et al. Identification and functional analysis of gene cluster involvement in biosynthesis of the cyclic lipopeptide antibiotic pelgipeptin produced by *Paenibacillus elgii*. *BMC Microbiology* **12**, 1-7 (2012).
64. Lu, S.-E. et al. Occidiofungin, a unique antifungal glycopeptide produced by a strain of *Burkholderia contaminans*. *Biochemistry* **48**, 8312-8321 (2009).
65. Gu, G., Smith, L., Liu, A. & Lu, S. E. Genetic and biochemical map for the biosynthesis of occidiofungin, an antifungal produced by *Burkholderia contaminans* strain MS14. *Appl. Environ. Microbiol.* **77**, 6189-6198 (2011).

66. Emrick, D. et al. The antifungal occidiofungin triggers an apoptotic mechanism of cell death in yeast. *Journal of Natural Products* **76**, 829-838 (2013).
67. Tan, W. et al. Nonclinical toxicological evaluation of occidiofungin, a unique glycolipopeptide antifungal. *International journal of toxicology* **31**, 326-336 (2012).
68. Lai-Hing, S. et al. Toxicological evaluation of occidiofungin against mice and human cancer cell lines. *Pharmacology & Pharmacy* **5**, 1085-1093 (2014).
69. Parke, J. L. & Gurian-Sherman, D. Diversity of the *Burkholderia cepacia* complex and implications for risk assessment of biological control strains. *Annual review of phytopathology* **39**, 225-258 (2001).
70. Chiarini, L., Bevivino, A., Dalmastrì, C., Tabacchioni, S. & Visca, P. *Burkholderia cepacia* complex species: health hazards and biotechnological potential. *Trends in microbiology* **14**, 277-286 (2006).
71. Lu, S., Woolfolk, S. & Caceres, J. Isolation and identification of Rhizobacteria antagonistic to plant fungal pathogens. *Phytopathology* **95**, 62-63 (2005).
72. Lu, S. & Gu, G. Characterization of the *occT* gene located in the *occ* gene cluster associated with production of occidiofungin in *Burkholderia contaminans* MS14. *Phytopathology* **99**, S76-S77 (2009).
73. Ellis, D. et al. Occidiofungin's chemical stability and in vitro potency against candida species. *Antimicrob. Agents Chemother.* **56**, 765-769 (2012).

74. Vidaver, A. K. Synthetic and Complex Media for the Rapid Detection of Fluorescence of Phytopathogenic Pseudomonads: Effect of the Carbon Source. *Applied Microbiology* **15**, 1523-1524 (1967).
75. Del Sal, G., Manfioletti, G. & Schneider, C. The CTAB-DNA precipitation method: a common mini-scale preparation of template DNA from phagemids, phages or plasmids suitable for sequencing. *BioTechniques* **7**, 514-520 (1989).
76. Rzhetsky, A. & Nei, M. A simple method for estimating and testing minimum-evolution trees. *Molecular Biology and Evolution* **9**, 945 (1992).
77. Zuckerkandl, E. & Pauling, L. in *Evolving Genes and Proteins* (Bryson, V. & Vogel, H.J. ed.) 97-166 (Academic Press, 1965).
78. Tamura, K., Dudley, J., Nei, M. & Kumar, S. MEGA4: Molecular Evolutionary Genetics Analysis (MEGA) software version 4.0. *Mol. Biol. Evol.* **24**, 1596-1599 (2007).
79. Alexeyev, M. F. Three kanamycin resistance gene cassettes with different polylinkers. *BioTechniques* **18**, 52-56 (1995).
80. Gu, G., Wang, N., Chaney, N., Smith, L. & Lu, S. E. AmbR1 is a key transcriptional regulator for production of antifungal activity of *Burkholderia contaminans* strain MS14. *FEMS microbiology letters* **297**, 54-60 (2009).
81. Prentki, P., Karch, F., Iida, S. & Meyer, J. The plasmid cloning vector pBR325 contains a 482 base-pair-long inverted duplication. *Gene* **14**, 289-299 (1981).



82. Plesa, M., Hernalsteens, J. P., Vandebussche, G., Ruyschaert, J. M. & Cornelis, P. The SlyB outer membrane lipoprotein of *Burkholderia multivorans* contributes to membrane integrity. *Research in microbiology* **157**, 582-592 (2006).
83. Ausubel, F. M. et al. *Current Protocols in Molecular Biology*. (John Wiley & Sons, 1988).
84. Gu, G., Smith, L., Wang, N., Wang, H. & Lu, S. E. Biosynthesis of an antifungal oligopeptide in *Burkholderia contaminans* strain MS14. *Biochemical and biophysical research communications* **380**, 328-332 (2009).
85. Lefebvre, M. D. & Valvano, M. A. Construction and evaluation of plasmid vectors optimized for constitutive and regulated gene expression in *Burkholderia cepacia* complex isolates. *Appl. Environ. Microbiol.* **68**, 5956-5964 (2002).
86. Wuthrich, K. *NMR of proteins and nucleic acids*. (Wiley, 1986).
87. Johnson, B. A. & Blevins, R. A. NMR View: A computer program for the visualization and analysis of NMR data. *Journal of biomolecular NMR* **4**, 603-614 (1994).
88. Marchler-Bauer, A. et al. CDD: a Conserved Domain Database for the functional annotation of proteins. *Nucleic Acids Res.* **39**, D225-229 (2011).
89. Vorholter, F. J. et al. The genome of *Xanthomonas campestris* pv. *campestris* B100 and its use for the reconstruction of metabolic pathways involved in xanthan biosynthesis. *Journal of biotechnology* **134**, 33-45 (2008).
90. Salzberg, S. L. et al. Genome sequence and rapid evolution of the rice pathogen *Xanthomonas oryzae* pv. *oryzae* PXO99A. *BMC Genomics* **9**, 1-16 (2008).

91. Campbell, J. A., Davies, G. J., Bulone, V. & Henrissat, B. A classification of nucleotide-diphospho-sugar glycosyltransferases based on amino acid sequence similarities. *Biochem J.* **326**, 929-939 (1997).
92. Coutinho, P. M., Deleury, E., Davies, G. J. & Henrissat, B. An evolving hierarchical family classification for glycosyltransferases. *J. Mol. Biol.* **328**, 307-317 (2003).
93. Deadman, M. E., Lundstrom, S. L., Schweda, E. K., Moxon, E. R. & Hood, D. W. Specific amino acids of the glycosyltransferase LpsA direct the addition of glucose or galactose to the terminal inner core heptose of *Haemophilus influenzae* lipopolysaccharide via alternative linkages. *The Journal of biological chemistry* **281**, 29455-29467 (2006).
94. Cantarel, B. L. et al. The Carbohydrate-Active EnZymes database (CAZy): an expert resource for Glycogenomics. *Nucleic Acids Res.* **37**, D233-238 (2009).
95. Balsalobre, C. et al. Complementation of the hha mutation in *Escherichia coli* by the ymoA gene from *Yersinia enterocolitica*: dependence on the gene dosage. *Microbiology* **142**, 1841-1846 (1996).
96. Alfano, J. R., Bauer, D. W., Milos, T. M. & Collmer, A. Analysis of the role of the *Pseudomonas syringae* pv. *syringae* HrpZ harpin in elicitation of the hypersensitive response in tobacco using functionally non-polar hrpZ deletion mutations, truncated HrpZ fragments, and hrmA mutations. *Mol Microbiol* **19**, 715-728 (1996).

97. Yethon, J. A., Vinogradov, E., Perry, M. B. & Whitfield, C. Mutation of the lipopolysaccharide core glycosyltransferase encoded by waaG destabilizes the outer membrane of Escherichia coli by interfering with core phosphorylation. *Journal of bacteriology* **182**, 5620-5623 (2000).
98. Fischbach, M. A. & Walsh, C. T. Assembly-line enzymology for polyketide and nonribosomal Peptide antibiotics: logic, machinery, and mechanisms. *Chemical Reviews* **106**, 3468-3496 (2006).
99. Koglin, A. et al. Structural basis for the selectivity of the external thioesterase of the surfactin synthetase. *Nature* **454**, 907-911 (2008).
100. Koglin, A. et al. Conformational switches modulate protein interactions in peptide antibiotic synthetases. *Science* **312**, 273-276 (2006).
101. Kohli, R. M., Takagi, J. & Walsh, C. T. The thioesterase domain from a nonribosomal peptide synthetase as a cyclization catalyst for integrin binding peptides. *Proceedings Of The National Academy Of Sciences* **99**, 1247-1252 (2002).
102. Lautru, S. & Challis, G. L. Substrate recognition by nonribosomal peptide synthetase multi-enzymes. *Microbiology* **150**, 1629-1636 (2004).
103. Samel, S. A., Wagner, B., Marahiel, M. A. & Essen, L.-O. The thioesterase domain of the fengycin biosynthesis cluster: a structural base for the macrocyclization of a non-ribosomal lipopeptide. *Journal Of Molecular Biology* **359**, 876-889 (2006).

104. Walsh, C. T. Polyketide and nonribosomal peptide antibiotics: modularity and versatility. *Science* **303**, 1805-1810 (2004).
105. White, C. J. & Yudin, A. K. Contemporary strategies for peptide macrocyclization. *Nature Chemistry* **3**, 509-524 (2011).
106. Boddy, C. N. Sweetening cyclic peptide libraries. *Chemistry & Biology* **11**, 1599-1600 (2004).
107. Boguslavsky, V., Hruby, V. J., O'Brien, D. F., Misicka, A. & Lipkowski, A. W. Effect of peptide conformation on membrane permeability. *The Journal Of Peptide Research* **61**, 287-297 (2003).
108. Fernandez-Lopez, S. et al. Antibacterial agents based on the cyclic D,L-alpha-peptide architecture. *Nature* **412**, 452-455 (2001).
109. Fridkin, G. & Gilon, C. Azo cyclization: peptide cyclization via azo bridge formation. *The Journal Of Peptide Research* **60**, 104-111 (2002).
110. Jelokhani-Niaraki, M., Hodges, R. S., Meissner, J. E., Hassenstein, U. E. & Wheaton, L. Interaction of gramicidin S and its aromatic amino-acid analog with phospholipid membranes. *Biophysical Journal* **95**, 3306-3321 (2008).
111. Jelokhani-Niaraki, M. et al. Conformation and other biophysical properties of cyclic antimicrobial peptides in aqueous solutions. *The Journal Of Peptide Research* **58**, 293-306 (2001).
112. Kohli, R. M., Walsh, C. T. & Burkart, M. D. Biomimetic synthesis and optimization of cyclic peptide antibiotics. *Nature* **418**, 658-661 (2002).

113. Rayan, A., Senderowitz, H. & Goldblum, A. Exploring the conformational space of cyclic peptides by a stochastic search method. *Journal Of Molecular Graphics & Modelling* **22**, 319-333 (2004).
114. Schwarzer, D., Mootz, H. D. & Marahiel, M. A. Exploring the impact of different thioesterase domains for the design of hybrid peptide synthetases. *Chemistry & Biology* **8**, 997-1010 (2001).
115. Ellis, D. et al. Occidiofungin's chemical stability and in vitro potency against *Candida* species. *Antimicrob. Agents Chemother.* **56**, 765-769 (2012).
116. Sieber, S. A. & Marahiel, M. A. Learning from nature's drug factories: nonribosomal synthesis of macrocyclic peptides. *Journal Of Bacteriology* **185**, 7036-7043 (2003).
117. Tseng, C. C. et al. Characterization of the surfactin synthetase C-terminal thioesterase domain as a cyclic depsipeptide synthase. *Biochemistry* **41**, 13350-13359 (2002).
118. Gu, G., Smith, L., Liu, A. & Lu, S.-E. Genetic and biochemical map for the biosynthesis of occidiofungin, an antifungal produced by *Burkholderia contaminans* strain MS14. *Applied And Environmental Microbiology* **77**, 6189-6198 (2011).
119. Gu, G., Smith, L., Wang, N., Wang, H. & Lu, S.-E. Biosynthesis of an antifungal oligopeptide in *Burkholderia contaminans* strain MS14. *Biochemical And Biophysical Research Communications* **380**, 328-332 (2009).

120. Gu, G., Wang, N., Chaney, N., Smith, L. & Lu, S.-E. AmbR1 is a key transcriptional regulator for production of antifungal activity of *Burkholderia contaminans* strain MS14. *FEMS Microbiology Letters* **297**, 54-60 (2009).
121. Tan, W. et al. Nonclinical Toxicological Evaluation of occidiofungin, a unique glycolipopeptide antifungal. *International Journal of Toxicology* **31**, 326-336 (2012).
122. Lu, S.-E., Scholz-Schroeder, B. K. & Gross, D. C. Characterization of the salA, syrF, and syrG regulatory genes located at the right border of the syringomycin gene cluster of *Pseudomonas syringae* pv. *syringae*. *Molecular Plant-Microbe Interactions: MPMI* **15**, 43-53 (2002).
123. Wüthrich, K. NMR of Proteins and Nucleic Acids. (Wiley, 1986).
124. Delaglio, F. et al. NMRPipe: a multidimensional spectral processing system based on UNIX pipes. *Journal Of Biomolecular NMR* **6**, 277-293 (1995).
125. Johnson, B. A. & Blevins, R. A. NMRView: a Computer-Program For the Visualization and Analysis of NMR Data. *J. Biomol. NMR* **4**, 603-614 (1994).
126. Heikkinen, S., Toikka, M. M., Karhunen, P. T. & Kilpeläinen, I. A. Quantitative 2D HSQC (Q-HSQC) via suppression of J-dependence of polarization transfer in NMR spectroscopy: application to wood lignin. *Journal Of The American Chemical Society* **125**, 4362-4367 (2003).
127. Rai, R. K., Tripathi, P. & Sinha, N. Quantification of metabolites from two-dimensional nuclear magnetic resonance spectroscopy: application to human urine samples. *Analytical Chemistry* **81**, 10232-10238 (2009).

128. Baysal, C. & Meirovitch, H. Free energy based populations of interconverting microstates of a cyclic peptide lead to the experimental NMR data. *Biopolymers* **50**, 329-344 (1999).
129. Bonmatin, J.-M., Laprévote, O. & Peypoux, F. Diversity among microbial cyclic lipopeptides: iturins and surfactins. Activity-structure relationships to design new bioactive agents. *Combinatorial Chemistry & High Throughput Screening* **6**, 541-556 (2003).
130. Eys, S., Schwartz, D., Wohlleben, W. & Schinko, E. Three thioesterases are involved in the biosynthesis of phosphinothricin tripeptide in *Streptomyces viridochromogenes* Tü494. *Antimicrob. Agents Chemother.* **52**, 1686-1696 (2008).
131. Liao, G., Shi, T. & Xie, J. Regulation mechanisms underlying the biosynthesis of daptomycin and related lipopeptides. *Journal Of Cellular Biochemistry* **113**, 735-741, (2012).
132. Vilhena, C. & Bettencourt, A. Daptomycin: a review of properties, clinical use, drug delivery and resistance. *Mini Reviews In Medicinal Chemistry* **12**, 202-209 (2012).
133. Brown, G. D., Denning, D. W. & Levitz, S. M. Tackling human fungal infections. *Science* **336**, 647-647 (2012).
134. Charlier, C. et al. Fluconazole for the management of invasive candidiasis: where do we stand after 15 years? *The Journal Of Antimicrobial Chemotherapy* **57**, 384-410 (2006).

135. Espinel-Ingroff, A. Mechanisms of resistance to antifungal agents: yeasts and filamentous fungi. *Revista Iberoamericana De Micología* **25**, 101-106 (2008).
136. Ghannoum, M. A. & Rice, L. B. Antifungal agents: mode of action, mechanisms of resistance, and correlation of these mechanisms with bacterial resistance. *Clinical Microbiology Reviews* **12**, 501-517 (1999).
137. Kavanagh, K. *New Insights in Medical Mycology*. (Springer, 2007).
138. Lorian, V. In *Antibiotics in laboratory medicine* (Lorian, V. ed., Lippincott Williams & Wilkins, 2005).
139. Hashimoto, S. Micafungin: a sulfated echinocandin. *The Journal Of Antibiotics* **62**, 27-35 (2009).
140. Ikeda, F. et al. Role of micafungin in the antifungal armamentarium. *Current Medicinal Chemistry* **14**, 1263-1275 (2007).
141. de Groot, P. W. J. et al. Proteomic analysis of *Candida albicans* cell walls reveals covalently bound carbohydrate-active enzymes and adhesins. *Eukaryotic Cell* **3**, 955-965 (2004).
142. Klis, F. M., de Groot, P. & Hellingwerf, K. Molecular organization of the cell wall of *Candida albicans*. *Medical Mycology* **39**, 1-8 (2001).
143. Munro, C. A. & Gow, N. A. Chitin synthesis in human pathogenic fungi. *Medical Mycology* **39**, 41-53 (2001).
144. Douglas, C. M. et al. The *Saccharomyces cerevisiae* FKS1 (ETG1) gene encodes an integral membrane protein which is a subunit of 1,3-beta-D-glucan synthase. *Proceedings Of The National Academy Of Sciences* **91**, 12907-12911 (1994).



145. Garcia-Effron, G., Lee, S., Park, S., Cleary, J. D. & Perlin, D. S. Effect of *Candida glabrata* FKS1 and FKS2 mutations on echinocandin sensitivity and kinetics of 1,3-beta-D-glucan synthase: implication for the existing susceptibility breakpoint. *Antimicrobial Agents And Chemotherapy* **53**, 3690-3699 (2009).
146. Ha, Y.-s., Covert, S. F. & Momany, M. FsFKS1, the 1,3-beta-glucan synthase from the caspofungin-resistant fungus *Fusarium solani*. *Eukaryotic Cell* **5**, 1036-1042 (2006).
147. Kanasaki, R. et al. FR220897 and FR220899, novel antifungal lipopeptides from *Coleophoma empetri* no. 14573. *The Journal Of Antibiotics* **59**, 149-157 (2006).
148. Radding, J. A., Heidler, S. A. & Turner, W. W. Photoaffinity analog of the semisynthetic echinocandin LY303366: identification of echinocandin targets in *Candida albicans*. *Antimicrob. Agents Chemother.* **42**, 1187-1194 (1998).
149. Falagas, M. E., Ntziora, F., Betsi, G. I. & Samonis, G. Caspofungin for the treatment of fungal infections: a systematic review of randomized controlled trials. *International Journal Of Antimicrobial Agents* **29**, 136-143 (2007).
150. Klepser, M. E., Ernst, E. J., Lewis, R. E., Ernst, M. E. & Pfaller, M. A. Influence of test conditions on antifungal time-kill curve results: proposal for standardized methods. *Antimicrob. Agents Chemother.* **42**, 1207-1212 (1998).
151. Naeger-Murphy, N. & Pile, J. C. Clinical indications for newer antifungal agents. *Journal Of Hospital Medicine* **4**, 102-111 (2009).
152. Pfaller, M. A. Anidulafungin: an echinocandin antifungal. *Expert Opinion On Investigational Drugs* **13**, 1183-1197 (2004).

153. Hacimustafaoglu, M. & Celebi, S. Candida infections in non-neutropenic children after the neonatal period. *Expert Review Of Anti-Infective Therapy* **9**, 923-940 (2011).
154. Maertens, J. et al. Multicenter, noncomparative study of caspofungin in combination with other antifungals as salvage therapy in adults with invasive aspergillosis. *Cancer* **107**, 2888-2897 (2006).
155. Fleury, C., Pampin, M., Tarze, A. & Mignotte, B. Yeast as a model to study apoptosis? *Bioscience Reports* **22**, 59-79 (2002).
156. Munoz, A. J., Wanichthanarak, K., Meza, E. & Petranovic, D. Systems biology of yeast cell death. *FEMS Yeast Research* **12**, 249-265 (2012).
157. Herker, E. et al. Chronological aging leads to apoptosis in yeast. *The Journal Of Cell Biology* **164**, 501-507 (2004).
158. Al-Dhaheri, R. S. & Douglas, L. J. Apoptosis in *Candida* biofilms exposed to amphotericin B. *Journal Of Medical Microbiology* **59**, 149-157 (2010).
159. Phillips, A. J., Sudbery, I. & Ramsdale, M. Apoptosis induced by environmental stresses and amphotericin B in *Candida albicans*. *Proceedings Of The National Academy Of Sciences* **100**, 14327-14332 (2003).
160. Yang, C., Gong, W., Lu, J., Zhu, X. & Qi, Q. Antifungal drug susceptibility of oral *Candida albicans* isolates may be associated with apoptotic responses to Amphotericin B. *Journal Of Oral Pathology & Medicine* **39**, 182-187 (2010).

161. Hwang, B. et al. Induction of yeast apoptosis by an antimicrobial peptide, Papiliocin. *Biochemical And Biophysical Research Communications* **408**, 89-93 (2011).
162. te Welscher, Y. M., van Leeuwen, M. R., de Kruijff, B., Dijksterhuis, J. & Breukink, E. Polyene antibiotic that inhibits membrane transport proteins. *Proceedings Of The National Academy Of Sciences* **109**, 11156-11159 (2012).
163. Wei, T. et al. Nonclinical Toxicological Evaluation of Occidiofungin, a Unique Glycolipopeptide Antifungal. *International Journal of Toxicology* **31**, 326-336 (2012).
164. Cormier, C. Y. et al. PSI:Biography-materials repository: a biologist's resource for protein expression plasmids. *Journal Of Structural And Functional Genomics* **12**, 55-62 (2011).
165. Riezman, H. et al. Import of proteins into mitochondria: a 70 kilodalton outer membrane protein with a large carboxy-terminal deletion is still transported to the outer membrane. *The EMBO Journal* **2**, 2161-2168 (1983).
166. Navarro-García, F., Eisman, B., Fiuza, S. M., Nombela, C. & Pla, J. The MAP kinase Mkc1p is activated under different stress conditions in *Candida albicans*. *Microbiology* **151**, 2737-2749 (2005).
167. Navarro-García, F., Sánchez, M., Pla, J. & Nombela, C. Functional characterization of the MKC1 gene of *Candida albicans*, which encodes a mitogen-activated protein kinase homolog related to cell integrity. *Molecular And Cellular Biology* **15**, 2197-2206 (1995).

168. Madeo, F., Fröhlich, E. & Fröhlich, K. U. A yeast mutant showing diagnostic markers of early and late apoptosis. *The Journal Of Cell Biology* **139**, 729-734 (1997).
169. Madeo, F. et al. Oxygen stress: a regulator of apoptosis in yeast. *The Journal Of Cell Biology* **145**, 757-767 (1999).
170. Frost, D. J., Brandt, K. D., Cugier, D. & Goldman, R. A whole-cell *Candida albicans* assay for the detection of inhibitors towards fungal cell wall synthesis and assembly. *The Journal Of Antibiotics* **48**, 306-310 (1995).
171. Escalante, A., Gattuso, M., Pérez, P. & Zacchino, S. Evidence for the mechanism of action of the antifungal phytolaccoside B isolated from *Phytolacca tetramera* Hauman. *Journal Of Natural Products* **71**, 1720-1725 (2008).
172. Millard, P. J., Roth, B. L., Thi, H. P., Yue, S. T. & Haugland, R. P. Development of the FUN-1 family of fluorescent probes for vacuole labeling and viability testing of yeasts. *Applied And Environmental Microbiology* **63**, 2897-2905 (1997).
173. Lushchak, V. I. Oxidative stress in yeast. *Biochemistry. Biokhimiia* **75**, 281-296 (2010).
174. Yasuaki, N., Akio, T. & Hiro, H. In vivo time-resolved Raman imaging of a spontaneous death process of a single budding yeast cell. *J. Raman Spectrosc.* **36**, 837-839 (2005).
175. Carmona-Gutierrez, D. et al. Apoptosis in yeast: triggers, pathways, subroutines. *Cell Death And Differentiation* **17**, 763-773 (2010).

176. Parker, R. RNA degradation in *Saccharomyces cerevisiae*. *Genetics* **191**, 671-702 (2012).
177. Beeler, T., Gable, K., Zhao, C. & Dunn, T. A novel protein, CSG2p, is required for Ca<sup>2+</sup> regulation in *Saccharomyces cerevisiae*. *The Journal Of Biological Chemistry* **269**, 7279-7284 (1994).
178. Cohen, A., Perzov, N., Nelson, H. & Nelson, N. A novel family of yeast chaperons involved in the distribution of V-ATPase and other membrane proteins. *The Journal Of Biological Chemistry* **274**, 26885-26893 (1999).
179. Ogawa, N., DeRisi, J. & Brown, P. O. New components of a system for phosphate accumulation and polyphosphate metabolism in *Saccharomyces cerevisiae* revealed by genomic expression analysis. *Molecular Biology Of The Cell* **11**, 4309-4321 (2000).
180. Samejima, I. & Yanagida, M. Identification of cut8<sup>+</sup> and cek1<sup>+</sup>, a novel protein kinase gene, which complement a fission yeast mutation that blocks anaphase. *Molecular And Cellular Biology* **14**, 6361-6371 (1994).
181. Smits, G. J., van den Ende, H. & Klis, F. M. Differential regulation of cell wall biogenesis during growth and development in yeast. *Microbiology* **147**, 781-794 (2001).
182. Bickle, M., Delley, P. A., Schmidt, A. & Hall, M. N. Cell wall integrity modulates RHO1 activity via the exchange factor ROM2. *The EMBO Journal* **17**, 2235-2245 (1998).

183. Banuett, F. Signalling in the yeasts: an informational cascade with links to the filamentous fungi. *Microbiology And Molecular Biology Reviews: MMBR* **62**, 249-274 (1998).
184. Reinoso-Martín, C., Schüller, C., Schuetzer-Muehlbauer, M. & Kuchler, K. The yeast protein kinase C cell integrity pathway mediates tolerance to the antifungal drug caspofungin through activation of Slt2p mitogen-activated protein kinase signaling. *Eukaryotic Cell* **2**, 1200-1210 (2003).
185. Walker, L. A. et al. Stimulation of chitin synthesis rescues *Candida albicans* from echinocandins. *Plos Pathogens* **4**, e1000040-e1000040 (2008).
186. Arana, D. M., Nombela, C., Alonso-Monge, R. & Pla, J. The Pbs2 MAP kinase kinase is essential for the oxidative-stress response in the fungal pathogen *Candida albicans*. *Microbiology* **151**, 1033-1049 (2005).
187. García, R., Rodríguez-Peña, J. M., Bermejo, C., Nombela, C. & Arroyo, J. The high osmotic response and cell wall integrity pathways cooperate to regulate transcriptional responses to zymolyase-induced cell wall stress in *Saccharomyces cerevisiae*. *The Journal Of Biological Chemistry* **284**, 10901-10911 (2009).
188. Narasimhan, M. L. et al. A plant defense response effector induces microbial apoptosis. *Molecular Cell* **8**, 921-930 (2001).
189. Djavaheri-Mergny, M., Maiuri, M. C. & Kroemer, G. Cross talk between apoptosis and autophagy by caspase-mediated cleavage of Beclin 1. *Oncogene* **29**, 1717-1719 (2010).

190. Maiuri, M. C., Zalckvar, E., Kimchi, A. & Kroemer, G. Self-eating and self-killing: crosstalk between autophagy and apoptosis. *Nature Reviews: Molecular Cell Biology* **8**, 741-752 (2007).
191. Kametaka, S., Okano, T., Ohsumi, M. & Ohsumi, Y. Apg14p and Apg6/Vps30p form a protein complex essential for autophagy in the yeast, *Saccharomyces cerevisiae*. *The Journal Of Biological Chemistry* **273**, 22284-22291 (1998).
192. Khan, M. A. S., Chock, P. B. & Stadtman, E. R. Knockout of caspase-like gene, YCA1, abrogates apoptosis and elevates oxidized proteins in *Saccharomyces cerevisiae*. *Proceedings Of The National Academy Of Sciences* **102**, 17326-17331 (2005).
193. Rezabek, G. H. & Friedman, A. D. Superficial fungal infections of the skin. Diagnosis and current treatment recommendations. *Drugs* **43**, 674-682 (1992).
194. Enoch, D. A., Ludlam, H. A. & Brown, N. M. Invasive fungal infections: a review of epidemiology and management options. *Journal of medical microbiology* **55**, 809-818 (2006).
195. Sheehan, D. J., Hitchcock, C. A. & Sibley, C. M. Current and emerging azole antifungal agents. *Clinical microbiology reviews* **12**, 40-79 (1999).
196. Sugar, A. The polyene macrolide antifungal drugs. In *Antimicrob. Agents Annu.* (Peterson, P.K. and Verhoef, J. ed.) 229-244 (Elsevier Science Publishers, 1987).
197. Hector, R. F. Compounds active against cell walls of medically important fungi. *Clinical microbiology reviews* **6**, 1-21 (1993).

198. Kurtz, M. B. & Douglas, C. M. Lipopeptide inhibitors of fungal glucan synthase. *Journal of medical and veterinary mycology : bi-monthly publication of the International Society for Human and Animal Mycology* **35**, 79-86 (1997).
199. Ghannoum, M. A. & Rice, L. B. Antifungal agents: mode of action, mechanisms of resistance, and correlation of these mechanisms with bacterial resistance. *Clinical microbiology reviews* **12**, 501-517 (1999).
200. Moseley, J. B. & Goode, B. L. The Yeast Actin Cytoskeleton: from Cellular Function to Biochemical Mechanism. *Microbiol. Mol. Biol. Rev.* **70**, 605-645 (2006).
201. Goode, B. L., Eskin, J. A. & Wendland, B. Actin and endocytosis in budding yeast. *Genetics* **199**, 315-358 (2015).
202. Pelham, R. J., Jr. & Chang, F. Role of actin polymerization and actin cables in actin-patch movement in *Schizosaccharomyces pombe*. *Nature cell biology* **3**, 235-244 (2001).
203. Pelham, R. J. & Chang, F. Actin dynamics in the contractile ring during cytokinesis in fission yeast. *Nature* **419**, 82-86 (2002).
204. Waddle, J. A., Karpova, T. S., Waterston, R. H. & Cooper, J. A. Movement of cortical actin patches in yeast. *The Journal of cell biology* **132**, 861-870 (1996).
205. Gourlay, C. W. & Ayscough, K. R. The actin cytoskeleton: a key regulator of apoptosis and ageing? *Nat. Rev. Mol. Cell Biol.* **6**, 583-589 (2005).
206. Desouza, M., Gunning, P. W. & Stehn, J. R. The actin cytoskeleton as a sensor and mediator of apoptosis. *Bioarchitecture* **2**, 75-87 (2012).



207. Bates, D. W. et al. Mortality and costs of acute renal failure associated with amphotericin B therapy. *Clinical infectious diseases : an official publication of the Infectious Diseases Society of America* **32**, 686-693 (2001).
208. Clements, J. S., Jr. & Peacock, J. E., Jr. Amphotericin B revisited: reassessment of toxicity. *The American journal of medicine* **88**, 22n-27n (1990).
209. Arikan, S. & Rex, J. H. Lipid-based antifungal agents: current status. *Current pharmaceutical design* **7**, 393-415 (2001).
210. Hamill, R. J. Amphotericin B formulations: a comparative review of efficacy and toxicity. *Drugs* **73**, 919-934 (2013).
211. Slavin, M. A. et al. Efficacy and safety of fluconazole prophylaxis for fungal infections after marrow transplantation--a prospective, randomized, double-blind study. *The Journal of infectious diseases* **171**, 1545-1552 (1995).
212. Girois, S. B., Chapuis, F., Decullier, E. & Revol, B. G. Adverse effects of antifungal therapies in invasive fungal infections: review and meta-analysis. *European journal of clinical microbiology & infectious diseases : official publication of the European Society of Clinical Microbiology* **25**, 138-149 (2006).
213. Lipp, H. P. Antifungal agents--clinical pharmacokinetics and drug interactions. *Mycoses* **51**, 7-18 (2008).
214. Vazquez, J. A. & Sobel, J. D. Anidulafungin: a novel echinocandin. *Clinical infectious diseases : an official publication of the Infectious Diseases Society of America* **43**, 215-222 (2006).

215. Chandrasekar, P. H. & Sobel, J. D. Micafungin: a new echinocandin. *Clinical infectious diseases : an official publication of the Infectious Diseases Society of America* **42**, 1171-1178 (2006).
216. Nett, J. E. & Andes, D. R. Antifungal Agents: spectrum of activity, pharmacology, and clinical indications. *Infectious disease clinics of North America* **30**, 51-83 (2016).
217. Chen, K.-C. et al. The *Burkholderia contaminans* MS14 ocfC gene encodes a xylosyltransferase for production of the antifungal occidiofungin. *Applied and Environmental Microbiology* **79**, 2899-2905 (2013).
218. Ravichandran, A., Gu, G., Escano, J., Lu, S.-E. & Smith, L. The presence of two cyclase thioesterases expands the conformational freedom of the cyclic peptide occidiofungin. *Journal of Natural Products* **76**, 150-156 (2013).
219. Barchiesi, F. et al. Comparison of the Fungicidal Activities of Caspofungin and Amphotericin B against *Candida glabrata*. *Antimicrob. Agents Chemother.* **49**, 4989-4992 (2005).
220. Wallace, T. L. et al. Activity of liposomal nystatin against disseminated *Aspergillus fumigatus* infection in neutropenic mice. *Antimicrob. Agents Chemother.* **41**, 2238-2243 (1997).
221. Scott, V. R., Boehme, R. & Matthews, T. R. New class of antifungal agents: jasplakinolide, a cyclodepsipeptide from the marine sponge, *Jaspis* species. *Antimicrob. Agents Chemother.* **32**, 1154-1157 (1988).